8-2012

Improving Complementary Methods To Predict Evapotranspiration For Data Deficit Conditions and Global Applications Under Climate Change

Fathi M. A. Anayah
Utah State University

IMPROVING COMPLEMENTARY METHODS TO PREDICT EVAPOTRANSPIRATION FOR DATA DEFICIT CONDITIONS AND GLOBAL APPLICATIONS UNDER CLIMATE CHANGE

by

Fathi (Moh'd Amin) Yousef Anayah

A dissertation submitted in partial fulfillment
of the requirements for the degree

of

DOCTOR OF PHILOSOPHY

in

Civil and Environmental Engineering

Approved:

Dr. Jagath Kaluarachchi Major Professor	Dr. Mac McKee Committee Member
Dr. A. Bruce Bishop Committee Member	Dr. Ronald Sims Committee Member
Dr. Mohammad Almasri Committee Member	Dr. Mark McLellan Vice President for Research and Dean of the School of Graduate Studies

UTAH STATE UNIVERSITY
Logan, Utah

2012

ABSTRACT

Improving Complementary Methods to Predict Evapotranspiration for Data Deficit Conditions and Global Applications under Climate Change

by

Fathi M.A. Anayah, Doctor of Philosophy

Utah State University, 2012

Major Professor: Dr. Jagath J. Kaluarachchi
Department: Civil and Environmental Engineering

A reliable estimate of evapotranspiration (ET) in river basins is important for the purpose of water resources planning and management. ET represents a significant portion of rainfall in the water budget; therefore, the uncertainty in estimating ET can lead to the inaccurate prediction of water resources. While remote sensing techniques are available to estimate ET, such methods are expensive and necessary data may not be readily available. Classical methods of estimating ET require detailed land use/cover information that are not readily available in rural river basins. Complementary methods provide simple and reliable approaches to estimate ET using meteorological data only. However, these methods have not been investigated in detail to assess the overall applicability and the needs for revisions if any. In this work, an improved approach to use the complementary methods using readily available meteorological data is presented. The methodology is validated using 34 global FLUXNET sites with heterogeneous land use/cover, climatic, and physical conditions. The method was compared with classical methods using Ghana as a study area where original pioneering studies of ET have been performed. The work was extended to develop global maps of ET and water surplus (precipitation - ET) for the 20th century followed by climate change-induced 21st century estimates for 2040-2069 and 2070-2099 periods. The emission scenario used was the moderate A1B with the global climate models CGCM3.1 and HADGEM1. The results were assessed at different scales from global to regional such as for potential outcomes of climate change on ET and water surplus.

(186 pages)

PUBLIC ABSTRACT

Improving Complementary Methods to Predict Evapotranspiration for Data Deficit Conditions and Global Applications under Climate Change

by

Fathi M.A. Anayah, Doctor of Philosophy

Agricultural water use across the world is about 70% to 80% of the total water use. Most rural river basins of the world depend on agriculture for food security as well as for livelihood. Evapotranspiration (ET) estimation is important to assess crop water use and therefore water balance for water resources planning and management. Classical methods of estimating ET require detailed land use/cover information that are not readily available in rural river basins. Complementary methods provide simple and reliable approaches to estimate ET using meteorological data only. However, these methods have not been investigated in detail to assess the overall applicability and the needs for revisions if any. In this work, an improved approach to use the complementary methods using readily available meteorological data is presented. The methodology is validated using 34 global FLUXNET sites with heterogeneous land use/cover, climatic and physical conditions. The method later compared with classical methods using Ghana as a study area where original pioneering works of ET have been performed. The work was extended to develop global maps of ET and water surplus (precipitation - ET) for the 20th century followed by climate change induced 21st century estimates for 2040-2069 and 2070-2099 periods. The emission scenario used was the moderate A1B with the global climate models CGCM3.1 and HADGEM1. The results were assessed by different scales from global to regional for potential outcomes of climate change on ET and water surplus.

(186 pages)

ACKNOWLEDGMENTS

All praise and thanks be to Allah, the Lord of all beings. The prophet Mohammad said: “He who does not thank people does not thank Allah." This dissertation is dedicated to my parents, Mohammad Amin and Layla, who spent all their lifetime looking after me and praying for me to get this high level of quality education. I also would like to thank my parents-in-law and all my siblings and their families.

Special thanks are due to my major advisor, Dr. Jagath J. Kaluarachchi, who offered me this great opportunity to pursue my doctoral degree. Many thanks from the heart for offering the guidance, support, and assistance and being a parent who provided dedicated advice. The assistance and guidance of Dr. Mohammad N. Almasri with whom I did my master’s degree in Palestine is unforgettable. I also would like to thank all my committee members, Dr. Mac McKee, Dr. Ronald Sims, Dr. A. Bruce Bishop, and Dr. Mohammad N. Almasri, for their guidance, assistance, and patience.

The financial and logistical support of the Utah Water Research Laboratory at Utah State University is fully acknowledged. I would also like to acknowledge the additional funding available from the International Water Management Institute, Sri Lanka. The faculty and staff at the Department of Civil and Environmental Engineering and the Utah Water Research Laboratory deserve a special thank you for their support. It is really a great honor to be a member of this great family.

Very special thanks are due to my wife, Sara, and my two little kids, Amin and Rashed, for the continuous encouragement, moral support, and patience during my doctoral study. I could not have done it without all of you.

Fathi Anayah

CONTENTS

Page

ABSTRACT.......... iii

PUBLIC ABSTRACT v

ACKNOWLEDGMENTS vii

LIST OF TABLES.......... x

LIST OF FIGURES xii

CHAPTER

1. INTRODUCTION.......... 1

References.......... 11

2. IMPROVING COMPLEMENTARY METHODS TO ESTIMATE EVAPOTRANSPIRATION UNDER VARIETY OF CLIMATIC AND PHYSICAL CONDITIONS 16

Abstract.......... 16
2.1 Introduction.......... 17
2.2 Existing Methods and Data.......... 24
2.3 Model Development and Results.......... 33
2.4 Summary and Conclusions 45
References.......... 47

3. USE OF MODIFIED COMPLEMENTARY METHODS TO PREDICT REGIONAL-SCALE EVAPOTRANSPIRATION: A COUNTRY-WIDE STUDY OF GHANA 65

Abstract.......... 65
3.1 Introduction.......... 66
3.2 Description of Ghana 72
3.3 Methodology.......... 74
3.4 Results and Discussion 81
3.5 Conclusions.......... 95
References.......... 97

4. GLOBAL APPLICATION OF A MODIFIED MODEL OF COMPLEMENTARY EVAPOTRANSPIRATION UNDER CLIMATE CHANGE.......... 113

Abstract ... 113
4.1 Introduction ... 114
4.2 Data Collection ... 120
4.3 Methodology ... 127
4.4 Current Conditions ... 135
4.5 Future Projections ... 144
4.6 Conclusions ... 149
References ... 151

5. SUMMARY, CONCLUSIONS, AND RECOMMENDATIONS ... 166

5.1 Summary and Conclusions ... 166
5.2 Recommendations ... 169
References ... 170

CURRICULUM VITAE ... 172

LIST OF TABLES

Table Page

2.1. Characteristics of the 34 EC sites with measured ET data used in the study. 52

2.2. Average values of RMSE, BIAS, and R^2 for the actual ET estimates of the different complementary methods, CRAE, AA, and GG, at each climatic class. 53

2.3. Details of the 39 model variations developed based on the complementary relationships.. 54

2.4. Results of the performance of different models in a given climatic class described through the best values of RMSE, BIAS, and R^2. 55

2.5. The values of the coefficients after optimization for the six promising model variations... 55

2.6. Average values of RMSE and BIAS for the complementary methods, six promising models, and post-optimized promising models at each climatic class. 56

2.7. Comparison of performance of GG18 to the most recently published ET studies.. .. 57

3.1. Characteristics of the 10 synoptic stations in Ghana. 102

3.2. Climatic class of each station using different aridity indices. 102

3.3. Average annual ETP estimates (mm) computed from different methods and the relative absolute difference (RAD) as %. 103

3.4. Percentage of crop cultivated in area of each station and related crop coefficients and heights.. 104

3.5. Computed average annual actual or crop ET (mm) and corresponding ET/P ratios as %.. 105

3.6. Comparison of annual ET estimates (mm) and percentage of annual ET to rainfall (%) of this study with results from prior studies conducted in the region.............. 106

4.1. The average annual values of the water budget components and ET/P ratios by continent. 158

4.2. The latitudinal distribution of the land areas in km^2, the volumes of the water budget components in km^3, and the share of each to its total value in % for every latitudinal slice. 158

4.3. The distribution of anomalies (%) in the water budget components in the globe, by Hemispheres, and by continents for the four climate change scenarios. 159

LIST OF FIGURES

Figure Page

2.1. A schematic representation of the complementary relationship between ET, ETW, and ETP. 58

2.2. World map showing the locations of the 34 EC sites with measured ET flux data... 59

2.3. Average values of RMSE, BIAS, and R^2 for the different estimates of net radiation, R_n (R_T in white, R_{TP} in dark gray, and R_{SZ} in light gray) for each climatic class. 60

2.4. Boxplots of RMSE, BIAS, and R^2 metrics of the selected six promising models for the different climatic classes. 61

2.5. Scatter plots of average ET estimates (mm/month) for GG18, GG20, and GG22 models in comparison to measured ET_{EC} fluxes from 33 sites (all except site 4) in the wet (triangle), moderate (circle), and dry (square) climatic classes. 62

2.6. RMSE, BIAS, and R^2 of the GG18 model at each site in the wet (triangle), moderate (circle), and dry (square) climatic classes and the dashed lines indicate the average values. 63

2.7. Schematic showing the structure of the proposed GG18 model. 64

3.1. A schematic representation of the complementary relationship between ET and ETP (after Morton, 1983). 107

3.2. Map of Ghana (within dark solid line) and the Volta River Basin in the hatched area. The dark squares show the synoptic stations used in the study and the interior divisions are administrative regions of Ghana. 108

3.3. Monthly potential evapotranspiration boxplots in mm (+: average value, ETP: GG model, ETW: GG model, GR: grass ET_o, AL: alfalfa ET_o, HV: Hargreaves ET_o, TC: Turc ET_o, and JH: Jensen Haise ET_o). 109

3.4. Average monthly actual ET, crop ET, and rainfall in mm (solid line: actual ET of GG model, dashed line: crop ET of GR method, and dotted line: rainfall). 110

3.5. Land use in areas surrounding Kete-Krachi, Wenchi, and Sunyani stations using the areal basemap feature enabled of ArcMap 10 at 1:250000 scale. 111

3.6. Spatial distribution of actual ET where the polygons show the representative areas falling within each synoptic station. The number inside each polygon is the volume of annual water loss from each area in km^3. 112

4.1. Seasonal wet enviornment ET in mm (Priestley and Taylor equation) of: (a) DJF (Dec, Jan, Feb), (b) MAM (Mar, Apr, May), (c) JJA (Jun, Jul, Aug), and (d) SON (Sep, Oct, Nov). 160

4.2. Annual Evapotranspiration of the modified GG model: (a) actual values in mm and (b) relative difference between ET and E_{TZhang} (Zhang et al., 2010) in %. 161

4.3. Spatial distribution of the Water Surplus (S): (a) annual values in mm and (b) anomalies between estimates of Fekete et al. (2000) and those of present study in mm. 162

4.4. The annual cycle of water budget components in the: (a) Globe, (b) Northern Hemisphere, and (c) Southern Hemisphere. 163

4.5. The latitudinal patterns of the water budget components and ET/P ratios (solid line) compared to those of Baumgartner and Reichel (1975) study (dashed line). 163

4.6. Annual anomalies of ET for: (a) HADGEM-2050, (b) CGCM-2050, (c) HADGEM-2080, and (d) CGCM-2080 models, and annual anomalies of Water Surplus (S) for: (e) HADGEM-2050, (f) CGCM-2050, (g) HADGEM-2080, and (h) CGCM-2080 models. 164

4.7. The difference in water surplus per capita ratios (S/capita) in percentage between the 2050s period and the baseline scenarios of: (a) the CGCM and (b) the HADGEM models. 165

CHAPTER 1

INTRODUCTION

A reliable estimate of Evapotranspiration (ET) in river basins is truly important for the purpose of water resources planning and management. The ET represents a significant portion of the rainfall in the water balance especially in semi-arid regions where most rainfall is typically lost as ET (FAO, 1989). Therefore, the uncertainty in estimating ET can lead to the inaccurate prediction of water balance and water resources needs. Generally, the concept of potential ET (ETP) is widely used by hydrologists, meteorologists, and agronomists. ETP was first introduced by Thornthwaite (1948) as the maximum ET from a large area covered completely and uniformly by plant if water supply is abundant. In water resources systems, the concept of potential ET (ETP) is widely used to indicate the climate driven water demand that is only governed by atmospheric conditions and not restricted by availability of water on the surface (Fortin and Seguin, 1975).

In the literature, the three classical approaches predominately used to estimate ETP are the temperature methods (e.g., Thornthwaite, 1948), radiation methods (e.g., Priestley and Taylor, 1972), and the combination methods (e.g., Penman, 1948). The combination methods are the most data intensive approaches whereas temperature methods are the least. Among all methods to estimate ETP, the Food and Agriculture Organization (FAO) version of the Penman-Monteith (P-M) equation (Allen et al., 1998) is currently considered to be the best method (Walter et al., 2000). Yet, the applicability of the P-M equation for hydrological purposes has many limitations (Morton, 1994). The

ETP is often estimated by meteorological data that are not necessarily measured under potential (Brutsaert, 1982) and required physical (Shuttleworth, 2006) conditions.

Typically, these classical methods are mainly applicable to predict crop ET from crop covered areas during the growing seasons to manage agricultural water demands. Crop ET is nothing but the potential ET multiplied by an applicable crop coefficient (Allen et al., 1998), which is called the two-step approach. These crop coefficients were specifically computed for water unstressed plant in humid environments. While the first condition is often unwarranted, extrapolation of the coefficients to arid and semi-arid climates is therefore doubtful (Mawdsley and Ali, 1985; Shuttleworth and Wallace, 2009).

However, actual water loss from the land surface is not restricted to crop areas only; instead evaporation happens from open water bodies as well as from open land surfaces with minimal vegetation cover. In water resources planning, the important estimate needed is the total water loss from the land surface that may or may not include transpiration from crop areas. More importantly, as the use of such methods does require detailed land cover/land use data and information, this will make applying such methods at global or even regional scale a daunting, if not impossible, task given the amount of field data collected and uncertainties inherent in the data to the methods. Another good example of such limitations to the methods will be the prediction of ET under the upcoming climate change projections where expected land cover/land use changes have not yet been predicted.

In contrast, the complementary methods, including the Complementary Relationship Areal ET (CRAE) method of Morton (1983), Advection-Aridity (AA) method developed by Brutsaert and Stricker (1979), and Granger and Gray (GG) method by Granger and Gray (1989), have the potential to provide competitive alternatives to calculate ET using only meteorological data in a diverse set of physical and climatic conditions.

The complementary methods offer simple, practical, and physically-based operational ET estimates at regional scale (Morton, 1983). The methods also consider the surrounding climatic conditions regardless of the underlying soil-plant system, avoid locally calibrated coefficients (Sophocleous, 1991), and require minimal meteorological data typically monitored in most rural areas (Hobbins et al., 2001; Nash, 1989). One other attractive feature of the complementary methods is the ability to use in climate change studies because the global climate models typically predict precipitation and temperature forecasts.

Do complementary methods have limitations? The answer is yes. As Morton (1983) summarized, the methods are best for weekly or monthly estimates but not for intervals of three days or less (see Armstrong et al., 2008; Doyle, 1990). In comparison, water resources studies focus on seasonal or annual estimates at regional scale as opposed to daily, local estimates. The methods cannot be used near sharp environmental discontinuities such as the edge of an oasis. Since an oasis effect is eliminated after 300 m (Davenport and Hudson, 1967), the impact of such discontinuities is limited. As for advantages, these methods do not require the knowledge of the soil-plant system, land use/cover, and terrain slope, which may affect the runoff coefficients that, in turn, could influence localized ET (Xu and Singh, 2005).

The concept of the complementary theory was initially introduced by Bouchet (1963) and states the presence of a complementary relationship between ET and ETP estimates. The methods also introduce a new concept named the wet environment ET (ETW) which is the ET that would occur if the soil-plant system is saturated and then ET could approach its potential rate, ETP (Granger, 1989). Simply, as the surface dries, areal ET decreases causing a decrease in humidity and an increase in temperature of the surrounding air at the same time, and as a result ETP will increase. This means that ETP is a function of ET in contrast to the model suggested by Penman (1948) where ETP is independent of ET. This latter claim is true for large moist areas when the effect of ET on temperature and humidity is fully developed and ET and ETP are equal, and for small moist areas in which the effect of ET is insignificant (Morton, 1983).

For several decades, the complementary methods have been studied and compared to other methods over diverse environments including different spatial and temporal scales and climates. Initially, the proper spatial scale of the Bouchet hypothesis was investigated by Fortin and Seguin (1975). Under spectrum of climates, the complementary relationship was found to be regionally valid over the conterminous United States (Hobbins et al., 2004) and the Volta Basin of West Africa (Oguntunde et al., 2005), but ET estimates have to be verified. For smaller scales in space and time, the complementary methods failed to estimate ET in semi-arid regions of Canada (Granger and Gray, 1990) and Northwestern China (Lemeur and Zhang, 1990) but not in an Irish humid basin (Doyle, 1990). Hobbins et al. (2001) evaluated the CRAE and AA methods for 139 basins in the United States. They found that as aridity increases, the CRAE method tends to overestimate ET and the AA method tends to underestimate ET. Xu and

Singh (2005), however, evaluated the three complementary methods for three sites of diverse climates and found that the predictive power of the three methods increases with humidity. In conclusion, previous studies had attempted to use the complementary methods with little success given the limited understanding of the methods and the confusion due to the definitions of various terms.

While the complementary methods have the potential to estimate actual ET with minimal data requirements, there are few limitations in predicting ET in a reliable and consistent manner for different spatial and temporal scales and hydrologic and climatic conditions. Given these conditions, this dissertation aims at assessing ET estimation using the complementary methods, improving the methods to better predict the regional ET, comparing the methods to the existing classical methods, and exploring the applicability of the methods at global scale in the context of climate change.

The research objectives to be achieved are summarized in the following questions: (1) What are the relative accuracies between the different complementary methods in predicting ET compared to measured data? (2) Does the performance of each method depend on the prevailing climate? (3) What improvements should be made in the complementary methods to better predict ET? (4) Can any of the complementary methods be modified to develop a single step ET prediction model (without local calibration) with the same advantages but can be used in a variety of physical and climatic conditions? (5) How reliable is such a modified model to predict ET at country scale such as Ghana where data are limited and climate variability is significant? (6) How close will be those estimates compared to the estimates from the existing classical methods? (7) Is there evidence to suggest that the complementary methods provide a regional-scale (or an areal) estimates of ET? (8) Is it possible to apply the methods at higher scale? What is the impact on the other components of the water budget? (10) Can the methods be used to assess climate change impacts? The dissertation consists of five chapters; Chapter 1 is the introduction, Chapter 5 includes the overall summary and conclusions, and the research questions will be addressed in the middle three chapters. The first four questions have been addressed in Chapter 2, questions (5) through (7) will be answered in Chapter 3, and Chapter 4 has addressed questions (8) through (10).

The aim of Chapter 2 is to develop a universal method incorporating complementary relationships that can be used in calculating regional ET with meteorological data in contrasting physical and climatic conditions. First, the validity of the three original complementary methods should be addressed under different climatic conditions in a scientifically justifiable manner. For this purpose, tens of FLUXNET global sites (Baldocchi et al., 2001) with measured meteorological and ET data are used to further evaluate the applicability of the complementary methods. The selection was based on data availability and climate variability. To classify the climatic conditions prevailing at each site, a simple aridity index developed by De Martonne (1925) is chosen. This index is widely used in hydrologic modeling as it indicates the availability of both water and energy in a simple way. The performance indicators used to explore the deviations between the model predictions and EC measurements are root mean square error (RMSE), absolute mean bias (BIAS), and coefficient of determination (R^2). As mentioned earlier, previous studies show that there is room for improvement to the complementary methods. Therefore, further review and test to the methods have to be conducted such that necessary modifications can be made. In this work, therefore, different combinations (variations) of model equations and their parameters are investigated to develop a set of potential models to improve ET predictions under variety of climatic conditions. Given the broad breadth and flexibility captured in these model variations, it is possible to assess the contribution of each model to the ET prediction such that the best model can be identified. Model calibration is typically used to improve the predictive power of the complementary methods too (see Hobbins et al., 2001 and Han et al., 2011). However, optimized models usually are locally calibrated with a set of coefficients that can be only applied to other areas of similar conditions and sometimes under specific circumstances (e.g., Xu and Singh, 2005). On the other hand, the purpose of this work is to develop a universal model independent of local calibration to estimate ET in diverse climates and environmental conditions using minimal data.

In Chapter 3, the purpose is to demonstrate the applicability of the proposed universal model in comparison to the classical methods. The study area consists of Ghana that has different climatic classes consisting of humid to semi-arid and a variety of land use patterns from traditional crop farming to forest. Daily meteorological data from ten synoptic stations between 2000 and 2005 are used.

There are many classical methods to estimate ET that are common among agronomists and hydrologists (see Jensen et al., 1990). Most of these methods are applied to calculate irrigation water requirements. In this work, four common classical methods are selected; American Society of Civil Engineers (ASCE) method (Allen et al., 2005), Hargreaves et al. (1985), Turc (1961), and Jensen and Haise (1963). The ASCE is the most recent and reliable method widely used all over the world which is basically P-M equation (Allen et al., 1998). The Hargreaves method is the alternative method suggested by Allen et al. (1998) when minimal data such as temperature is only available. Furthermore, the Hargreaves method was constructed using data from West Africa and grass as the crop reference (Hargreaves et al., 1985). The Turc method is a radiation method that was developed for Western Europe under humid climates for grass reference (Jensen et al., 1990). Although the Jensen and Haise method is a radiation method that was empirically developed for well-watered crops in the western United States, but it considers alfalfa to be the reference crop (Jensen et al., 1990). Thereby, the selection of these methods might capture the variability of classical methods in many aspects; methodology appropriateness, data requirement, and climate diversity.

Crop ET from the ASCE method is calculated following the procedure described by Allen et al. (1998) and the crop coefficients of the same source. Since the growing stages of each crop vary by region and climate, the data provided by Allen et al. (1998) cannot be directly used. Therefore, the detailed data published by the FAO for Ghana and Western Africa are used in this study. In the FAO database, the growing season for each crop is locally adapted to suit the four major agro-ecological zones of Ghana; namely Guinea Savannah zone, Transitional zone, Rain Forest zone, and Coastal Savannah zone. In addition to the cropping calendar of each crop, the other key information needed is the cropping pattern across Ghana. The distribution of each crop in all 138 districts in 2008 was made available from the Ministry of Food and Agriculture, Ghana to determine the cropping pattern across Ghana. The actual ET estimate of the proposed model can be easily compared to the predictions of crop ET from the classical methods. In addition, correlations and trends can be clearly identified.

In Chapter 4, the applicability of the proposed model to reliably predict regional ET at global scale is examined and compared to results of previous studies. In addition, the impacts of climate change on ET and water surplus are evaluated. The world water budget had been studied for some time (Budyko et al., 1962; FAO, 1973; Baumgartner and Reichel, 1975). The need for worldwide estimates of hydrological processes increases for the purpose of planning and management of water resources when demand for water increases with population growth. The major water fluxes of terrestrial water budget comprises of precipitation, ET, and runoff (Thornthwaite, 1948; Baumgartner and Reichel, 1975). Independent estimation of ET, therefore, is the challenging task in the water balance calculations (Zhang et al., 2010) given that 60-65% of the global precipitation is lost as ET (Brutsaert, 1982) and the fact that precipitation and runoff can be easily measured.

Currently, remote sensing techniques are used in predicting ET at large spatial scales. However, upscaling the estimates of such methods to a global scale has many difficulties that cannot be neglected. These difficulties include; remote sensing estimates always need secondary data that are not globally available, extending local or even regional parameterizations to a global scale is questionable, tower fluxes data should be checked for quality, coverage, and appropriateness of use, and the empirical upscaling of tower local measurements to global scale is sometimes unacceptable (Jimenez et al., 2011). In conclusion, global scale studies require “simplified formulations that are adapted to the existing global data sets and are also robust in the face of the data uncertainties” (Jimenez et al., 2011).

As mentioned earlier, classical methods presently available can estimate potential ET whereas estimating actual ET requires detailed local data such as land cover/land use, crop pattern, growing cycle, etc. Given the obvious data limitations worldwide especially in rural river basins, classical methods are difficult to use global scale and therefore only few ET studies are available presently (e.g., Zhang et al., 2010). Still the complementary methods offer a distinct advantage over the classical methods given the simplicity, ready availability of data, and the ability to estimate total water loss as opposed to crop ET. Another attractive feature of the complementary methods is the applicability in evaluating climate change driven impacts since general circulation models predict meteorological information such as temperature and precipitation that are key inputs to the complementary methods.

The meteorological data of New et al. (1999) are selected in this study for many reasons. The use of 30 minutes resolution data is still good enough for studies of global scale and data are accessible as global grids that can be easily imported into GIS applications. Furthermore, other datasets used such as runoff (Fekete et al., 2000) and soil moisture (Fan and van den Dool, 2004) have 30 minutes resolution. ET is estimated using the meteorological data on grid-by-grid basis of calculations. Once the worldwide ET maps are developed, water surplus which was defined by Thornthwaite (1948) to be the difference between precipitation and ET can also be produced. Water surplus here represents the excess water available for uses other than ET and simply can be runoff and/or groundwater recharge. In the context of climate change, climatological normal for two global climate models, CGCM3.1 and HADGEM1) are selected with A1B emission scenario for two time periods; 2050s (2040-2069) and 2080s (2070-2099). Since data of spatial resolution of 30 minutes are used, downscaled ClimGen data (Mitchell and Osborn, 2005) are made available and easily downloaded (Ramirez and Jarvis, 2008) as gridded data that can be imported into the GIS environment. It should be mentioned that Pattern-scaling method is used in downscaling GCM projections (Mitchell and Osborn, 2005). Parameterization techniques are used to predict missing downscaled data following the procedure described by Allen et al. (1998) and others. ModelBuilder tool enabled by the GIS environment was used in building the model to predict ET and water surplus.

In summary, this research provides: 1) an assessment of the applicability of the complementary methods to estimate total water loss, 2) a universal ET model that can estimate regional ET under different physical and climatic conditions without calibration and using meteorological data only, 3) a comparison of the proposed ET model to existing classical ET methods to assess broader applicability, and 4) the global application to the proposed model to assess water resources under existing and climate change scenarios.

References

Allen, R.G., Pereira, L.S., Raes, D., Smith, M., 1998. Crop evapotranspiration: Guidelines for computing crop water requirements. FAO Irrig. and Drain. Paper No. 56, Food and Agric. Orgn. of the United Nations, Rome, Italy.

Allen, R.G., Walter, I.A., Elliot, R., Howell, T., Itenfisu, D., Jensen M. (Eds), 2005. The ASCE Standardized Reference Evapotranspiration Equation. American Society of Civil Engineers Environmental and Water Resource Institute (ASCE-EWRI).

Armstrong, R.N., Pomeroy, J.W., Martz, L.W., 2008. Evaluation of three evaporation estimation methods in a Canadian prairie landscape. Hydrol. Process. 22, 2801-2815.

Baldocchi, D., Falge, E., Gu, L., Olson, R., Hollinger, D., Running, S., Anthoni, P., Bernhofer, C., Davis, K., Evans, R., Fuentes, J., Goldstein, A., Katul, G., Law, B., Lee, X., Malhi, Y., Meyers, T., Munger, W., Oechel, W., Paw, U.K.T., Pilegaard, K., Schmid, H.P., Valentini, R., Verma, S., Vesala, T., Wilson, K., Wofsy, S., 2001. FLUXNET: A new tool to study the temporal and spatial variability of ecosystem-scale carbon dioxide, water vapor, and energy flux densities. Bull. Am. Meteorol. Soc. 82, 2415-2434.

Baumgartner, A., Reichel, E., 1975. The world water balance: mean annual global, continental and maritime precipitation, evaporation and runoff, first ed. Elsevier Science Pub. Co., New York.

Bouchet, R.J., 1963. Evapotranspiration reelle ET potentielle, signification climatique. Int. Assoc. Sci. Hydrol. Pub. 62, 134-142.

Brutsaert, W., 1982. Evaporation into the Atmosphere: Theory, History, and Applications. D. Reidel Publishing Company, Dordrecht, Holland.

Brutsaert, W., Stricker, H., 1979. An advection aridity approach to estimate actual regional evaporation. Water Resour. Res. 15(2), 443-450.

Budyko, N.I., Efimova, Zubenok, L.I., Strokina, L.A., 1962. The heat balance of the earth’s surface. Izv. Akad. Nauk. SSSR. Ser. Geogr. Geofiz. 1, 6-16 (in Russian).

Davenport, D.C., Hudson, J.P., 1967. Changes in evaporation rates along a 17-km transect in the Sudan Gezira. Agric. Meteorol. 4, 339-352.

De Martonne, E., 1925. Traité de Géographie Physique, tome 1, Fourth ed. A. Colin, Paris.

Doyle, P., 1990. Modelling catchment evaporation: An objective comparison of the Penman and Morton approaches. J. Hydrol. 121, 257-276.

Fan, Y., van den Dool, H., 2004. Climate Prediction Center global monthly soil moisture data set at 0.5° resolution for 1948 to present. J. Geophys. Res. 109, D10102.

Fekete, B., Vorosmarty, C., Grabs, W., 2000. Global composite runoff fields on observed river discharge and simulated water balances. Water System Analysis Group, University of New Hampshire and Global Runoff Data Centre, Koblenz, Germany.

Food and Agriculture Organization (FAO), 1973. Man's influence on the hydrological cycle. Irrigation and Drainage Paper, Special Issue No. 17. Food and Agriculture Organization, Rome, Italy.

Food and Agriculture Organization (FAO), 1989. Arid zone forestry: A guide for field technicians. Food and Agriculture Organization of the United Nations, Rome, Italy.

Fortin, J.P., Seguin, B., 1975. Estimation de I'ETR regionale a partir de IETP locale: Utilization de la relation de Bouchet a differentes echelles de temps. Ann. Agron. 26(5), 537-554.

Granger, R.J., 1989. A complementary relationship approach for evaporation from nonsaturated surfaces. J. Hydrol. 111, 31-38.

Granger, R.J., Gray, D.M., 1989. Evaporation from natural nonsaturated surfaces. J. Hydrol. 111, 21-29.

Granger, R.J., Gray, D.M., 1990. Examination of Morton's CRAE model for estimating daily evaporation from field-sized areas. J. Hydrol. 120, 309-325.

Han, S., Hu, H., Yang, D. Tian, F., 2011. A complementary relationship evaporation model referring to the Granger model and the advection–aridity model. Hydrol. Process. 25, 2094-2101.

Hargreaves, G.L., Hargreaves, G.H., Riley, J.P., 1985. Agricultural benefits for Senegal River Basin. ASCE J. Irrig. and Drain. Engr. 111(2), 113-124.

Hobbins, M.T., Ramirez, J.A., Brown, T.C., 2004. Trends in pan evaporation and actual evapotranspiration across the conterminous U.S.: Paradoxical or complementary? Geophys. Res. Lett. 31(L13503), 1-5.

Hobbins, M.T., Ramirez, J.A., Brown, T.C., Claessens, L.H., 2001. The complementary relationship in estimation of regional evapotranspiration: The Complementary Relationship Areal Evapotranspiration and Advection-Aridity models. Water Resour. Res. 37(5), 1367-1387.

Jensen, M.E., Burman, R.D., Allen, R.G., 1990. Evapotranspiration and Irrigation Water Requirements. ASCE Manuals and Reports on Engineering Practice No. 70, Am. Soc. Civil Engr., New York.

Jensen, M.E., Haise, H.R., 1963. Estimating evapotranspiration from solar radiation. ASCE J. Irrig. Drain. Div. 89, 15-41.

Jimenez, C., Prigent, C., Mueller, B., Seneviratne, S.I., Mccabe, M.F., Wood, E.F., Rossow, W.B., Balsamo, G., Betts, A.K., Dirmeyer, P., Fisher, J.B., Jung, M., Kanamitsu, M., Reichle, R.H., Reichstein, M., Rodell, M., Sheffield, J., Tu, K., Wang, K., 2011. Global intercomparison of 12 land surface heat flux estimates. J. Geophys. Res. 116, D02102.

Lemeur, R., Zhang, L., 1990. Evaluation of three evapotranspiration models in terms of their applicability for an arid region. J. Hydrol. 114, 395-411.

Mawdsley, J.A., Ali, M.F., 1985. Modelling nonpotential and potential evapotranspiration by means of the equilibrium evaporation concept. Water Resour. Res. 21(3), 383-391.

Mitchell, T.D., Osborn, T.J., 2005. ClimGen: a flexible tool for generating monthly climate data sets and scenarios. Tyndall Centre for Climate Change Research, Norwich.

Morton, F.I., 1983. Operational estimates of areal evapotranspiration and their significance to the science and practice of hydrology. J. Hydrol. 66, 1-76.

Morton, F.I., 1994. Evaporation research - a critical review and its lessons for the environmental sciences, in: Critical Reviews in Environmental Science and Technology 24(3), Taylor and Francis Group, London, U.K., pp. 237-280.

Nash, J.E., 1989. Potential evaporation and the complimentary relationship. J. Hydrol. 111, 1-7.

New, M., Hulme, M., Hones, P., 1999. Representing twentieth-century space-time climate variability. Part I: Development of a 1961-90 mean monthly terrestrial climatology. Am. Meteorol. Soc. 12, 829-856.

Oguntunde, P.G., Van de Giesen, N., Andreini, M., 2005. Modeling regional evapotranspiration in the Volta Basin, West Africa: Testing the complementary relationship hypothesis. International Agricultural Research for Development Conference, Stuttgart-Hohenheim, Germany.

Penman, H.L., 1948. Natural evaporation from open water, bare soil, and grass. Proc. Roy. Soc. London A193, 120-146.

Priestley, C.H.B., Taylor, R.J., 1972. On the assessment of surface heat flux and evaporation using large-scale parameters. Month. Weather Rev. 100, 81-92.

Ramirez, J., Jarvis, A., 2008. High resolution statistically downscaled future climate surfaces. International Center for Tropical Agriculture (CIAT). CGIAR Research Program on Climate Change, Agriculture and Food Security (CCAFS). Cali, Colombia.

Shuttleworth, W.J., 2006. Towards one-step estimation of crop water requirements. Trans. ASABE. 49(4), 925-935.

Shuttleworth, W.J., Wallace, J.S., 2009. Calculating the water requirements of irrigated crops in Australia using the Matt-Shuttleworth approach. Trans. ASABE. 52(6), 1895-1906.

Sophocleous, M.A., 1991. Combining the soil water balance and water-level fluctuation methods to estimate natural groundwater recharge: practical aspects. J. Hydrol. 124, 229-241.

Thornthwaite, C.W., 1948. An approach toward a rational classification of climate. Geographical Review 38(1), 55-94.

Turc, L., 1961. Estimation of irrigation water requirements, potential evapotranspiration: a simple climatic formula evolved up to date. Ann. Agron. 12, 13-49.

Walter, I.A., Allen, R.G., Elliott, R., Mecham, B., Jensen, M.E., Itenfisu, D., Howell, T.A., Snyder, R., Brown, P., Echings, S., Spofford, T., Hattendorf, M., Cuenca, R.H.,Wright, J.L., Martin, D., 2000. ASCE standardized reference evapotranspiration equation, in: Evans, R.G., Benham, B.L., Trooien, T.P. (Eds.), Proc. National Irrigation Symposium ASAE. Phoenix, AZ. pp. 209-215.

Xu, C.Y., Singh, V.P., 2005. Evaluation of three complementary relationship evapotranspiration models by water balance approach to estimate actual regional evapotranspiration in different climatic regions. J. Hydrol. 308, 105-121.

Zhang, K., Kimball, J.S., Nemani, R.R., Running, S.W., 2010. A continuous satellite-derived global record of land surface evapotranspiration from 1983 to 2006. Water Resour. Res. 46, W09522.

CHAPTER 2

IMPROVING COMPLEMENTARY METHODS TO ESTIMATE EVAPOTRANSPIRATION UNDER VARIETY OF CLIMATIC AND PHYSICAL CONDITIONS

Abstract

Reliable estimation of evapotranspiration (ET) is important for the purpose of water resources planning and management. Complementary methods, including Complementary Relationship Areal Evapotranspiration (CRAE), Advection-Aridity (AA), and Granger and Gray (GG) methods, have been used to estimate ET because these methods are simple and practical in estimating ET at regional scale, using meteorological data only. However, prior studies have found limitations in the methods especially in contrasting climates. This study aims to develop a universal method incorporating complementary relationships that can be used in calculating regional scale ET with meteorological data in contrasting climatic and physical conditions. This work used 34 FLUXNET sites across the globe where eddy covariance (EC) fluxes of ET are available. A total of 39 model variations from the original complementary methods were proposed. Further analysis using statistical methods and simplified climatic class definitions produced one distinctly improved model based on the GG method when Priestley-Taylor equation is used to calculate the wet environment ET. The proposed model produced a single-step ET formulation with results equal or better than the recent studies using data-intensive, classical ET methods. Average root mean square error (RMSE), mean absolute bias (BIAS), and R^2 across 34 global sites were 20.57 mm/month, 10.55 mm/month and 0.64, respectively. The proposed model showed a step forward toward predicting ET in

large river basins with limited data to help assess water resources in a variety of physical and climatic conditions.

2.1 Introduction

In a recent research cooperative project with the International Water Management Institute, groundwater resources of northern Ghana was to be evaluated under climate change scenarios. Upon careful screening of available meteorological, land use/land class, and related hydrologic data suggested that *ET*, which is critical in any hydrologic analysis, is almost impossible to calculate given the limited data available in a large region such as the Volta Basin of northern Ghana. Data limitations in a rural river basin such as the Volta region highlighted the importance of using alternate methods as opposed to classical methods of calculating *ET* using land use/land cover data. Complementary methods initially proposed by *Bouchet* [1963] and others are potential candidate methods that can be used to calculate *ET* using meteorological data such as relative humidity, temperature, and sunshine hours.

There are several classical methods presently available to estimate potential *ET* whereas estimating actual *ET* requires detailed local data such as land cover/land use, crop pattern, growing cycle, etc. Typically, these classical methods are mainly applicable to predict crop *ET* from crop covered areas during the growing seasons to manage agricultural water demands. Crop *ET* is nothing but the potential *ET* multiplied by an applicable crop coefficient, which is sometimes called the two-step approach [*Allen et al.*, 1998]. However, actual water loss from the land surface is not restricted to crop areas only; instead evaporation happens from open water bodies as well as from open land surfaces with minimal vegetation cover. *Chen and Hu* [2004] showed that shallow groundwater contributes to *ET* at the surface. In water resources planning, the important estimate needed is the total water loss from the land surface that may or may not include transpiration from crop areas.

For several decades, complementary methods, including the CRAE [*Morton,* 1983], AA [*Brutsaert and Stricker,* 1979], and the GG [*Granger and Gray*, 1989] methods, have been used to estimate *ET*. These methods are attractive due to simplicity, practicability, and reliability in estimating *ET*, wet environment *ET* (*ETW*), and potential *ET* (*ETP*) at regional scale using meteorological data only. Previous studies attempted to use the complementary methods with little success given the limited understanding of the methods and the confusion due to the definitions of various terms. Still the complementary methods offer a distinct advantage over the classical methods given the simplicity, ready availability of data, and the ability to estimate total water loss as opposed to crop *ET*.

Model building and validating using the complementary methods cannot be conducted without the use of *ET* measurements. As a part of this study, it was important to use measured *ET* data for model validation. Typically, two approaches are commonly used to measure *ET*. The oldest and probably the most accurate is the use of lysimeters where the results are typically used in estimating irrigation water requirements [*Hipps and Kustas*, 2001]. Another popular approach is the eddy covariance (EC) method that uses surface energy fluxes for weather forecasting, irrigation scheduling, and hydrologic modeling [*Chavez et al.*, 2009]. Those fluxes include net radiation (R_n), soil heat flux (G_{soil}), sensible heat (H), and latent heat (LE). Although weighing lysimeter is considered to be the most accurate method to measure *ET*, yet EC method outperforms it in many aspects. An EC system is attractive given the low cost for equipment, simplicity in operation, minimal physical disturbance, and the availability of a sound theoretical basis with minimum experimental parameters while capturing the areal fluxes within the footprint area [*Wang et al.,* 2008; *Luo et al.,* 2010]. Most importantly, EC data are freely accessible worldwide, for example, FLUXNET (http://www.fluxnet.ornl.gov/fluxnet/index.cfm) which is a global network of micrometeorological sites that use EC methods to measure land-atmosphere exchange of carbon dioxide, water vapor, and energy fluxes [*Baldocchi et al.*, 2001]. FLUXNET comprises of tens of free-access regional networks such as AmeriFlux (http://public.ornl.gov/ameriflux/dataproducts.shtml#), AsiaFlux (http://www.asiaflux.net/), EuroFlux (http://gaia.agraria.unitus.it/newtcdc2/IMECC-TCDC_home.aspx), CarboAfrica (http://gaia.agraria.unitus.it/newtcdc2/CarboAfrica_home.aspx), and OzFlux (http://www.ozflux.org.au/index.html).

The major limitation of the EC methods is the lack of energy balance closure ($H + LE \neq R_n - G_{soil}$) that causes underestimation of *ET*. This shortcoming can be overcome by the use of different forcing closure techniques [*Twine et al.,* 2000; *Wang et al.,* 2008]. The energy imbalance may often underestimate the turbulent fluxes ($LE + H$) by 10-30% relative to the available energy ($R_n - G_{soil}$) [*Twine et al.,* 2000; *Castellvi et al.,* 2008]. *Wilson et al.* [2002] found that the imbalance across 22 FLUXNET sites was only about 20%. Several studies such as those conducted by *Twine et al.* [2000], *Wilson et al.* [2002], and *Chavez et al.* [2009] showed that forcing energy balance would improve EC measurements considerably. While this imbalance could be attributed to instrumental errors or missing surface energy fluxes, EC is the “primary” and “preferred” method for directly measuring *ET* [*Mauder et al.,* 2007; *Castellvi et al.,* 2008]. The question is whether the imbalance is attributed to the method itself or to the instrumentation. It was proved that RMSE and bias of *LE* sensors normally range from 35.7 to 57.1 W/m^2 and from -26.9 to 28.0 W/m^2, respectively [*Mauder et al.,* 2007]. Meanwhile, the authors mentioned that measurement accuracy can be < 5% for some sensor combinations when maintained properly. From a study at Waikato dairy farm in New Zealand in 2008, *ET* was measured by lysimeters to verify if EC-based *ET* requires closure forcing [*Kuske*, 2009]. The results did not support that hypothesis and instead EC-based *ET* measurements were, on average, higher than those of lysimeters. *Huntington et al.* [2011] found that the imbalance is < 10%, which is within the “uncertainty of measurement accuracy.” In a recent study, it was found that EC data are comparable to weighing lysimeter *ET* measurements [*Castellvi and Snyder,* 2010] when the RMSE was 23.8 W/m^2 and R^2 was 0.98. Those studies showed that the impact of energy imbalance in the EC method on *ET* estimates may not be as significant as thought earlier. The EC method is still attractive for direct measurement of *ET* fluxes and the “results of this method are often used as the inspection standard for other methods” [*Luo et al.,* 2010]. As a result, energy balance closure techniques were not considered in this study.

EC systems are currently used to calibrate, validate, and evaluate hydrologic models, particularly remote sensing models [e.g., *Chavez et al.,* 2009]. *Suleiman and Crago* [2004] estimated hourly *ET* using radiometric surface temperatures in two grassland sites in Oklahoma and Kansas and used EC systems to validate the results. In this work, the RMSE ranged from 30 to 50 W/m^2 while R^2 varied between 0.78 and 0.94.

Data from 19 AmeriFlux EC sites were used to validate the estimates of a remotely sensed *LE* modified model based on a revised Penman-Monteith equation [*Mu et al.*, 2007]. The average RMSE, bias, and R^2 of this model over the 19 sites were 27.3 W/m^2, -5.8 W/m^2, and 0.76, respectively. These results were further improved where the average RMSE, absolute bias, and R^2 over 46 AmeriFlux sites were 0.84 mm/day, 0.33 mm/day, and 0.65, respectively [*Mu et al.*, 2011]. In the study of *Kuske* [2009], the *ET* estimates based on Penman-Monteith and Priestley-Taylor equations were compared to those of the EC method. Both models were significantly overestimating high *ET* fluxes and slightly underestimating low *ET* fluxes. *Thompson et al.* [2011] tested *ET* “null” model that couples the Penman-Monteith equation to a soil moisture model at 14 AmeriFlux sites of which eight sites are used in the present study. The RMSE of the base model varied between 56 and 208 mm/month and therefore, modifications were made to improve model performance. The RMSE improved to the range of 34 to 175 mm/month.

Complementary methods to predict *ET* have not been extensively used especially using EC-based *ET*. With the exception of the work of *Ali and Mawdsley* [1987], researchers have recently started paying attention to the complementary methods to investigate the potential in estimating *ET* at regional scale and compare estimates to measurements. The monthly *ET* map of a modified Morton method over Hungary was produced using MODIS imagery [*Szilagyi and Kovacs*, 2010] and verified using three EC sites. At Bugac and Matra sites, *ET* estimates matched with EC systems. Monthly R^2 values were 0.79 and 0.80 and errors were -6 mm/year and 13 mm/year for Bugac and Matra sites, respectively. The bias ranged between -19 mm/month and 21 mm/month. At Hegyhatsal site, however, the authors found an imbalance of 44% with the EC measurements and then *ET* results were corrected accordingly. In another study, *Shifa* [2011] examined the wind speed function of the AA model using data under wet and dry conditions in Spain. For the original AA model, the RMSE was 0.55 mm/day and 0.95 mm/day for the wet and dry conditions, respectively. The author found that the AA model is performing best using calibrated wind function coefficients under wet conditions in which RMSE and R^2 were 0.4 mm/day and 0.7, respectively. *Huntington et al.* [2011] tested the AA method using data from arid shrublands in five EC sites in eastern Nevada. It was found that the RMSE, R^2, and percent bias were 13 mm/month, 0.77, and 18%, respectively. The RMSE, R^2, and percent bias of a modified AA model were 11 mm/month, 0.71, and 1%, respectively. The R^2 of the modified model was lower than that of the original model, but *ET* estimates were closer to the 1:1 line. *Han et al.* [2011] proposed an enhanced GG model for four sites under different land covers and compared the original GG model and the enhanced GG model using EC-based *ET* values. The enhanced model was better than the original GG model at three sites only. The RMSE of the enhanced GG model ranged from 3.43 to 15.02 W/m^2.

Hobbins et al. [2001] and *Xu and Singh* [2005] found limitations to the complementary methods in different physical and climatic conditions especially in arid settings. Some of these limitations lead to many questions such as; how applicable are the complementary relationship based *ET* methods? Are these methods only valid under humid climates? If these methods do not produce good results, what are the limitations in the different methods? Given these unanswered questions related to the complementary methods, it is important to address the validity of the methods under different physical and climatic conditions in a scientifically justifiable manner.

It was found that there is no single study where the *ET* estimates of the complementary methods have been extensively predicted and evaluated using EC sites at which surface and physical conditions vary significantly. To evaluate the applicability of the complementary methods and to propose suitable changes to a given model, the applicability of the model needs to be evaluated under a variety of land cover/land use classes, physical conditions, and climatic conditions. None of the previous studies have attempted to evaluate the applicability of the complementary methods under such broad conditions and even the most extensive study used a classical method for sites within the same region [e.g., *Mu et al.,* 2011]. Generally, any improvement to a complementary method-based *ET* prediction model will be valuable given the simplicity of the data requirement, ready availability of data that are mostly meteorological data, and the value of the results of such models especially for deficit regions located in the developing world. In addition, the three complementary methods, CRAE, AA, and GG, have not been cross-compared and evaluated using the EC-based *ET* measurements.

The objectives of this study are to: (1) investigate the applicability of the complementary methods in estimating *ET* in contrasting environments, (2) perform necessary revisions to the existing methods to improve estimates if necessary, and (3) using the results of these objectives, propose a global model of estimating *ET* using the complementary methods that is simple and robust, uses minimum data, and reliable to estimate *ET* in diverse climates and environmental conditions.

2.2 Existing Methods and Data

2.2.1 Complementary Relationship

Complementary methods describe the relationships between *ET*, *ETW*, and *ETP* that are correlated by the complementary theory first introduced by *Bouchet* [1963]. The theory dictates a complementary relationship between the *ET* and *ETP* estimates [*Morton*, 1983]. As shown in Figure 2.1, the complementary relationship between *ET* and *ETP* for unsaturated water supply is not necessarily linear and does not follow a particular law. In spite of the fact that *ET* is negatively correlated to *ETP*, there is no exact shape of that relationship [*Davenport and Hudson*, 1967]. *ETW*, however, is *ET* that would occur if the soil-plant surface is wet enough so that *ET* could approach its potential rate, *ETP* [*Granger*, 1989]. The three types of *ET* are related as

$$ET = 2ETW - ETP \tag{1}$$

where *ET*, *ETW*, and *ETP* are in W/m^2 in consistence with *Morton* [1983] and can be expressed in equivalent water depth (such as mm/day) if divided by the latent heat of vaporization and multiplying by the number of days in each month [*Morton*, 1983]. Equation (1) indicates that an increase in *ET* is accompanied by an equivalent decrease of *ETP*, i.e., $\delta ET = - \delta ETP$. In other words, as the surface dries, actual *ET* decreases causing a reduction in humidity and an increase in temperature of the surrounding air at the same time, and as a result *ETP* will increase.

2.2.2 CRAE Method

ETP is estimated by solving the energy balance and vapor transfer equations iteratively [*Morton*, 1983]. *Morton* [1983] calculated *ETP* by solving for the equilibrium temperature (T_P in °C) at which the energy balance and vapor transfer equations for a moist surface are equivalent. The procedure of the iterative solution is given by *Morton* [1983, Appendix C]. The energy balance equation used to estimate *ETP* is given as

$$ETP = R_T - \lambda f_T (T_P - T) \tag{2}$$

where R_T is the net radiation for soil-plant surfaces (W/m^2) at air temperature T (°C), λ is the heat transfer coefficient (mbar/°C), and f_T is the vapor transfer coefficient (W/m^2/mbar). To estimate *ETW* in equation (4), net radiation for soil-plant surfaces at T_P (R_{TP}) has to be computed first using equation (3).

$$R_{TP} = ETP + \gamma f_T (T_P - T) \tag{3}$$

$$ETW = \mathrm{b}_1 + \mathrm{b}_2 (1 + \gamma / \Delta_P)^{-1} R_{TP} \tag{4}$$

where γ is the psychrometric constant (mbar/°C), b_1 is a constant representing advection energy and equals to 14 W/m^2, b_2 is a constant that equals 1.2, and Δ_P is the rate of change of saturation vapor pressure at T_P (mbar/°C). Constants b_1 and b_2 are calibrated by climatic data in arid regions in North America and Africa as illustrated by *Morton* [1983]. The value of *ETP* from equation (2) and the value of *ETW* from equation (4) are used in equation (1) to calculate the *ET* flux of the CRAE method.

2.2.3 AA Method

In the AA method, *Penman* [1948] equation (ET_{PEN}) is used to estimate *ETP* as shown in equation (5) and equation (6).

$$ET_{PEN} = \frac{\Delta}{\gamma + \Delta}(R_n - G_{soil}) + \frac{\gamma}{\gamma + \Delta} E_a \tag{5}$$

$$E_a = 0.35(\beta + 0.54U)[(e_s - e_a) \times \mathrm{a}_1] \tag{6}$$

where Δ is the rate of change of saturation vapor pressure with T (mbar/°C), R_n is the net radiation (mm/d), G_{soil} is the soil heat flux (mm/d), E_a is the drying power of air (mm/day), β is a constant and usually equals to 1.0, U is the wind speed at 2 m above ground level (m/s), e_s is saturation vapor pressure at T (mbar), e_a is the vapor pressure of air (mbar), and a_1 is a unit conversion factor equals to 0.75 mm Hg/mbar. In order to obtain E_a in mm/day in equation (6), factor a_1 is required to convert the units of vapor pressure to mm Hg. In the *Penman* [1956] formula of wind function, constant β is updated to 0.5. Although both wind function formulae (when β = 1 or 0.5) are widely used in hydrology, Penman preferred β of 1 over 0.5 [*Thom and Oliver,* 1977]. The first term of equation (5) is usually called equilibrium *ET* and the second is the aerodynamic *ET* that is generated by large scale advection effects. When advection is minimal, the interactions of atmosphere with the soil-plant system will be completely developed and will be approaching an equilibrium condition [*Brutsaert and Stricker,* 1979].

ETW of the AA method is calculated using the *Priestley and Taylor* [1972] equation (ET_{PT}) in which minimal advection occurs as shown in equation (7).

$$ET_{PT} = \alpha \frac{\Delta}{\gamma + \Delta}(R_n - G_{soil}) \tag{7}$$

where α is the well-known coefficient of ET_{PT} equation that typically equals to 1.26 or 1.28. The AA method in this study has α value of 1.28 and β value of 1. The value of *ETP* from equation (5) and the value of *ETW* from equation (7) are used in equation (1) to calculate the *ET* fluxes of the AA method.

2.2.4 GG Method

The complementary relationship given in equation (1) is primarily used by CRAE and AA methods. In the GG method, *Granger and Gray* [1989] adopted a modified version that is given in equation (8). Equation (8) could be reduced to equation (1) only when $\gamma = \Delta$. The theory behind this argument in the GG method is given by *Granger* [1989].

$$ET = (1 + \frac{\gamma}{\Delta})ETW - \frac{\gamma}{\Delta}ETP \tag{8}$$

In this method, two new concepts were identified and empirically correlated together; the relative drying power (*D*) and the relative evaporation (*G*) shown in equation (9) and equation (10), respectively.

$$D = \frac{E_a}{E_a + (R_n - G_{soil})} \tag{9}$$

$$G = \frac{ET}{ETP} \tag{10}$$

D indicates the dryness of the surface, i.e., *D* becomes larger as surface becomes dryer. *G* is *ET* that occurs under similar wind and humidity conditions from a saturated surface at its actual temperature [*Granger and Gray,* 1989].

In the first work by the authors, *G* was defined as G_1 through equation (11) where this equation was empirically derived using data from two stations in a semi-arid region of western Canada. *Granger and Gray* [1989] claimed that it is independent of land use.

$$G_1 = \frac{1}{c_1 + c_2 e^{c_3 D}} \tag{11}$$

where c_1 = 1.0, c_2 = 0.028, and c_3 = 8.045. Equation (11) was later modified by *Granger* [1998] to account for different surface conditions as shown in equation (12).

$$G_2 = \frac{1}{c_4 + c_5 e^{c_6 D}} + c_7 D \tag{12}$$

where c_4 = 0.793, c_5 = 0.2, c_6 = 4.902, and c_7 = 0.006. This means that G in equation (10) can be substituted by either G_1 of equation (11) or G_2 of equation (12). *ETW* required to solve equation (8) is obtained from equation (5) earlier used in the AA model. Thereafter G_1 is used in equation (10) together with equation (9) to solve for *ET* in equation (8). The final equation for *ET* of the GG method is therefore given as

$$ET = \frac{\Delta G}{\gamma + \Delta G}(R_n - G_{soil}) + \frac{\gamma G}{\gamma + \Delta G} E_a \tag{13}$$

where ET, R_n, G_{soil}, and E_a are in mm/day. Therefore, the GG method enables direct predicting of *ET* without the need for surface parameters (temperature, vapor pressure) or any prior estimate of *ETP* [*Granger,* 1989].

2.2.5 American Society of Civil Engineers (ASCE) Method

Allen et al. [2005] provided the details of the ASCE method to calculate the ASCE standardized reference *ET* (ET_{SZ}) shown in equation (14) for two reference crops, grass and alfalfa.

$$ET_{SZ} = \frac{\Delta(R_n - G_{soil}) + \gamma \frac{C_n}{T + 273} U[(e_s - e_a) \times a_2]}{\Delta + \gamma(1 + C_d U)} \tag{14}$$

where C_n and C_d are constants that change with reference crop and calculation time step and a_2 is a unit conversion factor equals to 0.10 kPa/mbar. Factor a_2 is needed as vapor pressure in equation (14) is in kPa not mbar. ET_{SZ} for grass reference crop is almost identical to the FAO version of the Penman-Monteith equation [*Allen et al.*, 1998] that is currently considered as the best method to estimate *ETP*. To differentiate R_n estimated by the ASCE method than those of the CRAE method, it is denoted R_{SZ}. C_n and C_d constants used are for short crop reference (grass) on a daily time step. The effect of G_{soil} is negligible compared to R_n specifically as the calculations are performed on a monthly basis, and therefore G_{soil} is ignored in the calculations [e.g., *Hobbins et al.*, 2001].

2.2.6 Sites of Eddy Covariance System

This study selected 34 global sites with measured meteorological and flux data and those sites are distributed around the world as follows: 17 from AmeriFlux sites, 11 from EuroFlux sites, five from AsiaFlux sites, and one CarboAfrica site (see Figure 2.2). Unfortunately, efforts to obtain data from other sites in CarboAfrica have not been successful. The selection of the 34 sites was mainly based on data availability and climate variability. The details of the sites selected and data collected are shown in Table 2.1 and Figure 2.2. The reason to select this large number of sites is that prior studies have typically used a handful of sites and in most cases under similar climatic conditions. By using a variety of global sites in contrasting physical and climatic conditions and measured *ET* data, we proposed to demonstrate the validity of the *ET* methods in a broad selection of land use/land class categories.

To classify the climatic conditions prevailing at each site, a simple aridity index developed by *De Martonne* [1925], AI_M (in mm/°C), is chosen and given by equation (15).

$$AI_M = \frac{P_{ann}}{T_{ann} + 10} \qquad (15)$$

where P_{ann} is the average annual precipitation in mm and T_{ann} is the average annual T in °C.

AI_M is found to be an accurate measure to define the prevailing climate from the six climate classes defined here and has been successfully applied in meteorological and agricultural applications [*Baltas,* 2007]. Unlike other aridity indices, AI_M indicates the availability of both water and energy from basic, readily available data. Although AI_M tends to classify the climate as more humid than it is when compared to other indices (results not shown), it is still a good index to classify the 34 sites into a number of clusters. In effect, the sites were sorted based on the following climatic classes; very humid ($AI_M \geq 35$), humid ($28 \leq AI_M < 35$), sub-humid ($24 \leq AI_M < 28$), Mediterranean ($20 \leq AI_M < 24$), semi-arid ($10 \leq AI_M < 20$), and arid ($AI_M < 10$).

As shown in Table 2.1, the 34 sites have different geographic and climatic conditions. The P_{ann} ranges from 196 mm at site 25 to 2231 mm at site 4 and the T_{ann} varies between -1.7 °C at site 3 and 26.3 °C at site 4. It is noticed that many sites fall within the very humid climatic class. The surface conditions also differ varying from grasslands to forests. Data are available from 12 to 120 months in the period from 1992 to 2010 depending on the site. At site 1, for example, 24 month data are collected in 2006 and 2007, while at site 4 there are no ET data in April 2003. Therefore, the total number of months included in the calculations from 2002 to 2005 is 47 instead of 48. Compared to the lowest value of average ET_{EC} flux (10.5 mm/month) that occurs at site 25, site 4 has a maximum value of 134.3 mm/month. It is observed that site 4 has the highest ET_{EC} fluxes across the 34 sites because the site is located in tropical peat swamp forests where soil moisture is relatively high throughout the year [*Hirano et al.*, 2005] and the site is also exposed to high energy demands. In general, the wide ranges of ET_{EC} fluxes and AI_M values reflect the diversity of hydrologic and climatic conditions covered in this study.

In addition to the energy balance closure discussed earlier in the introduction, there are other issues that have to be addressed such as the physical settings of the EC measurements. For example, the level at which the meteorological variables are monitored is not the same for all variables at each site, which is a common problem in any *ET* method [*Shuttleworth,* 2006]. To keep the effect of vertical gradient of these variables to a minimum, it is important to measure these variables at the same elevation as the heat flux measurements. Minimizing uncertainty of measurement and instrumentation errors will definitely improve model predictions and help answer many of the research questions discussed earlier with better precision.

2.2.7 Input Data

Monthly data are usually easier to collect in data-scarce areas, less problematic to process poor quality data, and more appropriate for regional-scale studies. *Thompson et al.* [2011] examined model performance using different time scales from half hourly to inter-annual and found that monthly time scale was preferable. Here data were downloaded from each EC site using its regional network website and sometimes obtained by personal communication with the primary investigator. In cases when monthly data are not readily available, average monthly data were aggregated from finer time resolution data, e.g., daily or hourly. To keep minimal changes to the input data, months of available data (50% or more) only were considered in the calculations. Moreover, negative flux rates at night such as those shown in Table 2.1 have been included in the calculations.

Input data requirements are often the driver to select a specific method to estimate *ET*. Even in rural regions where data deficits are common, data to calculate R_n from the CRAE method [*Morton*, 1983] requires monthly averages of temperature, humidity (or dew-point temperature), and sunshine hours (or solar radiation) only. Again, the CRAE method calculates two types of R_n; R_T and R_{TP} at the same time. It is obvious that the CRAE method can also estimate *ETP*, *ETW*, and *ET* using the same data used to calculate R_T, however, the AA and GG methods cannot do so without wind speed measurements.

In the ASCE method [*Allen et al.*, 2005], input data to calculate R_n (i.e., R_{SZ}) are similar to those of the CRAE method. More specifically, the ASCE method requires minimum and maximum temperature data, which sometimes are not available. In this case the procedure described by *Allen et al.* [2005, equation E.5] is followed. One of the main differences between the CRAE and ASCE methods is the albedo calculation. In the former, albedo is calculated using a set of equations whereas it is fixed to 0.23 in the latter. The ASCE method also requires wind speed measurements to calculate *ETP* while estimating crop *ET* requires detailed information about the land cover/ land use, crop cultivated, cropping pattern, growing cycle, etc. and this is beyond the scope of this study. The ASCE method is utilized to compare R_{SZ} with R_T and R_{TP} as well as to examine the complementary relationships on primary *ETP* equations as illustrated in the results.

The complementary methods compute the total water loss from the soil surface irrespective of the land cover or class. Therefore, the estimates from the complementary methods have much wider applicability in water resources than for irrigation purposes only. It should be mentioned that aggregated data used here include monthly average time series of air temperature, relative humidity, wind speed, precipitation, solar radiation, net radiation, and latent heat fluxes.

The EC measurements used for comparisons are net radiation (R_n) and latent heat flux (ET_{EC}). The performance indicators used to explore the deviations between the model predictions and EC measurements are RMSE, absolute mean bias (BIAS), and R^2. It is common to use the RMSE as the key indicator of model performance [e.g., *Mu et al.*, 2007; *Castellvi and Snyder*, 2010; *Han et al.*, 2011; *Huntington et al.*, 2011; *Thompson et al.*, 2011]. As the number of sites is large, using the absolute value of the mean bias (BIAS), which indicates the disparity of predicted and measured ET, is preferred over the mean bias value. Thereby, the distinction is made between BIAS and the actual mean bias.

2.3 Model Development and Results

Model development is conducted in three stages using the results of models in each stage compared to the EC measurements. First, the original complementary methods are evaluated across all sites. Based on the results obtained especially in predicting net radiation, a set of model variations representing the different model structures of the complementary methods will be developed. In the second stage, these models variations will be tested for accuracy in comparison to measured EC data and the results of this work will help in further narrowing the set to a suitable model(s). In the third stage, a statistical analysis will be conducted to differentiate between the final set of models capable of predicting ET in a universal manner independent of land use/cover. In essence, the approach will be to define a wide range of model variations and to narrow this set of model variations to a single universal model where at each stage, direct comparisons with measured EC data will be made.

2.3.1 Net Radiation (R_n)

Given the importance of net radiation in *ET* calculation and the availability of these data from the EC sites, a comparison of R_n estimates predicted by *Morton* [1983] and *Allen et al.* [2005] methods is made. Net radiation computed by the method of *Morton* [1983] is denoted as R_T that is the net radiation at T and R_{TP} is the net radiation at T_P. Net radiation from the *Allen et al.* [2005] method is denoted as R_{SZ}. The three estimates were compared to the R_n measurements at the EC sites and shown in Figure 2.3.

The three methods perform better as humidity increases given the fact that the number of sites within the humid climatic class is large. It is clear that the semi-arid class has the lowest performance. The reason is site 26 at which none of the methods can estimate R_n. At this site, R_{SZ} estimates are the best compared to R_T and R_{TP}. The RMSE and BIAS values of R_{SZ} estimates are high and approach 60.3 mm/month and 36.5 mm/month, respectively. In contrast, the RMSE and BIAS values of R_T at site 25 are the lowest in the semi-arid climatic class and approach 13.4 mm/month and 3.1 mm/month, respectively.

Scientifically, R_{TP} estimate at T_P developed by *Morton* [1983] has a vague physical meaning. It is noticed that R_{TP} estimates do not properly simulate R_n except in few occasions. However, the average RMSE values of R_{SZ} estimates are much better than those of R_T under almost all climates except arid (semi-arid and arid) climates. The behavior of the BIAS is similar to that of the RMSE. In general, the average RMSE value of R_T is close to that of R_{SZ} estimates given the difference is only 0.32 mm/month, similar to the average BIAS and R^2 values. The average R^2 values of R_T and R_{SZ} estimates range from 88 to 98% and from 92 to 98%, respectively. These elevated values suggest that R_T and R_{SZ} estimates explain the variation of R_n. Of all 34 sites, the RMSE of R_{SZ} estimates varies between 7.6 mm/month at site 9 and 75.7 mm/month at site 6. In summary, the average RMSE and R^2 values are marginally different for R_{SZ} than those of R_T that in turn have a lower BIAS value. While R_{SZ} is commonly used and recommended by the ASCE, R_T performs much better in arid and semi-arid regions and can be an effective indicator of net radiation across all regions.

2.3.2 Comparison to ET Values

The net radiation R_n is obviously the most important parameter in estimating *ET*. Given the discrepancy in estimating R_n, the uncertainty in *ET* predictions using the complementary methods is expected to be comparatively larger. The original complementary methods were applied to the 34 sites and the *ET* estimates were compared to the values from the EC sites (ET_{EC}) as shown in Table 2.2. It is no surprise that the sub-humid climatic class has the poorest performance as there are only two sites in this class of which site 19 has one of the poorest values of RMSE, BIAS, and R^2. For the CRAE method, the sites with arid climates have the lowest RMSE and BIAS values and sites with humid (very humid and humid) climates have the highest R^2 values. The AA method was developed for a watershed of severe drought, and therefore, it was expected to outperform the other two methods in arid climates. Yet, this claim is only valid in the semi-arid class. On one hand, *Hobbins et al.* [2001] evaluated the CRAE and AA methods for 120 basins in the United States. They found that as aridity increases, the CRAE method tends to overestimate *ET* and the AA method tends to underestimate *ET*.

On the other hand, *Xu and Singh* [2005] evaluated the three complementary methods for three sites of diverse climates and found that the predictive power of the three methods increases with humidity. This contradicts with the results shown in Table 2.2 as the CRAE and AA methods perform best under arid climates. Broadly speaking, the three methods work relatively well under extreme climatic conditions, either arid or humid. In addition, predictions of the GG method are slightly better in humid climates than arid as found by *Xu and Singh* [2005]. Overall, the CRAE method is the best according to the RMSE and R^2 values while the GG method has the lowest BIAS value.

Still, the computed *ET* estimates are not close to the ET_{EC} measurements indicating that the three complementary methods may need improvements. Since net radiation estimates are accurate enough to predict R_n, efforts are needed to improve the remaining *ET* analysis of the complementary methods.

2.3.3 Model Improvements

The results shown in Figure 2.3 clearly indicate that the accuracy of the net radiation prediction is dependent on the climatic class and therefore, any improvements in a proposed model should consider climate dependency. Selecting the correct equation to calculate *ETP*, *ETW*, and even *ET* may significantly influence the accuracy of the estimates. It is also noticed that the different methods discussed here have some similarities leading to the final calculation of *ET*.

In this work, therefore, different combinations of model equations and their parameters are considered to develop a set of potential models to improve *ET* predictions under a variety of climatic conditions. For instance, these different models can help to decide if R_T is a better estimator of net radiation compared to R_{SZ} or not. Similarly to answer if the complementary relationships are adequately presented by equation (1) or equation (8). Accordingly, 39 different *ET* models are proposed and given in Table 2.3. In selecting these different models, the criteria used were dependent on the following: the method to calculate R_n, the complementary relationship representation to calculate *ET*, the value of α in the ET_{PT} equation, the value of β in the wind function of the ET_{PEN} equation, the relative evaporation function (*G*) in the GG method, and the equations to calculate both *ETW* and *ETP* in each model.

Based on the criteria given earlier, the CRAE method produced three different models that capture the importance of R_n and the complementary relationships. With the AA method, four criteria, namely R_n, complementary relationships, α, and β, are important and therefore 16 model variations are possible. However, *Hobbins et al.* [2001] found that changes to the AA method did not necessarily produce superior results and the improvements were minor especially when the advection part of the method is perturbed by β. For these reasons, only seven model variations are proposed to the original AA method. The initial results from this study indicate that the model variations to the GG method are much better than those of the CRAE and AA methods. *ETW* of the original CRAE method is derived from the ET_{PT} equation (equation 7) that is simply adopted by the AA method to calculate *ETW* while the original GG method uses the ET_{PEN} equation [*Brutsaert and Stricker,* 1979; *Morton,* 1983; *Granger and Gray,* 1989; *Szilagyi and Kovacs*, 2010]. To test the sensitivity of the results to the different forms of calculating *ETW*, it is possible to develop 16 model variations with different *ETW* calculations. Similarly, the possibility of using either ET_{PT} or ET_{PEN} to calculate *ETW* also exists. Considering these possibilities, additional 16 model variations are developed given that β will no longer be altered. Table 2.3 therefore shows the 33 different model variation proposed from the three original complementary models. In addition, the ASCE method added six more variations to test the complementary relationships in the *ETW* and *ETP* calculations. The complete set of model variations between the three original complementary methods and the ASCE methods is 39. Given the broad breadth captured in the 39 model variations, it is possible to assess the contribution of each model to the *ET* prediction such that the best model can be identified.

For the purpose of narrowing and identifying the best model variation, each model was used at each site and key performance statistics, RMSE, BIAS, and R^2, were computed. Thereafter the best model variation for each climatic class and performance statistic was identified. For example, the lowest RMSE, lowest BIAS, or the highest R^2 for each climatic class was identified. The results are given in Table 2.4 from all 39 model variations. In the first pass, 10 models were identified to have the best average metric value for each climatic class. GG20, as an example, is considered the best for five combinations of metric and climatic class. In contrast, GG3 is the best only for RMSE for the very humid climatic class. GG1, GG3, GG11, and GG13 are the best models each for only one combination of metric and climatic class. Given the large size of ten models selected from the proposed 39 models, it is important to perform further investigations to narrow the final selection. In this process, models that showed good performance only once were eliminated reducing the total to six, namely GG7, GG14, GG18, GG20, GG22, and CRAE2.

A careful review of Table 2.3 especially a comparison between R_T and R_{SZ} shows that although the GG method originally used the complementary relationship given by equation (8) [*Granger*, 1989], yet, five of the six promising models used equation (1) instead to represent the complementary relationship. In essence, equation (1) is effective in capturing the variability of *ET* and therefore it is preferred over equation (8). It is important to observe that four of the five promising models adopted ET_{PT} equation to calculate *ETW* indicating the strong applicability of the GG method. Lastly, it seems that altering α in ET_{PT} equation and the equation describing *G* did not alter the results.

Before moving to further analysis, the results given in Figure 2.3 and Table 2.2, indicate that the six-class discretization of climatic conditions is unnecessarily complex and this sorting may be simplified further to better assess the accuracy of a proposed model. With this in mind, the subsequent analysis was restricted to three simple climatic classes: wet (very humid and humid), moderate (sub-humid and Mediterranean), and dry (semi-arid and arid). With this new definition, the original 34 global sites are now reallocated as 18, 6, and 10 into wet, moderate, and arid classes, respectively.

Figure 2.4 shows the results of all performance statics to these six models based on the new definition of climatic classes consisting of wet, moderate, and dry. For all climatic classes, CRAE2 has the highest RMSE and BIAS. GG7 perform well only in the wet climatic class, while it performs poor in moderate and dry classes. It is also noticed that GG14 could not simulate *ET* in the moderate climatic class. Overall, GG22 has the lowest median and average values of RMSE that are 16.20 and 20.23 mm/month, respectively, introducing the possibility to be the best model variation. Based on BIAS for all sites, the lowest average value is 10.55 mm/month for GG18, while the lowest median value is 7.45 mm/month for GG20. Comparing the three models together, both GG18 and GG20 have the same R^2 of 0.64 and GG22 produced a value of 0.62. It is therefore correct to state that GG18, GG20, and GG22 are the best of the six selected earlier. There is no evidence to suggest that a specific model is superior in a particular climatic class. The climate class with poorest performance is the moderate class. The reason may be the low number of sites in this class and therefore extreme values such as those of site 24 can dramatically influence the results. Also in the moderate climatic class, it is worth to mention that the GG22 model has the lowest average values of RMSE and BIAS, however, models GG18 and GG20 share the highest average value of R^2. It is also worth to note that all three models have the following similarities; the models use the GG method while using R_{SZ} to calculate net radiation, equation (1) to represent the complementary relationship, and ET_{PT} equation shown in equation (7) to compute *ETW*.

2.3.4 Model Calibration through Optimization

Model calibration is typically used to improve the predictive power of the complementary methods [e.g., *Hobbins et al.*, 2001; *Han et al.*, 2011]. However, optimized models are usually locally calibrated with a set of coefficients that can be only applied to other areas of similar conditions and sometimes under specific circumstances [e.g., *Xu and Singh*, 2005; *Shifa*, 2011]. The purpose of this section is to find if optimization could improve *ET* predictions of the six best model variations selected earlier GG7, GG14, GG18, GG20, GG22, and CRAE2. For optimization to provide improvements, the improved models through this approach should not only work in selected sites but should be applicable in a variety of physical and climatic settings. Therefore the goal of model calibration via optimization is to improve the six models to minimize RMSE and identify a single model that can be universally applied under a variety of conditions. Following *Shuttleworth* [2006], this approach consists of a “two-step *ET* estimation method." The first step is selecting the corresponding values of coefficients for the prevailing climate and second is the actual calculation of *ET*.

The coefficients optimized are as follows: b_1 and b_2 in equation (4) for the CRAE2 model, c_1, c_2, and c_3 in equation (11) for the GG18 and GG20 models, and c_4, c_5, c_6, and c_7 in equation (12) for the GG7, GG14, and GG22 models. The coefficients were optimized for each site and then the average and median values of each coefficient in the same climatic class were computed and shown in Table 2.5. These average and median values were then used again at each site to re-calculate the RMSE value for the set of coefficients specified for that particular climatic class. The final set of RMSE and BIAS values for each optimized model is compared to the values obtained from the original complementary methods and non-optimized models and the results are given in Table 2.6. It is noted that only the median values of coefficients are used in these results as similar results were obtained with average values too. It is evident that optimization did not significantly improve the results compared to the improvement already produced by the proposed six promising models except CRAE2 and, less importantly, by GG7. Sometimes, the results of the optimized model are worse than those of the original promising models. It is not surprising because the median values of the coefficients optimized for some sites greatly differ than those locally optimized at the site. The average RMSE for GG14 in the wet class, for instance, is higher than that of the optimized model. Almost seven out of the 18 sites in the wet climatic class are worse in terms of the average RMSE value. Also the poor results are obvious at sites 11, 16, and 17. In short, CRAE2 in its initial formulation has the poorest performance (see Figure

2.4), however, the optimized CRAE2 model becomes the best model in terms of RMSE and BIAS metrics (Table 2.6) and R^2 alike (not shown).

Given the additional work and complexity added through optimization and marginal improvements of the results (except CRAE2), it can be concluded that optimization of these six model variations did not produce a universal model to predict *ET* under a variety of conditions. Essentially, the focus of developing a single step prediction model for *ET* is still the desirable option to investigate. With this in mind, the subsequent work will focus on further improving the three model variations, GG18, GG20, and GG22.

2.3.5 Statistical Analysis

The applicability of the three models GG18, GG20, and GG22 was further investigated using the analysis of variance (ANOVA) to assess if these three models are similar or not [*Berthouex and Brown*, 2002]. The ANOVA test is applied to the time series consisting of 1657 estimates each of ET_{EC}, ET_{GG18}, ET_{GG20}, and ET_{GG22} and the average values across 34 sites are 35.9, 33.8, 33.2, and 32.0 mm/month, respectively. There is a marginal tendency to underestimate the average *ET* value in all three models for some reason. This similar trend among the three models is because there are only minor differences in between the models. F statistic is computed for the degree of freedom of 3 and at 95% confidence level and its value is compared to that of the F test of ANOVA. Simply, if the F test is smaller, methods are alike. In this case, $F_{3,1653,0.05}$ is found to be 2.60 [*Berthouex and Brown*, 2002, Table C in the Appendix] while the F test is 4.58. Therefore, it can be concluded that with 95% confidence, the averages of the four time series are not equal, yet, the difference cannot be identified which is one of the ANOVA test shortcomings.

For this purpose, another statistical analysis known as the Dunnet's method [*Berthouex and Brown*, 2002] was used to compare the three models to the ET_{EC} fluxes. The Dunnet's method has the advantage to answer two questions; (1) a confidence interval in which average values are alike and (2) the direction of the difference. The results of the Dunnet's method showed that at 95% confidence interval, the average *ET* is between 32.3 and 39.4 mm/month. In other words, GG22 is considered to be statistically different while the difference in each of the other two models is likely to be insignificant. Figure 2.5 shows the average *ET* estimates for 33 sites according to the climatic class. At site 4, none of the models can simulate the elevated *ET* fluxes measured therein and so this site can be ignored as it represents an extreme case in which trends of *ET* values cannot be easily captured [see *Hirano et al.*, 2005]. In general, GG22 underestimates *ET* as humidity increases. However, the scatter of data around the 1:1 line for almost all climatic classes is more pronounced in GG18 and GG20. The similarity between the GG18 and GG20 models is visible because the only difference between the two models is the coefficient α in the ET_{PT} equation that does not influence the results. In fact, GG18 has two advantages over the other two models; it has the closest average *ET* value to that of the ET_{EC} fluxes and it has the highest slope and therefore the closest to the 1:1 line (see Figure 2.5). Hence, GG18 is deemed to be the best over the six promising models developed and therefore represents the one-step estimation method proposed in this study.

In Figure 2.6, the performance indicators for GG18 are shown for each site in the three climatic classes. The R^2 values have a minor increasing trend with humidity. The R^2 values at the sites of wet climatic class mostly lie above the average value and vice versa for the sites of the dry climatic class. There is no such trend for RMSE and BIAS. However, the RMSE and BIAS values at most sites of dry climatic class lie below the average value. Again, it is emphasized that site 4 has specific issues that have to be further inspected as discussed earlier. Generally, Figure 2.6 demonstrates that GG18 is consistent and reliable among the diverse sites of the different climates with no noteworthy preference.

It is worth to mention that the average R^2 for GG18 over the wet, moderate, and dry classes are 0.72, 0.61, and 0.52, respectively. Since the *ET* fluxes in general differ between the wet and dry climates, the absolute values of RMSE may not be simply compared to each other. Instead, the RMSE value at each site was divided by the average ET_{EC} value shown in Table 2.1 so that the relative RMSE is computed and all sites can be correspondingly cross-compared. The values of the relative RMSE for GG18 range from 0.23 at site 11 to 1.59 at site 34 with an average value of 0.69.

In comparison to the outcomes of most recently published *ET* studies such as those conducted by *Han et al.* [2011], *Mu et al.* [2011], and *Thompson et al.* [2011], the results of the GG18 model in Table 2.7 are equal or even better and more reliable taking into account the wide range of physical and climatic conditions. More importantly, the *ET* estimates of GG18 outperforms the estimates of *ET* in the other studies by the minimal data requirement as well as the minimal cost and resources needed to compute reliable regional *ET* using meteorological data only. Although the two-step estimation method (optimized CRAE2) is providing slightly better results, GG18 produced through the one-step estimation method (without any optimization) is recommended due to the simplicity and straight-forward application of the model regardless of the physical and climatic conditions. As shown in Figure 2.7, it is obvious that this proposed simple model can be applied reliably and efficiently to estimate ET in data scarce areas where detailed information are not readily available.

2.4 Summary and Conclusions

Complementary methods have the potential to predict regional *ET* using minimal meteorological data. However, prior studies used small data sets representing limited climatic variability and physical conditions and were not successful in improving the methods. A few of the successful studies used locally calibrated parameters that may not have the universal applicability simply due to the two-step approach required to compute *ET*. In addition, water resources studies require the total water loss from the land surface irrespective of the land use/land class. In this regard, complementary methods provide the distinct advantage over the classical methods that only provide crop *ET* using detailed input data such as land use/land class, cropping patterns, and crop calendar. However, the state of the complementary methods is such that there is no single methodology consistently used or adapted for universal use over a wide variety of climatic and physical conditions. Most studies opt to use locally calibrated model parameters to compute *ET*. Therefore, more research is needed to improve the applicability of the complementary methods. This study is aimed at developing such a single step model using the complementary relations that require simple meteorological data only while being able to compute regional scale *ET* independent of the land use/land class.

In this work, 34 global sites with measured *ET* data via the eddy covariance method were used to develop the proposed model. The sites have different climatic and physical conditions to ensure the universal application of the proposed model. The original complementary methods consisting of CRAE, AA, and GG were first evaluated for the proposed 39 model variations based on the model structure. Climate of these sites were initially sorted to six different climatic classes based on the aridity index proposed by *De Martonne* [1925]. Initial results identified a set of six promising model variations. Calibration of the six models did not provide significant improvements to the results as the two-step approach proposed by optimization added the limitation of local applicability as opposed to universal applicability combined with additional effort. Given the complexity of using six different climatic classes, the analysis later reduced this number to three distinct climatic classes consisting of wet, moderate, and dry climates. This simplification identified three promising models from the earlier six. Statistical analyses conducted via ANOVA testing and the Dunnet method showed that two of the models are similar while one model, GG18, clearly provided different patterns and better results. Therefore the GG18 model that consists of one-step estimation method is considered the best over the two-step method (using optimization) in which the coefficients are locally calibrated. Also the comparison of results from recent studies using the complementary relationships showed that the GG18 model is capable of producing equal or better results while capturing a wide variety of physical and climatic conditions.

In the GG18 model, net radiation R_n is computed using R_{SZ}. However, both R_{SZ} and R_T estimates are able to better predict net radiation if albedo calculations can be improved. It is evident that the simple complementary relationships suggested by equation (1) can describe the behavior of *ET* fluxes better than the more generic complementary relationship of equation (8). Most importantly, the predictive power of the GG method [*Granger and Gray*, 1989] is improved when the ET_{PT} equation is used to calculate the wet environment *ET*, *ETW*. There is a strong indication that this proposed GG18 model can significantly enhance the accuracy of *ETW* calculations using the GG method and consequently to predict *ET* at regional scale using meteorological data only. Furthermore, this one-step estimation method can reliably estimate *ET* regardless of the prevailing climatic conditions. Such an estimate will unequivocally lead to reliable predictions of water resources, in particular recharge estimation and impacts due to climate change. The outcome of this study is improved estimation of *ET* with high confidence in areas where actual *ET* fluxes are not routinely monitored.

References

Ali, M. F., and J. A. Mawdsley (1987), Comparison of two recent models for estimating actual ET using only regularly recorded data, *J. Hydrol.*, *93*, 257-276, doi:10.1016/0022-1694(87)90099-0.

Allen, R.G., L. S. Pereira, D. Raes, and M. Smith (1998), Crop evapotranspiration: Guidelines for computing crop water requirements, *FAO Irrig. and Drain. Paper No. 56*, Food and Agric. Orgn. of the United Nations, Rome, Italy.

Allen, R.G., I. A.Walter, R. Elliot, T. Howell, D. Itenfisu, and M. Jensen (Eds.) (2005), *The ASCE Standardized Reference Evapotranspiration Equation*, Environment and Water Resources Institute of the Am. Soc. Civil Eng. (ASCE), Task Committee on Standardization of Reference Evapotranspiration, Final Rep., ASCE, Reston, VA.

Baldocchi, D., E. Falge, L. Gu, R. Olson, D. Hollinger, S. Running, P. Anthoni, C. Bernhofer, K. Davis, R. Evans, J. Fuentes, A. Goldstein, G. Katul, B. Law, X. Lee, Y. Malhi, T. Meyers, W. Munger, W. Oechel, U. K. T. Paw, K. Pilegaard, H. P. Schmid, R. Valentini, S. Verma, T. Vesala, K. Wilson, and S. Wofsy (2001), FLUXNET: A new tool to study the temporal and spatial variability of ecosystem-scale carbon dioxide, water vapor, and energy flux densities. *Bull. Am. Meteorol.*

Soc., 82, 2415-2434, doi:10.1175/1520-0477(2001)082<2415:FANTTS>2.3.CO;2.

Baltas, E. (2007), Spatial distribution of climatic indices in northern Greece, *Meteorol. Appl., 14*(1), 69-78, doi: 10.1002/met.7.

Berthouex, P., and L. Brown (2002), *Statistics for Environmental Engineers*, Second edition, Lewis Publishers, CRC Press LLC, Boca Raton, FL, USA.

Bouchet, R. J. (1963), Evapotranspiration reelle et potentielle, signification climatique, *Int. Assoc. Sci. Hydrol., 62*, 134-142.

Brutsaert, W., and H. Stricker (1979), An advection aridity approach to estimate actual regional evaporation, *Water Resour. Res., 15*(2), 443-450, doi:10.1029/WR015i002p00443.

Castellvi, F., and R. L. Snyder (2010), A comparison between latent heat fluxes over grass using a weighing lysimeter and surface renewal analysis, *J. Hydrol., 381*, 213-220, doi: 10.1016/j.jhydrol.2009.11.043.

Castellvi, F., R. L. Snyder, and D. D. Baldocchi (2008), Surface energy-balance closure over rangeland grass using the eddy covariance method and surface renewal analysis, *Agric. For. Meteorol., 148*, 1147-1160, doi: 10.1016/j.agrformet.2008.02.012.

Chavez, J. L., T. A. Howell, and K. S. Copeland (2009), Evaluating eddy covariance cotton ET measurements in an advective environment with large weighing lysimeters, *Irrig. Sci., 28*, 35-50, doi: 10.1007/s00271-009-0179-7.

Chen, X., and Q. Hu (2004), Groundwater influences on soil moisture and surface evaporation, *J. Hydrol., 297*, 285-300, doi: 10.1016/j.jhydrol.2004.04.019.

Davenport, D. C., and J. P. Hudson (1967), Changes in evaporation rates along a 17-km transect in the Sudan Gezira, *Agric. Meteorol., 4*, 339-352.

De Martonne, E. (1925), *Traité de Géographie Physique*, tome 1, Fourth edition, A. Colin, Paris.

Granger, R. J. (1989), A complementary relationship approach for evaporation from nonsaturated surfaces, *J. Hydrol., 111*, 31-38, doi: 10.1016/0022-1694(89)90250-3.

Granger, R. J. (1998), Partitioning of energy during the snow-free season at the Wolf Creek Research Basin, in *Proceedings of Wolf Creek Research Basin: Hydrology, Ecology, and Environment Workshop*, edited by Pomeroy, J. W., and R. J. Granger, pp. 33-44, Whitehorse, Yukon, Canada.

Granger, R. J., and D. M. Gray (1989), Evaporation from natural nonsaturated surfaces, *J. Hydrol., 111*, 21-29, doi: 10.1016/0022-1694(89)90249-7.

Han, S., H. Hu, D. Yang, and F. Tian (2011), A complementary relationship evaporation model referring to the Granger model and the advection–aridity model, *Hydrol. Process., 25*, 2094-2101, doi: 10.1002/hyp.7960.

Hipps, L., and W. P. Kustas (2001), Patterns and organization in evaporation, in *Spatial Patterns in Catchment Hydrology: Observations and Modeling*, edited by Grayson, R., and G. Bloschl, pp. 105-122, Cambridge University Press, UK.

Hirano, T., H. Segah, S. Limin, T. June, S. J. Tuah, K. Kusin, R. Hirata, and M. Osaki (2005), Energy balance of a tropical peat swamp forest in Central Kalimantan, Indonesia, *Phyton, 45*(4), 67-71.

Hobbins, M. T., J. A. Ramirez, T. C. Brown, L. H. Claessens (2001), The complementary relationship in estimation of regional evapotranspiration: The Complementary Relationship Areal Evapotranspiration and Advection-Aridity models, *Water Resour. Res., 37*(5), 1367-1387, doi: 10.1029/2000WR900358.

Huntington, J. L., J. Szilagyi, S. W. Tyler, and G. M. Pohll (2011), Evaluating the complementary relationship for estimating evapotranspiration from arid shrublands, *Water Resour. Res., 47*, W05533, doi: 10.1029/2010WR009874.

Kuske, T. J. (2009), Fluxes of energy and water vapour from grazed pasture on a mineral soil in the Waikato, M.S. thesis, The Univ. of Waikato, New Zealand.

Luo, X., K. Wang, H. Jiang, J. Sun, J. Xu, Q. Zhu, and Z. Li (2010), Advances in research of land surface evapotranspiration at home and abroad, *Sciences in Cold and Arid Regions*, *2*(2), 0104–0111.

Mauder, M., S. P. Oncley, R. Vogt, T. Weidinger, L. Ribeiro, C. Bernhofer, T. Foken, W. Kosiek, H. A. R. De Bruin, and H. Liu (2007), The energy balance experiment EBEX-2000. Part II: Intercomparison of eddy-covariance sensors and post-field data processing methods, *Bound. Layer Meteorol., 123*, 29-54, doi: 10.1007/s10546-006-9139-4.

Morton, F. I. (1983), Operational estimates of areal evapotranspiration and their significance to the science and practice of hydrology, *J. Hydrol., 66*, 1-76, doi:10.1016/0022-1694(83)90177-4.

Mu, Q., F. A. Heinsch, M. Zhao, and S. W. Running (2007), Development of a global evapotranspiration algorithm based on MODIS and global meteorological data, *Remote Sens. Environ., 111*(4), 519-536, doi: 10.1016/j.rse.2007.04.015.

Mu, Q., M. Zhao, and S. W. Running (2011), Improvements to a MODIS global terrestrial evapotranspiration algorithm, *Remote Sens. Environ., 115*, 1781-1800, doi: 10.1016/j.rse.2011.02.019.

Penman, H. L. (1948), Natural evaporation from open water, bare soil, and grass, *Proc. R. Soc. London, Ser. A, 193*, 120-145, doi:10.1098/rspa.1948.0037.

Penman, H. L. (1956), Evaporation: An introductory survey, *Neth. J. Agric. Sci., 4*, 9-29.

Priestley, C. H. B., and R. J. Taylor (1972), On the assessment of surface heat flux and evaporation using large-scale parameters, *Mon. Weather Rev., 100*, 81-92, doi:10.1175/1520-0493(1972)100<0081:OTAOSH>2.3.CO;2.

Shifa, Y. B. (2011), Estimation of evapotranspiration using advection aridity approach, M.S. thesis, Univ. of Twente, The Netherlands.

Shuttleworth, W. J. (2006), Towards one-step estimation of crop water requirements, *Trans. ASABE., 49*(4), 925-935.

Suleiman, A,, and R. Crago (2004), Hourly and daytime ET from grassland using radiometric surface temperatures, *Agron. J., 96*, 384-390.

Szilagyi, J., and A. Kovacs (2010), Complementary-relationship-based evapotranspiration mapping (cremap) technique for Hungary, *Per. Pol. Civil Eng., 54*(2), 95-100, doi: 10.3311/pp.ci.2010-2.04.

Thom, A. S., and H. R. Oliver (1977), On Penman's equation for estimating regional evaporation, *Quart. J. R. Meteorol. Soc., 103*(436), 345-357, doi: 10.1002/qj.49710343610.

Thompson, S. E., C. J. Harman, A. G. Konings, M. Sivapalan, A. Neal, and P. A. Troch (2011), Comparative hydrology across AmeriFlux sites: The variable roles of climate, vegetation, and groundwater, *Water Resour. Res., 47*, W00J07, doi: 10.1029/2010WR009797.

Twine, T., W. P. Kustas, J. M. Norman, D. R. Cook, P. R. Houser, T. P. Meyers, J. H. Prueger, P. J. Starks, and M. L. Wesely (2000), Correcting eddy-covariance flux underestimates over a grassland, *Agric. For. Meteorol., 103*, 279-300, doi:10.1016/S0168-1923(00)00123-4.

Wang, T., W. Sammis, and D. R. Miller (2008), Eddy covariance measurements of crop water uses: The energy closure problem and potential solutions, in *Agricultural Water Management Research Trends*, edited by Sorenson, M. L., pp. 1-7, Nova Science Publishers Inc., New York.

Wilson, K., Goldstein, A., Falge, E., Aubinet, M., Baldocchi, D.D., Berbigier, P., Bernhofer, C., Ceulemans, R., Dolman, H., Field, C., Grelle, A., Ibrom, A., Law, B.E., Kowalski, A., Meyers, T., J. Moncrieff, R. Monson, W. Oechel, J. Tenhumen, R. Valentini, and S. Verma (2002), Energy balance closure at FLUXNET sites, *Agric. For. Meteorol., 113*, 223-243, doi: 10.1016/S0168-1923(02)00109-0.

Xu, C. Y., and V. P. Singh (2005), Evaluation of three complementary relationship evapotranspiration models by water balance approach to estimate actual regional evapotranspiration in different climatic regions, *J. Hydrol.*, *308*, 105-121, doi:10.1016/j.jhydrol.2004.10.024.

Table 2.1. Characteristics of the 34 EC sites with measured *ET* data used in the study

#	Site	Country	Lat. °	Long. °	Data availability from-to (# months)	ET_{EC}, mm/month min	mean	max	AI_M, mm/°C	Land cover
					Very humid					
1	Takayama	Japan	36.1	137.4	06-07 (24)	9.4	44.4	91.7	83.2	Coniferous forest
2	Walker Branch, TN	USA	36.0	-84.3	95-98 (48)	10.5	47.4	116.2	76.5	Deciduous forest
3	Qinghai	China	37.6	101.3	02-04 (36)	1.6	36.2	110.5	68.3	Alpine meadow
4	Palangkaraya	Indonesia	2.3	114.0	02-05 (47)	82.4	134.3	164.0	61.5	Tropical forest
5	Harvard Forest, MA	USA	42.5	-72.2	92-99 (96)	5.1	37.5	108.4	61.2	Mixed forest
6	Flakaliden	Sweden	64.2	19.8	96-98 (31)	-0.1	23.0	63.4	51.5	Coniferous forest
7	Bondville, IL	USA	40.0	-88.3	97-06 (120)	1.7	50.1	135.4	49.6	Cropland
8	Goodwin Creek,MS	USA	34.3	-89.9	03-06 (48)	2.4	55.5	138.7	47.9	Cropland
9	Tharandt	Germany	51.0	13.6	96-99 (42)	6.5	39.2	95.9	47.1	Coniferous forest
10	Sarrebourg	France	48.7	7.1	96-99 (32)	-0.1	32.8	102.3	42.7	Deciduous forest
11	Kennedy Oak, FL	USA	28.6	-80.7	02-06 (53)	6.0	49.1	120.3	40.4	Evergreen forest
12	Loobos	Netherland	52.2	5.7	96-98 (30)	7.4	32.4	63.1	39.7	Coniferous forest
13	Sakaerat	Thailand	14.5	101.9	01-03 (32)	37.7	63.8	109.5	36.8	Tropical forest
					Humid					
14	Norunda	Sweden	60.1	17.5	96-98 (29)	1.3	30.9	80.8	34.0	Mixed forest
15	Fort Peck, MT	USA	48.3	-105.1	00-06 (84)	1.3	26.0	164.0	33.0	Grassland
16	Freeman, TX	USA	29.9	-98.0	05-08 (48)	6.0	49.1	120.3	30.9	Grassland
17	Little Washita, OK	USA	35.0	-98.0	96-98 (32)	8.9	41.6	104.4	30.7	Grassland
18	Mehrstedt 2	Germany	51.3	10.7	04-06 (34)	0.0	27.0	95.3	29.6	Grassland
					Sub-humid					
19	Evora	Portugal	38.5	-8.0	05-05 (12)	-0.3	13.7	34.8	26.2	Evergreen forest
20	Mauzac	France	43.4	1.3	05-07 (34)	8.3	37.2	91.4	25.5	Grassland
					Mediterranean					
21	Bugac	Hungary	46.7	19.6	02-08 (72)	2.3	37.5	103.9	23.8	Grassland
22	Metolius, OR	USA	44.3	-121.6	04-08 (60)	2.3	30.3	71.0	22.8	Woody savanna
23	Tonzi Ranch, CA	USA	38.4	-121.0	01-09 (80)	1.4	29.8	95.5	21.0	Woody savanna
24	Vaira Ranch, CA	USA	38.4	-121.0	01-09 (108)	-5.1	25.1	88.0	21.0	Woody savanna
					Semi-arid					
25	Kherlenbayan	Mongolia	47.2	108.7	03-10 (88)	-2.3	10.5	50.8	17.5	Grassland
26	Llano de los Juanes	Spain	36.9	-2.8	05-05 (12)	7.2	18.7	36.7	15.4	Olive plantation
27	Audubon, AZ	USA	31.6	-110.5	02-09 (87)	2.0	24.4	92.5	13.5	Open shrubland
28	Kendall, AZ	USA	31.7	-109.9	04-09 (68)	2.2	20.2	72.4	13.2	Grassland
29	Santa Rita, AZ	USA	31.8	-110.9	04-07 (48)	4.3	26.0	91.1	10.7	Open shrubland
					Arid					
30	Corral Pocket, UT	USA	38.1	-109.4	01-07 (39)	4.6	14.8	33.3	9.8	Grassland
31	Sevilleta grass, NM	USA	34.4	-106.7	07-08 (19)	4.5	22.2	69.7	9.0	Grassland
32	Sevilleta shrub, NM	USA	34.3	-106.7	07-08 (24)	3.3	23.5	74.7	9.0	Grassland
33	Demokeya	Sudan	13.3	30.5	97-98 (17)	6.1	38.1	106.3	8.9	Savanna/grassland
34	Yatir	Israel	31.3	35.1	01-09 (48)	5.7	17.8	57.3	8.6	Evergreen forest

Table 2.2. Average values of RMSE, BIAS, and R^2 for the actual *ET* estimates of the different complementary methods, CRAE, AA, and GG, at each climatic class

Climatic class	RMSE (mm/month)			BIAS (mm/month)			R^2		
	CRAE	AA	GG	CRAE	AA	GG	CRAE	AA	GG
Very humid	27.6	29.0	22.6	15.8	12.2	10.6	0.73	0.71	0.73
Humid	31.2	35.2	27.1	19.2	16.5	14.3	0.77	0.73	0.75
Sub-humid	46.6	54.7	45.0	31.9	28.7	26.5	0.39	0.33	0.41
Mediterranean	35.3	58.1	47.4	18.6	28.8	25.3	0.51	0.42	0.45
Semi-arid	16.6	18.9	22.1	9.6	8.4	13.3	0.56	0.61	0.41
Arid	22.4	31.9	29.5	9.4	14.4	19.5	0.53	0.54	0.42
All classes	27.80	33.76	28.43	15.73	15.54	15.50	0.64	0.61	0.59

Table 2.3. Details of the 39 model variations developed based on the complementary relationships. Also shown in bold/underline are the six promising models identified using preliminary analysis

Criteria	R_n		CR		α		β		*G*		*ETW*			*ETP*		
Equation			1	8					11	12	5	7	14	5	7	14
Value	R_T	R_{SZ}			1.26	1.28	0.5	1.0								
CRAE1	✓			✓												
CRAE2		✓	✓													
CRAE3		✓		✓												
AA1	✓			✓		✓		✓				✓		✓		
AA2	✓			✓	✓		✓					✓		✓		
AA3		✓	✓			✓		✓				✓		✓		
AA4		✓		✓		✓		✓				✓		✓		
AA5		✓	✓		✓		✓					✓		✓		
AA6		✓		✓	✓		✓					✓		✓		
AA7	✓		✓		✓		✓					✓		✓		
GG1	✓		✓					✓	✓		✓					
GG2	✓			✓				✓		✓	✓					
GG3	✓		✓					✓		✓	✓					
GG4		✓		✓				✓	✓		✓					
GG5		✓	✓					✓	✓		✓					
GG6		✓		✓				✓		✓	✓					
GG7		✓	✓					✓		✓	✓					
GG8	✓		✓		✓			✓		✓		✓				
GG9	✓			✓	✓			✓		✓		✓				
GG10	✓		✓		✓			✓	✓			✓				
GG11	✓			✓	✓			✓	✓			✓				
GG1	✓		✓			✓		✓	✓			✓				
GG13	✓			✓		✓		✓	✓			✓				
GG14	✓		✓			✓		✓		✓		✓				
GG15	✓			✓		✓		✓		✓		✓				
GG16		✓	✓			✓		✓		✓		✓				
GG17		✓		✓		✓		✓		✓		✓				
GG18		✓	✓			✓		✓	✓			✓				
GG19		✓		✓		✓		✓	✓			✓				
GG20		✓	✓		✓			✓	✓			✓				
GG21		✓		✓	✓			✓	✓			✓				
GG22		✓	✓		✓			✓		✓		✓				
GG23		✓		✓	✓			✓		✓		✓				
ASCE1		✓	✓					✓					✓	✓		
ASCE2		✓		✓				✓					✓	✓		
ASCE3		✓	✓		✓							✓				✓
ASCE4		✓		✓	✓							✓				✓
ASCE5		✓	✓		✓			✓				✓		✓		
ASCE6		✓		✓	✓			✓				✓		✓		

Table 2.4. Results of the performance of different models in a given climatic class described through the best values of RMSE, BIAS, and R^2

Metric	Climatic Class						
	Very humid	Humid	Sub-humid	Mediterranean	Semi-arid	Arid	All classes
RMSE	G3	GG7	GG22	GG22	GG20	GG20	GG22
R^2	CRAE2	GG11 and GG13	GG18 and GG20	GG18 and GG20	CRAE2	CRAE2	CRAE2
BIAS	GG1	GG7	GG20	GG22	GG14	GG14	GG18

Table 2.5. The values of the coefficients after optimization for the six promising model variations

Class	Coefficient	GG7		GG14		GG18		GG20		GG22		CRAE2	
		Mean	Median	Mean	Median	Mean	Median	Mean	Media	Mean	Median	Mean	Median
Wet	c_1					1.99	1.98	1.92	1.89				
	c_2					0.05	0.00	0.05	0.00				
	c_3					8.66	8.73	8.46	8.15				
	c_4	1.79	1.77	2.15	1.93					1.56	1.54		
	c_5	0.07	0.01	0.00	0.00					0.04	0.01		
	c_6	9.20	8.63	7.95	5.75					9.75	9.13		
	c_7	0.06	0.02	0.03	0.06					0.21	0.10		
	b_1											14.31	14.53
	b_2											1.02	1.03
Moderate	c_1					1.49	1.13	1.92	1.57				
	c_2					0.02	0.02	0.19	0.02				
	c_3					10.09	10.15	11.09	10.12				
	c_4	1.52	1.33	1.24	1.47					1.25	1.07		
	c_5	0.02	0.01	0.01	0.01					0.02	0.01		
	c_6	11.93	11.75	12.97	13.00					10.63	10.11		
	c_7	0.08	0.05	0.07	0.05					0.05	0.01		
	b_1											17.76	15.94
	b_2											0.80	0.95
Dry	c_1					0.88	0.98	1.20	1.03				
	c_2					0.03	0.01	0.03	0.02				
	c_3					8.55	8.52	8.79	8.04				
	c_4	1.54	1.25	1.23	1.01					1.31	0.87		
	c_5	0.09	0.05	0.07	0.05					0.03	0.02		
	c_6	8.65	8.68	7.48	5.32					8.14	8.10		
	c_7	-0.03	-0.02	-0.14	-0.13					-0.09	-0.04		
	b_1											13.62	14.71
	b_2											1.03	1.09

Table 2.6. Average values of RMSE and BIAS for the complementary methods, six promising models, and post-optimized promising models at each climatic class

Model		RMSE (mm/month)				BIAS (mm/month)			
		Wet	Moderate	Dry	All	Wet	Moderate	Dry	All
Complementary methods	CRAE	28.6	39.1	19.5	27.8	16.7	23.1	9.5	15.7
	AA	30.7	57.0	25.4	33.8	13.4	28.8	11.4	15.5
	GG	23.8	46.6	25.8	28.4	11.6	25.7	16.4	15.5
Promising models	GG7	19.7	26.4	27.2	23.1	10.0	15.0	19.1	13.6
	GG14	21.2	27.2	17.6	21.2	12.5	12.0	7.7	11.0
	GG18	22.5	21.4	16.6	20.6	12.4	8.3	8.6	10.6
	GG20	22.4	21.0	16.6	20.4	12.5	8.1	8.5	10.6
	GG22	21.9	20.1	17.3	20.2	13.7	7.7	8.1	11.0
	CRAE2	30.1	38.4	26.2	30.4	21.2	26.6	16.0	20.6
Optimized promising models	GG7	19.3	16.2	20.6	19.1	9.6	6.8	13.1	10.1
	GG14	22.5	19.8	20.3	21.4	12.0	9.9	9.2	10.8
	GG18	19.3	16.2	19.2	18.7	10.2	6.4	11.0	9.8
	GG20	19.5	17.1	19.9	19.2	10.4	10.3	11.7	10.7
	GG22	20.2	18.1	17.2	18.9	10.2	6.6	9.6	9.4
	CRAE2	18.9	16.3	18.4	18.3	8.6	6.1	9.9	8.6

Table 2.7. Comparison of performance of GG18 to the most recently published *ET* studies. When *ET* is given in power units of W/m^2, it can be converted to evaporation depth of mm units by multiplying it by the average number of days for each month (365 day/12 month) and dividing it by the heat of vaporization that is 28.5 W-day/kg

Citation	Theory	# of sites	RMSE (mm/month)			BIAS (mm/month)			R^2		
			min	max	mean	min	max	mean	min	max	mean
Present study	**GG18**	**34**	**10.3**	**59.9**	**20.6**	**0.5**	**58.1**	**10.6**	**0.01**	**0.94**	**0.64**
Present study	**Optimized CRAE2**	**34**	**7.4**	**50.0**	**18.3**	**0.0**	**48.3**	**8.6**	**0.02**	**0.94**	**0.67**
Suleiman and Crago [2004]	Radiometric surface temperature	2	32.0	53.4					0.78	0.94	
Mu et al. [2007]	Revised remote sensing and Penman-Montieth	19	7.7	56.4	29.2	2.9	41.1	15.6	0.13	0.96	0.76
Szilagyi and Kovacs [2010]	CRAE method	3	2.6	39.7	15.3	0.0	21.0	8.4			
Han et al. [2011]	Enhanced GG method	4	3.7	16.0	10.7				0.82	0.98	0.92
Huntington et al. [2011]	Modified AA method	5			11.0						0.71
Mu et al. [2011]	Modified remote sensing and Penman-Montieth	46	9.4	52.0	25.6	0.3	28.6	10.0	0.02	0.93	0.65
Thompson et al. [2011]	Penman-Montieth and soil moisture model	14	34.0	175.0	94.1						

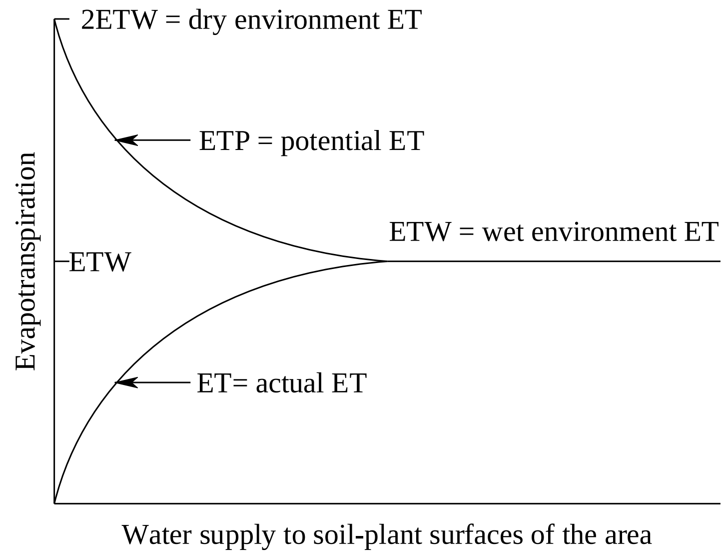

Figure 2.1. A schematic representation of the complementary relationship between ET, ETW, and ETP [after *Morton*, 1983].

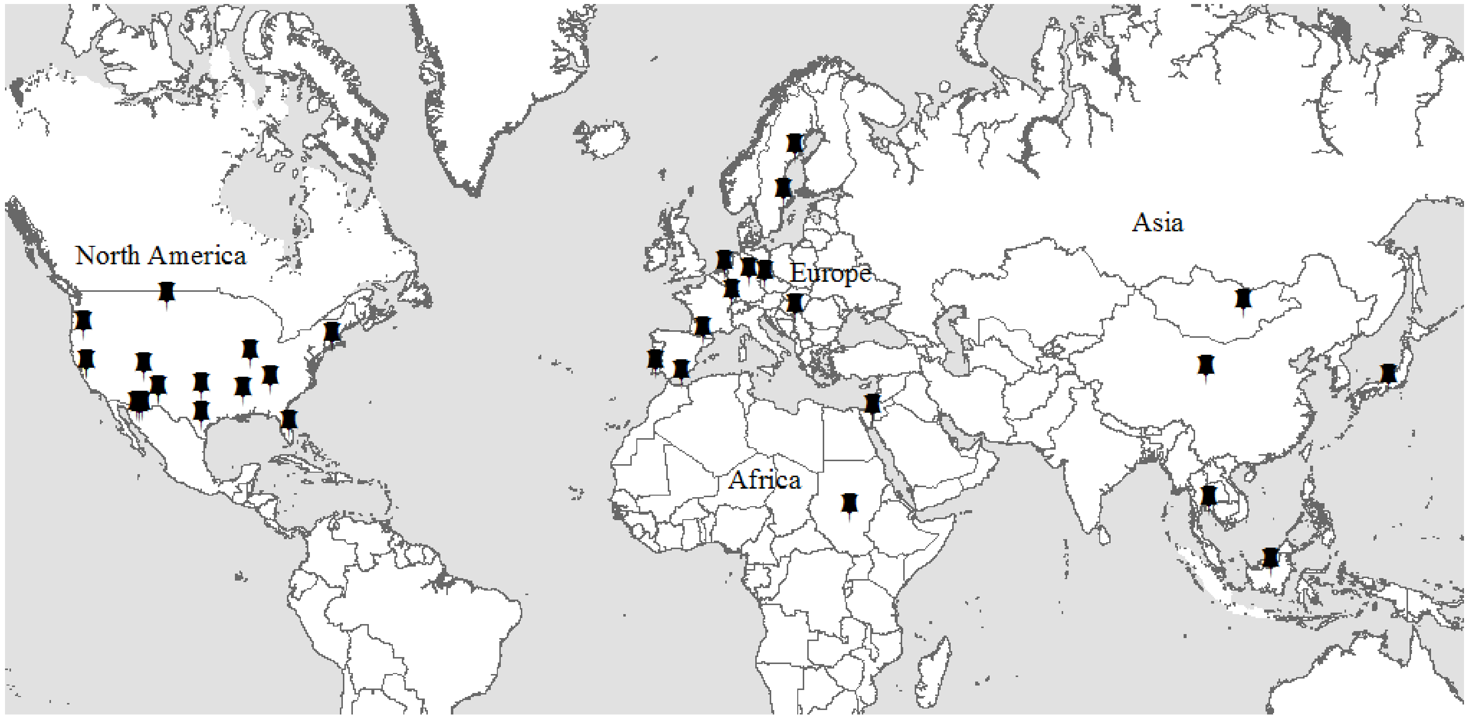

Figure 2.2. World map showing the locations of the 34 EC sites with measured *ET* flux data.

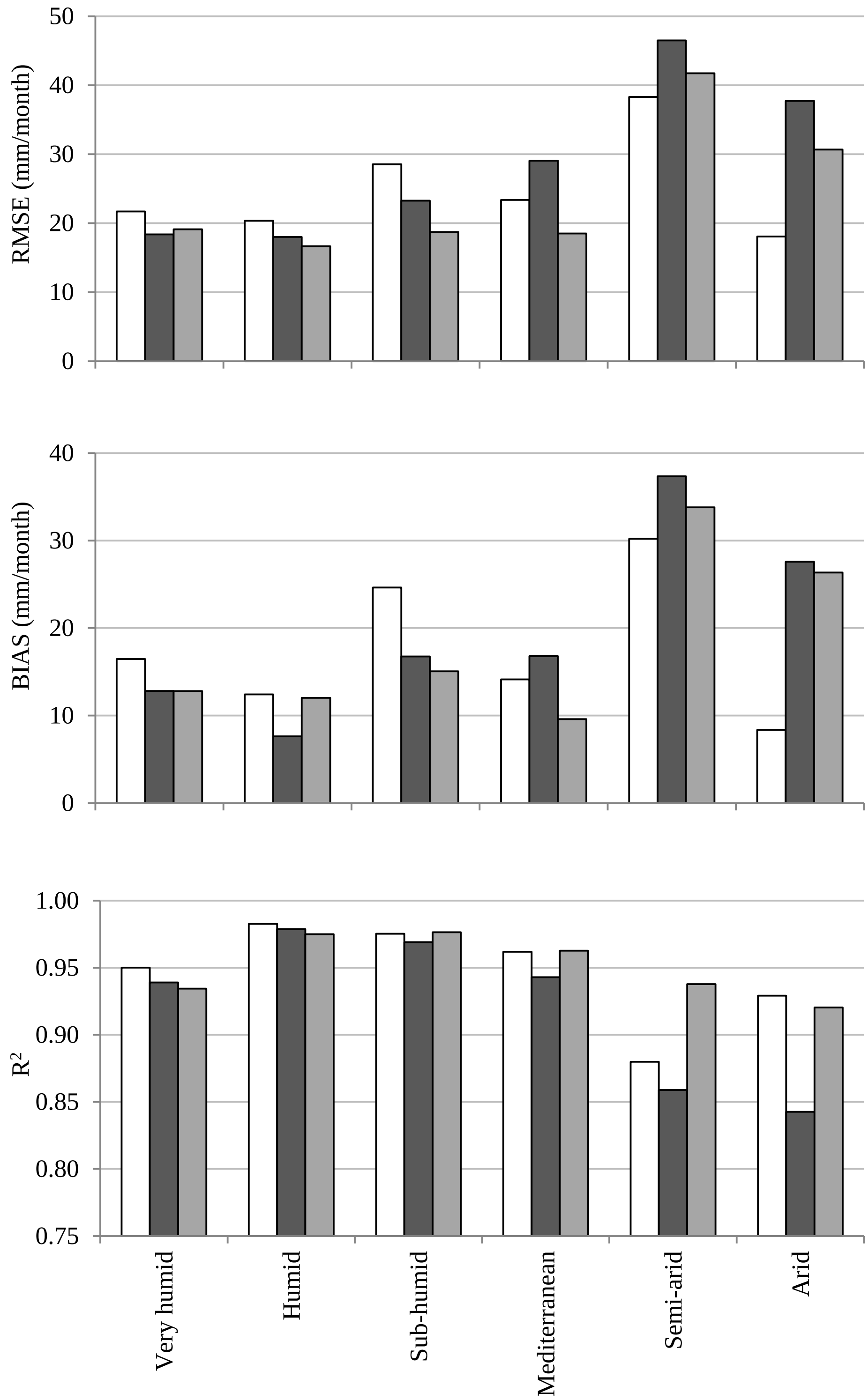

Figure 2.3. Average values of RMSE, BIAS, and R^2 for the different estimates of net radiation, R_n (R_T in white, R_{TP} in dark gray, and R_{SZ} in light gray) for each climatic class.

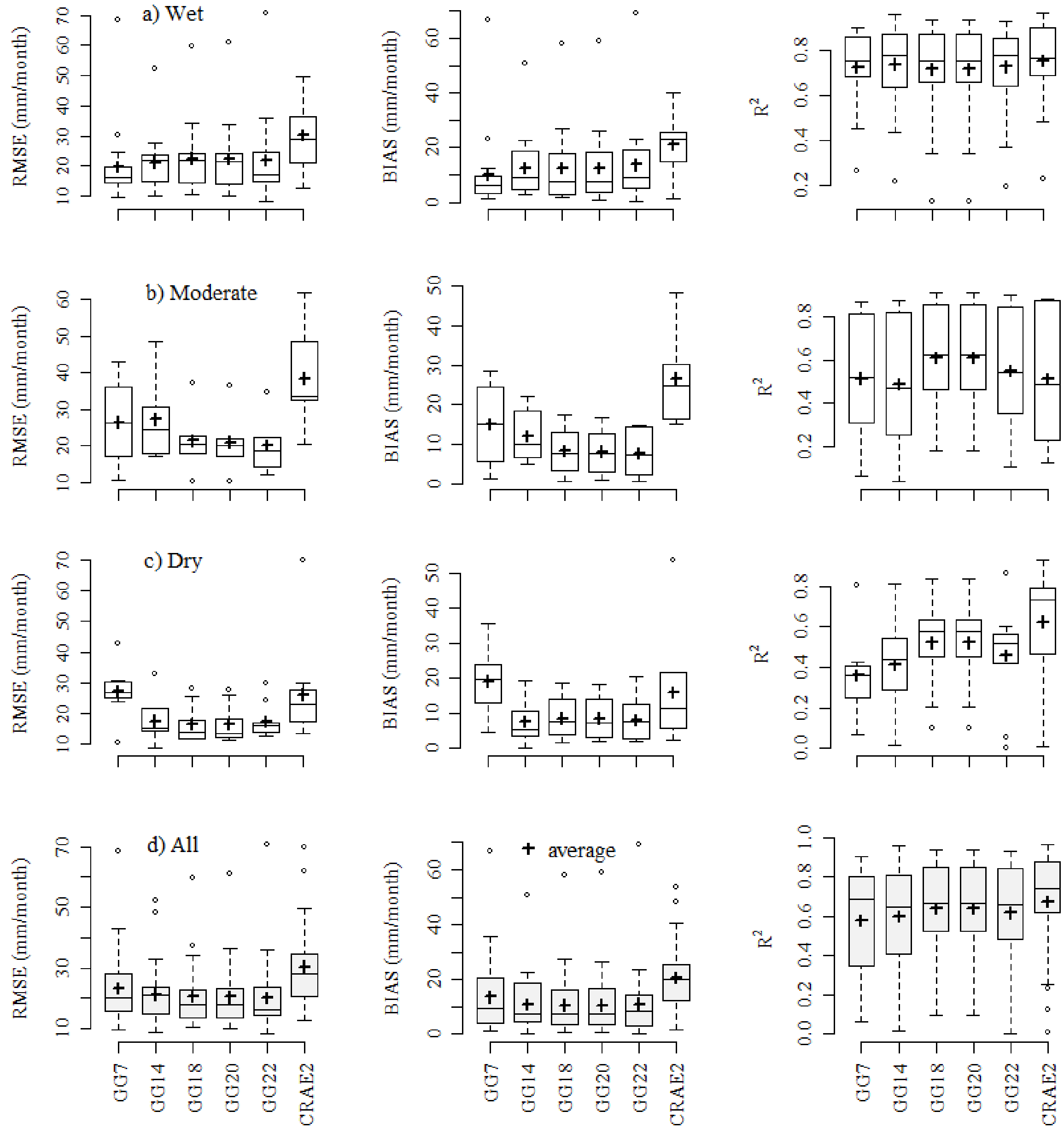

Figure 2.4. Boxplots of RMSE, BIAS, and R^2 metrics of the selected six promising models for the different climatic classes.

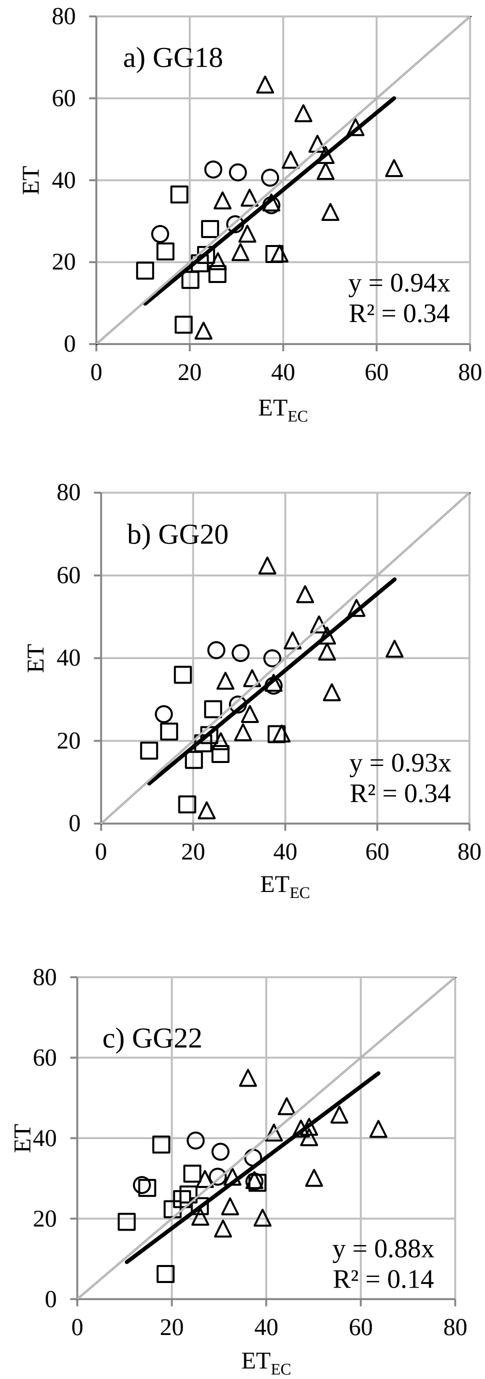

Figure 2.5. Scatter plots of average *ET* estimates (mm/month) for GG18, GG20, and GG22 models in comparison to measured ET_{EC} fluxes from 33 sites (all except site 4) in the wet (triangle), moderate (circle), and dry (square) climatic classes.

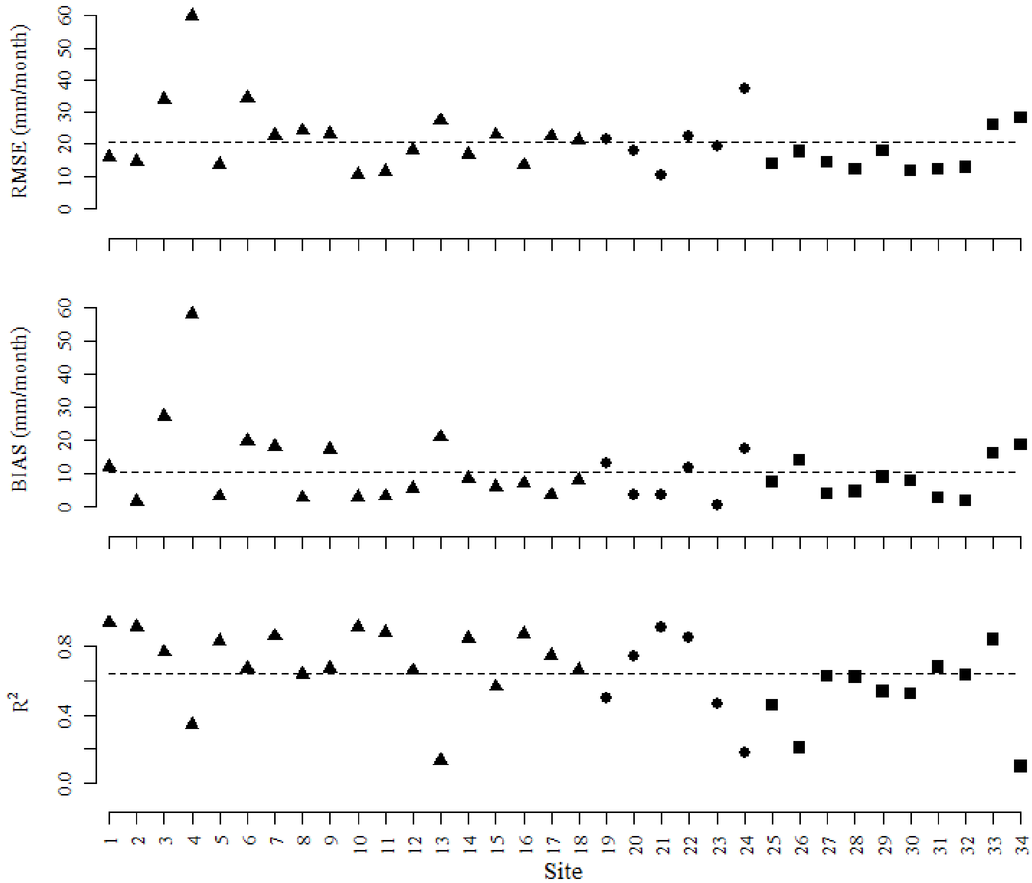

Figure 2.6. RMSE, BIAS, and R^2 of the GG18 model at each site in the wet (triangle), moderate (circle), and dry (square) climatic classes and the dashed lines indicate the average values.

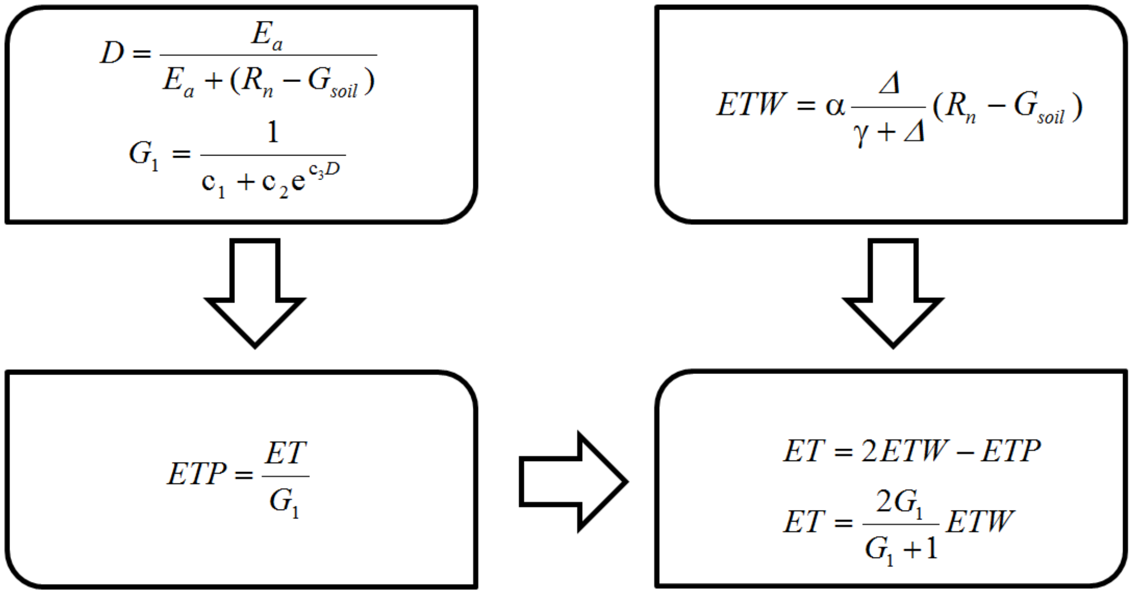

Figure 2.7. Schematic showing the structure of the proposed GG18 model.

CHAPTER 3

USE OF MODIFIED COMPLEMENTARY METHODS TO PREDICT REGIONAL-SCALE EVAPOTRANSPIRATION: A COUNTRY-WIDE STUDY OF GHANA

Abstract

Most classical evapotranspiration (ET) estimation methods require detailed data such as land use/class, hydrology, crop patterns, growing cycle, etc. However, studies have shown that the complementary methods are more attractive due to simplicity and minimal data requirements consisting of meteorological data only. Yet, complementary methods have not received adequate acceptance given the inability to accommodate contrasting physical and climatic conditions. Recent work by Anayah and Kaluarachchi (Chapter 2) proposed a modified form of the Granger and Gray (GG) method (Granger and Gray, 1989) that can estimate regional ET under different land use/class and physical conditions and the model was validated using measured data from 34 global sites. The purpose of this study is to demonstrate the applicability of this modified GG model in comparison to classical methods. The study area covers Ghana that has different climatic classes consisting of humid to semi-arid and a variety of land use patterns from traditional crop farming to forest. Daily meteorological data from ten synoptic stations between 2000 and 2005 are used. The results show that the modified GG model estimates of ET agree with crop ET predictions from ASCE, Hargreaves, and two other methods especially in northern Ghana where semi-arid climate prevails. The predicted regional ET values are 51 to 74% of the annual rainfall. The Priestley-Taylor equation used to compute wet environment ET of the modified GG model is close to the Penman-Monteith equation used in the ASCE grass reference method and the relative absolute difference of

annual values is 9%. Comparing the ET estimates of the modified GG model and the ASCE grass method showed the average RMSE and R^2 over the 10 stations are 22 mm/month and 0.65, respectively. The overall results prove that the modified GG model is capable of reliably predicting regional ET using a small number of monitoring stations with meteorological data only.

3.1 Introduction

Climate of a region cannot be classified based on rainfall only; it also depends on ET (Thornthwaite, 1948). ET represents a significant portion of the rainfall in the water balance especially in semi-arid regions where most rainfall is typically lost as ET (FAO, 1989). Given the inter-annually and intra-annually variable rainfall patterns in these regions, planning and managing water resources is difficult without reliable information of ET.

Generally, the concept of potential ET (ETP) is widely used by hydrologists, meteorologists, and agronomists. ETP was first introduced by Thornthwaite (1948) as the maximum ET from a large area covered completely and uniformly by plant if water supply is abundant. Three concepts are common among the scientific community and sometimes used interchangeably; these are ETP, reference ET (ET_o), and open water evaporation (E_p) (see Doorenbos and Pruitt, 1977). In water resources systems, the concept of ETP is widely used to indicate the climate driven water demand that is only governed by atmospheric conditions and not restricted by availability of water on the surface (Fortin and Seguin, 1975). However, there is a difference between ETP and reference ET in which both crop and weather data are specified (Irmak and Haman, 2003). Moreover, the concept of ET_o is extensively used in irrigation practices. On the other hand, open water evaporation introduced by Penman (1948) is different than ETP since the latter could be influenced by the soil-plant system. In effect, the ambiguity in using ETP is still present and it is largely depends on the application. Brutsaert (1982) mentioned that ETP is often estimated by meteorological data that are not necessarily measured under potential conditions. In comparison, water resources studies focus on seasonal or annual estimates at regional-scale as opposed to local estimates.

Worldwide, the three classical approaches predominately used to estimate ETP are the temperature methods such as Thornthwaite (1948), radiation methods such as Priestley and Taylor (1972), and the combination methods such as Monteith (1965). The combination methods, well known as the Penman's methods (Penman, 1948, 1956), are the most data intensive approaches whereas temperature methods are the least. Among all methods to estimate ETP, the Food and Agriculture Organization (FAO) version of the Penman-Monteith (P-M) equation (Allen et al., 1998), which is similar to the American Society of Civil Engineers (ASCE) version (Allen et al., 2005), is currently considered to be the best method (Walter et al., 2000). Yet, the applicability of the P-M equation for hydrological purposes has been criticized due to existing shortcomings (see Morton, 1994). For example, meteorological parameters are not measured at 2 m elevation from ground level and not at crop elevation as required by the P-M method (Shuttleworth, 2006).

Although the P-M equation considers the physical processes of ET from plant communities, it does not adequately consider the plant-atmospheric interactions especially under limited soil moisture (Mawdsley and Ali, 1985). As described by Allen et al. (1998) and Allen et al. (2005), ETP is computed for a reference crop such as grass or alfalfa and then multiplied by a crop coefficient for a given crop to determine crop ET. These crop coefficients are computed using prevailing climatic conditions for water unstressed plant communities and mostly under humid environments. Extrapolation of these coefficients to arid and semi-arid climates is therefore questionable (Shuttleworth and Wallace, 2009). In addition, Shuttleworth (2006) suggested that there is a need for "crop-specific surface-resistance estimates" similar to the crop coefficients. Another limitation is the lack of information of crop coefficients and growing cycles for different regions or countries. Examples include crops such as yam, cocoyam, and plantain that are common in Ghana. For instance, maize is grown in Ghana and not addressed by Allen et al. (1998) except the same crops grown in Nigeria have information listed. Although Nigeria is relatively close to Ghana, the climatic variation is significant and therefore, the variation of growing cycle is also high.

In contrast, the complementary methods, including the Complementary Relationship Areal ET (CRAE) method of Morton (1983), Advection-Aridity (AA) method developed by Brutsaert and Stricker (1979), and Granger and Gray (GG) method by Granger and Gray (1989), have the potential to provide competitive alternatives to calculate ET using meteorological data only in a diverse set of physical and climatic conditions. According to Morton (1983), complementary methods offer simplicity, practicality, and provide reliable physically-based operational ET estimates at regional scale. The methods also consider the surrounding climatic conditions regardless of the underlying soil-plant system, avoid locally calibrated coefficients (Sophocleous, 1991), and require minimal meteorological data typically monitored in most rural areas (Hobbins et al., 2001; Nash, 1989). One other attractive feature of the complementary methods is the ability to use in climate change studies because the general circulation models typically predict precipitation and temperature forecasts.

Do complementary methods have limitations? The answer is yes. As Morton (1983) summarized, the methods are best for monthly estimates and cannot be used for intervals of three days or less (see Armstrong et al., 2008; Doyle, 1990). Still this is not a serious limitation in water resources studies given the long-term outlook of such studies. The methods cannot be used near sharp environmental discontinuities such as the edge of an oasis. Since an oasis effect is eliminated after 300 m (Davenport and Hudson, 1967), the impacts of such discontinuities are limited. As for advantages, these methods do not require the knowledge of the soil-plant system, land use/cover, and terrain slope, which may affect the runoff coefficients that, in turn, could influence localized ET (Xu and Singh, 2005).

In the complementary methods, wet environment ET (ETW) is the ET that would occur if the soil-plant system is saturated and then ET could approach its potential rate, ETP (Granger, 1989). In spite of the fact that ET is negatively correlated to ETP (Fig. 3.1), there is no exact shape of that relationship (see Davenport and Hudson, 1967). The concept of the complementary theory was initially introduced by Bouchet (1963) and states the presence of a complementary relationship between ET from an area and point ETP estimate in that area. Accordingly, the relationship between ET and ETP under limited water supply is not linear and does not follow a given law. The three types of ET used in the complementary methods are mathematically related as

$$\mathrm{ET} + \mathrm{ETP} = 2\mathrm{ETW} \tag{1}$$

where ET, ETW, and ETP are in mm/d. Eq. (1) indicates that an increase in ET will be accompanied by an equivalent decrease in ETP, i.e., $\delta ET = - \delta ETP$. In other words, as the surface dries, areal ET decreases causing a decrease in humidity and an increase in temperature of the surrounding air at the same time, and as a result ETP will increase. This means that ETP is a function of ET in contrast to the model suggested by Penman (1948) where ETP is independent of ET. This latter claim is true for large moist areas when the effect of ET on temperature and humidity is fully developed and ET and ETP are equal, and for small moist areas in which the effect of ET is insignificant (Morton, 1983).

The CRAE and AA methods use the same complementary relationship originally developed as shown by Eq. (1). However, Granger and Gray (1989) modified that relationship as follows:

$$\mathrm{ET} + \frac{\gamma}{\Delta}\mathrm{ETP} = \left(1 + \frac{\gamma}{\Delta}\right)\mathrm{ETW} \qquad (2)$$

where γ is the psychrometric constant (kPa/°C) and Δ is the rate of change of saturation vapor pressure with temperature (kPa/°C). Hence, Eq. (2) can be reduced to Eq. (1) only when $\gamma = \Delta$.

For several decades, the complementary methods have been studied and compared to other methods over different environments including different spatial and temporal scales and climates. Initially, the proper spatial scale of the Bouchet hypothesis was investigated by Fortin and Seguin (1975). Over semi-arid to sub-humid tropical regions of West Africa, Oguntunde et al. (2005) applied the AA method and noted that the complementary relationship hypothesis is evidently valid across the Volta Basin, but ET estimates have to be verified. Similar work proved that the trends in pan evaporation and ET across the U.S. have a complementary relationship (Hobbins et al., 2004). For smaller scales of space and time in cold semi-arid regions of Canada, it was found that the CRAE method is not suitable for short periods or field-size areas (Granger and Gray, 1990). However, Doyle (1990) compared the CRAE method and the Thornthwaite soil moisture model on an Irish humid basin to water balance data and found that the CRAE method is valid. Under semi-arid climates in Northwestern China, Lemeur and Zhang (1990) used the CRAE and AA methods on a daily basis to estimate ET and large errors were found compared to the water balance approach. In addition, the results emphasized that the CRAE method overestimated annual ET in the mountainous areas and the P-M method is still preferable over both methods. In the U.S., the CRAE and AA methods produced ET values at 139 minimally-impacted basins (Hobbins et al., 2001) and the results showed that as aridity increases, ET is overestimated by the CRAE method and underestimated by the AA method. Still, the CRAE method predicted monthly ET over the climate spectrum. Additional studies conducted using the three complementary methods, their applicability, and limitations have been recently discussed by Anayah and Kaluarachchi (Chapter 2).

While the complementary methods such as the GG method have the potential to estimate actual ET with minimal data requirements, there are few limitations in predicting ET in a reliable and consistent manner for different spatial and temporal scales and hydrologic and climatic conditions. Given these limitations, there exist obvious research questions such as: (1) What are the relative accuracies between the different complementary methods in predicting ET compared to measured data? (2) Does the performance of each method depend on the prevailing climate? (3) What improvements should be made in the complementary methods to better predict ET? (4) Can any of the complementary methods be modified to develop a single step ET prediction model (without local calibration) with the same advantages but can be used in a variety of physical and climatic conditions? (5) How reliable is such a modified model to predict ET at country scale such as Ghana where data are limited and climate variability is significant? (6) How close will be those estimates compared to the estimates from the existing classical methods? (7) Is there evidence to suggest that the complementary methods provide a regional-scale (or an areal) estimates of ET? The first four questions have been addressed in a recent study by Anayah and Kaluarachchi (Chapter 2) using the proposed modified GG model that was validated using measured ET data from 34 global sites with contrasting climatic and physical conditions. The purpose of this study is to extend the earlier work to address the remaining questions related to the ability to reliably predict regional ET using the modified complementary method proposed by Anayah and Kaluarachchi (Chapter 2) and to evaluate the applicability of the work compared to results of existing classical methods.

3.2 Description of Ghana

The land area of the Volta River Basin exceeds 400,000 km^2 and overlays six countries of which Ghana occupies 42% of the land area (Fig. 3.2). The basin comprises four principle sub-basins; Black, White, Oti, and the Lower Volta. The area of Ghana is 238,538 km^2 of which the agricultural land area is about 57% (SRID, 2010). Ghana is administratively divided into ten regions as shown in Fig. 3.2. The population of Ghana in 2009 was 24 million with a growth rate of 2.1% of which 68.2% were rural population living in nine regions excluding the capital city of Accra (SRID, 2010). Agriculture is the major source of income and employment for most people especially for rural communities. Globally, agricultural water use accounts for 70 to 80% of water used, and therefore, efficient planning and management of water resources in countries such as Ghana is important for food security and rural livelihood.

Ghana in the Volta River Basin was selected for this study for several reasons. This region was the focus of several important studies that were conducted more than 50 years ago by many pioneering scientists such as Penman (1956) as discussed by Rietveld (1978). It is also a pilot study region where many water related field studies are conducted by research institutions such as the International Water Management Institute (IWMI), the GLOWA Volta project funded by the German Technical Cooperation (GTZ), and the work of the Canadian International Development Agency (CIDA). Since the Volta River Basin is a transboundary water source, there are political and economic interests among the riparian countries for the equitable allocation of water for all users.

All data used in this work were originally monitored and maintained by the Meteorological Services Department of Ghana. Except for Koforidua and Akim Oda stations, data were provided by the Water Resources Commission (WRC) of Ghana and CIDA. Data of the remaining two stations were provided by IWMI. Information related to these ten synoptic stations are shown in Table 3.1 and Fig. 3.2. Daily values of minimum air temperature (T_{min}), maximum air temperature (T_{max}), minimum relative humidity (RH_{min}), maximum relative humidity (RH_{max}), sunshine hour (S), and average wind speed (U) at the ten synoptic stations from 2000 to 2005 were used in this research.

Ghana lies within four major agro-ecological zones and the ten synoptic stations fall across all four zones; Guinea savannah zone (includes Navrongo, Wa, Tamale, Yendi, and Bole stations), Transitional zone (includes Kete-Krachi and Wenchi stations), Rain Forest zone (includes Sunyani and Akim Oda stations), and Coastal Savannah zone (includes Koforidua station). The smooth transition of environments in Ghana does uniquely vary from semi-arid climates in the north with a mono-modal rainfall pattern to sub-tropical humid climates in the south with a bi-modal rainfall pattern. The average annual rainfall varies from north to south between 963 and 1432 mm, respectively. At Akim Oda station in the south, for instance, the major rainfall season extends from March to August while the minor season extends from September to October. In contrast, there is only one rainfall season that starts in May and ends by September at Navrongo station in northern Ghana, i.e., summer rainfall. Rainfall is high during these months and ET is low probably due to the increased humidity. In this humid climate, recharge is most likely high. As in most semi-arid regions, surface water resources are considerably unreliable due to the high inter- and intra-annual variability in rainfall in the north. The average daily temperature (T) marginally varies from 26.4 to 29.3°C, however, the average daily relative humidity (RH) fluctuates considerably between 53.8% and 79.2% and the same is true with S and U. Topography is relatively undulating with gentle slopes and the average elevation is about 190 m above mean sea level. The topsoil is mostly sandy loam and loam and the gravel content in the sandy soils increases with depth indicating lower soil stability, but, the drainage characteristics are better during the rainy season (SRID, 2010).

3.3 Methodology

3.3.1 Modified Complementary Method

The modified GG model proposed by Anayah and Kaluarachchi (Chapter 2) is an enhanced version of the complementary methods in which two significant changes are made to the original GG method. It is found that the complementary relationship shown in Fig. 3.1 and Eq. (1) can precisely describe the behavior of ET fluxes better than the more generic expression derived in the original work by Granger and Gray (1989), i.e., Eq. (2). More importantly, the predictive power of the GG method is improved when the Priestley and Taylor (1972) equation (P-T) shown in Eq. (3) is adopted to calculate the wet environment ET, ETW, instead of the Penman (1948) equation used in the original GG method.

$$ETW = \alpha \frac{\Delta}{\gamma + \Delta}(R_n - G_{soil}) \qquad (3)$$

where α is the coefficient of the P-T equation that typically equals to 1.26, R_n is the net radiation in mm/d, and G_{soil} is the soil heat flux density in mm/d. The procedure described by Allen et al. (2005) is used to calculate the daily net radiation for both actual and crop ET estimates. Daily data required to calculate R_n are simply: T_{min}, T_{max}, RH_{min}, RH_{max}, and S. It is noticed that soil heat flux (G_{soil}) density is negligible for daily periods especially when compared to R_n.

In the GG method, two new parameters were identified and empirically correlated together; relative drying power (D) and relative evaporation (G) shown in Eq. (4) and Eq. (5), respectively. Parameter D indicates the dryness of the surface, i.e., D increases with dryness of the surface. Parameter G is ET that occurs under similar wind and humidity conditions from a saturated surface at its actual temperature (Granger and Gray, 1989). It should be mentioned that Eq. (6) was empirically derived using data from two stations in a semi-arid region of western Canada. Granger and Gray (1989) claimed that it is independent of land use.

$$D = \frac{E_a}{E_a + R_n} \tag{4}$$

$$G = \frac{ET}{ETP} \tag{5}$$

$$G = \frac{1}{1 + 0.028e^{8.045D}} \tag{6}$$

where E_a is the drying power of air in mm/day. The average daily values of U are required to calculate E_a. Substituting ETP of Eq. (5) in Eq. (1) will provide an estimate of ET in the modified GG model as shown in Eq. (7).

$$ET = \frac{2G}{G + 1} ETW \tag{7}$$

3.3.2 Classical Methods

There are many classical methods to estimate ET that are common among agronomists and hydrologists (see Jensen et al., 1990). Most of these methods are applied to calculate irrigation water requirements. In this work, four common classical methods are selected; American Society of Civil Engineers (ASCE) method (Allen et al., 2005), Hargreaves et al. (1985), Turc (1961), and Jensen and Haise (1963). It should be noted that the classical methods described here require the calculation of ET_o first followed by the use of K_c to calculate ET compared to calculating ET directly using the modified GG model that does not require crop data.

3.3.2.1 ASCE method

Allen et al. (2005) described the method to calculate the ASCE standardized reference ET (ET_o) shown in Eq. (8) for two reference crops, grass and alfalfa. The use of ET_o for grass as the reference crop (Allen et al., 2005) is almost identical to the FAO version of the P-M equation (Allen et al., 1998) that is currently considered to be the best method to estimate ET_o.

$$ET_o = \frac{\Delta(R_n - G_{soil}) + \gamma \frac{C_n}{T+273} U(e_s - e_a)}{\Delta + \gamma(1 + C_d U)} \tag{8}$$

where T is the average daily air temperature in °C, U is the average daily wind speed in m/s, e_s is the average daily saturation vapor pressure in kPa, e_a is the average daily vapor pressure in kPa, and C_n and C_d are constants that change with reference crop and calculation time step. C_n and C_d are 900 and 0.34, respectively, for grass and daily time steps.

$$ET_c = K_c ET_o \tag{9}$$

According to Eq. (9), crop ET (ET_c) is the multiplication of ET_o by the crop coefficient (K_c). In Allen et al. (1998), there are three tabulated values for K_c according to the growing stage; K_c for the initial stage ($K_{c\ ini}$), K_c for the mid-season ($K_{c\ mid}$), and K_c for the late season ($K_{c\ end}$). Since the tabulated crop coefficients were computed under sub-humid climates where RH_{min} is 45% and U is 2 m/s, it is recommended to adjust $K_{c\ mid}$ and $K_{c\ end}$ according to the actual value of RH_{min} and U as shown in Eq. (10).

$$(K_c)_{Adjusted} = (K_c)_{Tabulated} + [0.04(U-2) - 0.004(RH_{min} - 45)]\left(\frac{h}{3}\right)^{0.3} \tag{10}$$

where h is the average plant height during the mid-season in m. Similarly, ET_o for alfalfa is computed using the same Eq. (8) with C_n and C_d at 1600 and 0.38 (see Allen et al., 2005), respectively, for daily time steps. To calculate ET_c, the alfalfa-based crop coefficients are different than those of grass reference crops. The alfalfa-based crop coefficients are calculated using Eq. (11) and Eq. (12).

$$K_{c\,(alfalfa)} = K_{c\,(grass)} / K_{ratio} \quad (11)$$

$$K_{ratio} = 1.2 + [0.04(U - 2) - 0.004(RH_{min} - 45)]\left(\frac{h}{3}\right)^{0.3} \quad (12)$$

3.3.2.2 Hargreaves method

The Hargreaves method is the alternative method suggested by Allen et al. (1998) when minimal data such as temperature is only available. In essence, this method is recommended when humidity, wind speed, and solar radiation data are missing. This method estimates ET_o and uses K_c for grass reference to calculate crop ET. Furthermore, the Hargreaves method was constructed using data from West Africa, more specifically Senegal (see Hargreaves et al., 1985). ET_o of the Hargreaves method for grass reference is given as

$$ET_o = 0.0022(T + 17.8)\sqrt{T_{max} - T_{min}}\,R_a \quad (13)$$

where T, T_{max}, and T_{min} are in °C, and R_a is the extraterrestrial radiation in mm/d.

3.3.2.3 Turc method

The Turc method, on the other hand, was developed for western Europe under humid climates (Jensen et al., 1990) for grass reference. To accommodate general climatic conditions, the model is adjusted by a humidity factor for less humid conditions as shown in Eq. (14) and Eq. (15).

$$ET_o = 0.013\frac{T}{T + 15}(58.56R_s + 50) \quad \text{for RH} > 50\% \quad (14)$$

$$ET_o = 0.013\frac{T}{T+15}(58.56R_s + 50)\left(1+\frac{50-RH}{70}\right) \qquad \text{for RH < 50\%} \qquad (15)$$

where R_s is the solar radiation in mm/d. The conversion factor 58.56 enables estimating R_s in mm/d instead of cal/cm^2/d units in the original equation. In comparison, the Hargreaves method is solely dependent on temperature, whereas the Turc method is different since it depends on RH and solar radiation. It is a simple empirical radiation method in which the crop coefficients are based on grass reference.

3.3.2.4 Jensen Haise method

This is a radiation method to estimate ET_o that was empirically developed for well-watered crops in the western United States (Jensen et al., 1990). It is simple and straightforward and it considers alfalfa to be the reference crop. According to Jensen et al. (1990), ET_o is estimated by Eq. (16).

$$ET_o = \frac{1}{38 - \frac{2L}{305} + \frac{36.5}{e_{max} - e_{min}}}\left(T + 2.5 + 1.4(e_{max} - e_{min}) + \frac{L}{550}\right)R_s \qquad (16)$$

where L is the elevation in m, e_{max} is the saturation vapor pressure at T_{max} in kPa, and e_{min} is the saturation vapor pressure at T_{min} in kPa.

The latter three methods, Hargreaves, Turc, and Jensen Haise methods, are empirical and have been developed under different physical conditions and contrasting climates. Therefore, it will be interesting to find the applicability of these models and their comparisons with the proposed modified complementary method. Hereafter, GR stands for the ASCE grass reference method, AL stands for the ASCE alfalfa reference method, HV stands for the Hargreaves method, TC stands for the Turc method, and JH stands for the Jensen Haise method.

3.3.3 Climate Classification

Aridity index (AI) is used to specify the climatic class and the definitions differ in complexity and data requirements. The prevailing climate of each station is defined by different aridity indices. As mentioned in the introduction, Thornthwaite (1948) assumed that climate of a region can be classified based on rainfall and ET. Therefore, every aridity index should indicate the availability of both water and energy. The aridity indices used here are AI_M of De Martonne (1925), AI_T of Thornthwaite and Mather (1955), AI_B of Budyko (1958), and AI_U defined by UNEP (1992). The definition of each index is given below.

$$AI_M = \frac{P_{ann}}{T_{ann} + 10} \tag{17}$$

$$AI_T = 100\left(\frac{P_{ann}}{ETP_{ann}} - 1\right) \tag{18}$$

$$AI_B = \frac{R_{ann}}{P_{ann}} \tag{19}$$

$$AI_U = \frac{P_{ann}}{ETP_{ann}} \tag{20}$$

where P_{ann} is the average annual rainfall in mm, T_{ann} is the average annual temperature in °C, ETP_{ann} is the average annual ETP in mm, and R_{ann} is the average annual R_n in mm. Using an index such as AI_M is straightforward and easy given the simplicity of input data. The other aridity indices are seemingly more accurate but complex because R_{ann} and ETP_{ann} estimates have to be calculated first. It should be noted that there is no universally accepted method to define aridity. In this work, R_{ann} is the average annual R_n calculated by the procedure described by Allen et al. (2005) and ETP_{ann} is similar to the average annual ET_o for short reference crop.

3.4 Results and Discussion

3.4.1 Climate Class

Given the significant climate variability across Ghana from semi-arid north to humid south, it is important to classify the prevailing climatic conditions. In this work, the four aridity indices defined by Eqs. (17) through (20) were used and the results are shown in Table 3.2. One would expect the most recent index AI_U that captures both precipitation and energy may be able to identifying the contrasting climates present across Ghana. Instead, this index provides a more uniform climatic distribution across Ghana similar to AI_B. Both AI_M and AI_T indicate different degrees of humid conditions. On the other hand, AI_T indicates more contrasting climates varying between semi-arid climate in three stations in the north to dry and wet sub-humid conditions towards the south. It seems that the oldest index, AI_M, outperforms the other three indices by capturing the variability of humid categories and in the use of simple input data.

3.4.2 Potential Evapotranspiration

ETP or ET_o is the first step of calculating actual or crop ET with any of the classical methods. In this work, the proposed modified GG model is estimating ETP and ETW while ET_o of grass and alfalfa are estimated using the classical methods and the results are shown in Fig. 3.3. It is observed that ETP of the modified GG model is high compared to the other estimates showing an “unrealistic representation of the upper constraint on actual ET” as discussed by Chiew and Leahy (2003). Furthermore, these authors found that ETP of the complementary method (CRAE in their case) is similar to the pan evaporation value that considers ideal conditions where neither energy nor water is typically limited. This reason can be explained if the procedure to calculate ETP in the GG method is well understood. ETP is calculated using G in Eq. (5) which indicates dryness of the surface that is empirically correlated to D in Eq. (6) which reflects how much convective is the environment. As illustrated by Granger and Gray (1989), the "surface conditions play a predominant role in the partitioning of the available energy to evaporation, and thus also control the ETP." Higher values of ETP indicate convective environments (high D values) under dry surface conditions (low G values) prevail. Apparently, ETP values in the north are considerably higher than those in the south.

In contrast, ETW of the modified GG model is very much comparable to other ET_o estimates. For example, the mean values of ETP predicted by the modified GG model range from 157 to 222 mm/month whereas mean ETW values from the same model vary between 116 and 138 mm/month. The corresponding mean values of ET_o for grass and alfalfa range from 100 to 155 and from 109 to 199 mm/month, respectively. Hence it is possible to compare ETW of the modified GG model with ET_o of the GR method. Compared to the ETW estimates, the GR method is slightly overestimating ET_o under arid climates and underestimating ET_o under humid climates. The variability of ET_o of the GR method is slightly higher than ETW with the modified GG model. It is noticed that the AL method is overestimating ET_o compared to the GR method, however, the difference gradually diminishes as humidity increases.

Acheampong (1986) estimated ET_o in Ghana using Walker-modified Penman, Thornthwaite, and Papadakis approaches and compared those estimates with class A pan evaporation measurements. This study was one of the first few studies conducted across

Ghana and the comparisons were made at six synoptic stations of which three are included in this research; Navrongo, Tamale, and Wenchi. The monthly ET_o estimates from this earlier study were available in low-quality charts and the approximate values of the pan evaporation measurements at Navrongo, Tamale, and Wenchi were 212, 257, and 165 mm/month, respectively. The average monthly ET_o estimates from the other three methods for Navrongo, Tamale, and Wenchi vary between 152 and 178, 153 and 193, and 111 and 135 mm, respectively. It is noticed that ETP of the modified GG model is the closest to the pan evaporation measurements. The ET_o measurements of Acheampong (1986) and the results of ETP from the modified GG model are very much close and comparable. Similarly, both Hobbins et al. (2001) and Chiew and Leahy (2003) found that ETP of the CRAE method is a good estimator of pan evaporation.

Table 3.3 shows the annual estimates of ETP, ETW, and ET_o given by the different methods used in this study. The ETW estimates are more consistent and the variation among the stations is not substantial. The relative absolute difference (RAD) is simply defined as the absolute value of the difference between ETW of the modified GG model and ET_o of a classical method divided by ETW. It is noticed however that the RAD_{GR} ranges from zero at Bole to 16% at Akim Oda with an average of 9% and no obvious trend. Although advection energy is lumped into the radiation energy of the P-T equation in the modified GG model, still the P-T equation is a good substitute to the P-M equation. With other classical methods, the results from the JH method are close to those of the AL method. The performance of the HV method is improving with aridity whereas the TC method is performing in the opposite direction. One reason for the criticism of these two methods is the results from the two methods tend to move in opposite directions. A possible reason for this behavior may be the parameters used in these methods are locally developed in specific circumstances and may not be applicable otherwise. Nevertheless, an interesting trend is observed when ETW and the average of the five ET_o estimates of the classical methods are compared by RAD_{AVG} values as shown in column [10] of Table 3.3. The closure between these two estimates significantly increases with humidity.

Acheampong (1986) estimated pan evaporation rates at Navrongo, Tamale, and Wenchi as 2550, 3085, and 1985 mm/year, respectively. These estimates are close to the ETP values of the modified GG model except at Tamale where the difference is about 18%. The estimates from the other three methods used in this study are fairly in agreement with the estimates of the modified GG method. At Navrongo, for instance, Compaore et al. (2008) stated that average annual ETP from 1961 to 2003 is 2423 mm. Carrier (2008) studied ET of northern Ghana that included eight stations discussed in this work. It is no surprise that ET_o of the GR method agreed at around 90 to 95% with the estimates of Carrier (2008) who used the P-M equation. Two other studies (Martin, 2006; Obuobie, 2008) have been conducted in northern Ghana specifically using the Navrongo station that is well maintained and used by many international research projects. In a total of seven previous studies (e.g., Acheampong, 1986; Carrier, 2008; Compaore et al., 2008), ET_o was estimated using both Penman and Thornthwaite methods, at Navrongo station and the average annual ET_o ranged from 1647 to 2423 mm. In Table 3.3, the values of ETW and ETP at Navrongo are 1623 and 2662 mm/year and correspond to the lower and upper bounds of the ET_o range for the seven previous studies, respectively.

3.4.3 Actual ET

Actual ET is the total water loss from the land surface which may or may not include vegetation, but includes evaporation from water bodies and soil moisture. On the other hand, crop ET occurs only during the growing cycle of a crop. In rural areas where agriculture is the dominant land use, it is expected that crop ET represents a significant proportion of actual ET. In other words, actual ET is crop ET when the contribution to ET from water bodies and soil moisture is minimal. Since the stations used in this study are located within agricultural areas, crop ET is comparable to actual ET. As discussed earlier, actual ET predicted by the complementary methods, specifically the modified GG method is areal ET representing the area surrounding a given station since climatic variables are used exclusively to calculate ET. Another argument is that ET is a representation of the climatic variables in the surrounding area as opposed to the argument by classical methods where ET is a measure of water outflow from a given land cover/use. ET estimates from the classical methods are complex given the high uncertainty associated with land use/cover as well as the soil-plant interactions.

It is worth to mention that data used by Anayah and Kaluarachchi (Chapter 2) were monthly time series while data used here are daily. The question is whether this time scale difference may affect the results of the modified GG model or not as found by Xu and Singh (2005). For this purpose, the time-series of monthly meteorological data were made available from the Meteorological Services Department of Ghana from 1961 to 2005 for five northern stations, namely Navrongo, Tamale, Wa, Bole, and Yendi. Monthly data of these five stations from 2000 to 2005 were used for comparison with daily estimates of the modified GG model. The root mean square errors (RMSEs) of the two estimates ranged from 2.8 mm/month at Wa to 5.9 mm/month at Tamale. The bias of the mean values (Bias) is -1.6 mm/month at Bole and 2.6 mm/month at Tamale and the lowest coefficient of determination (R^2) is 0.96 at Bole. These results suggest that the modified GG model can accommodate both daily and monthly time steps to produce consistent results.

3.4.4 Crop ET

Crop ET from the ASCE method is calculated following the procedure described by Allen et al. (1998) and the crop coefficients used are shown in Table 3.4. These values were adjusted as discussed earlier to suit the existing climatic conditions of each station. In computing crop ET at each station, the variety of crops cultivated in the region was considered and the corresponding contribution was properly accounted. All calculations were made on daily basis as discussed earlier while crop coefficient relevant calculations were made on monthly basis. Later aggregated ET_o or ETP were used to find the monthly values to use with crop coefficients to compute the monthly crop ET values.

Since the growing stages of each crop given in Table 3.4 can vary by region and climate, the data provided by Allen et al. (1998) cannot be directly used. Therefore, the detailed data published by FAO for Ghana and western Africa (http://www.fao.org/agriculture/seed/cropcalendar/welcome.do) was used in this study. For example, the growing seasons for 29 crops are locally adapted to suit the four major agro-ecological zones of Ghana. In addition to the cropping calendar of each crop, the other key information needed was the cropping pattern across Ghana. The distribution of each crop in all 138 districts in 2008 was available from the Ministry of Food and Agriculture, Ghana (http://mofa.gov.gh/site/) to determine the cropping pattern across

Ghana as given in Table 3.4. For this calculation, the representative area of each station was determined using the Thiessen Polygon method. These calculations were conducted on the basis "agriculture is predominantly on a smallholder basis in Ghana" and "about 90% of farm holdings are less than 2 hectares in size" (personal communication with Ministry of Food and Agriculture; SRID, 2010).

For other classical methods, such as HV, TC, and JH methods, the procedure to calculate crop ET is straightforward where crop coefficient computed earlier can be used with the corresponding ET_o.

3.4.5 Comparison of Actual and Crop ET

One strong argument for the use of complementary methods is its' ability to predict regional ET from point observations of meteorological data (Morton, 1983). Classical methods compute point estimates of ETP or ET_o and to compute areal ET, still detailed land cover/use information is needed. In the modified GG model used here, point observations from ten synoptic stations are used to predict ET across Ghana using meteorological data only. If good comparison can be obtained between the ET estimates of the classical methods (which is crop ET here) and the modified GG model (or actual ET), then the capability of the complementary methods to predict regional ET can be confirmed.

Fig. 3.4 shows the average monthly actual ET computed from the modified GG model and crop ET computed from the GR method. The actual ET estimates in most stations are close to those of crop ET in particular during the growing seasons. There is one major exception at Sunyani and another minor discrepancy at Tamale. Also, Kete-Krachi has shown a unique behavior that does not exist in any of the other stations.

Sunyani is the only station where crop ET is always higher than the actual ET. This station exists in a residential area (see Table 3.1), and it is well known that ET of a residential area is less than that of an agricultural area. It is similar to the urbanization effect explained by Morton (1983) as it increases runoff and decreases ET. This argument is proven here too where the modified GG model is capturing the land cover/land use effect using climatic variables only. In essence, the complementary methods represented here using the modified GG model are recognizing the effect of land use/cover on the adjacent atmospheric layer without the details of the soil-plant interactions. A similar effect is noticed at Tamale where crop ET is higher than actual ET in the last half of the year during the growing cycle. This could be simply referred to the “urbanization” effect as Tamale is the capital city of the northern region and the economic hub of northern Ghana. Crop ET is marginally higher than actual ET during the growing season in other semi-arid stations, Navrongo and Wa, indicating that there could be fewer crops that may not actually exist. Kete-Krachi is uniquely different than all other stations. Kete-Krachi is situated at the confluence of the river discharging from the Oti sub-basin and the river discharging from both Black and White sub-basins. Therefore, Kete-Krachi is influenced by the “oasis effect” explained by Morton (1983) where an open water body surrounding the station causing ET to elevate beyond typical values of crop ET. The single exception is when the peak of the growing season is reached in September/October and water on the land surface is abundant. Hence, the difference between actual ET and crop ET at this station could be justified by the additional amount of evaporation from the water bodies in the surrounding area.

In summary, three key observations are made: when actual ET is higher than crop ET, which is the case at Kete-Krachi; when actual and crop ET estimates are equal similar to Wenchi; and when actual ET is smaller than crop ET as with Sunyani. These three stations are almost at the same latitude. Fig. 3.5 shows the areal basemap generated by ArcMap 10 showing the land use pattern of each station. The information shown in Fig. 3.5 clearly shows that Kete-Krachi is surrounded by large water bodies where as Wenchi and Sunyani are not. Based on the discussion made earlier and the information shown in Fig. 3.5, it is clearly shown that the complementary methods proposed through the modified GG model are capable of predicting ET or water loss from the land surface using meteorological data only and independent of land use/cover information.

It is also noticed that actual ET is higher than crop ET in late spring and early summer. It is the onset of the rainfall season where the crops are in the initial stages of growing with a high water demand (high R_n and therefore high ETP). Therefore ET is high during this period. However, this is not the case during the minor rainfall season since soil moisture is still high enough to accommodate the water demand; therefore actual ET and crop ET are almost same during this period. In the fall season, actual ET in many stations is again higher that crop ET due to the end of the growing cycle while the soil is moderately moist.

In this discussion, the reader should keep in mind that many assumptions are made in calculating crop ET using the classical methods. Most importantly, the crop pattern and calendar are presumed to be the same between 2000 and 2005. The minor variations between actual and crop ET can be explained by such assumptions. In addition, the contributing area to each station is delineated by the Thiessen polygons method and the accuracy of this delineation can be improved if more stations are present. This limitation is important especially in southern Ghana where urbanization is higher than the north, less agriculture is present, and the climate is more humid.

3.4.6 Annual ET Estimates

To better understand the ET distribution among the stations, the average annual actual and crop ET estimates and percentage of ET to the rainfall are shown in Table 3.5. The trend that ET decreases with latitude is primarily expected. At Navrongo, the actual ET estimates are in good agreement with all crop ET estimates while Sunyani is the contrary. In general, the agreement between the actual ET and crop ET estimates increases with latitude. The crop ET estimates of GR and AL methods are almost identical as expected.

Comparing actual ET of the modified GG model and crop ET of the GR method, it is found that the absolute difference between the two estimates (as percentage of rainfall) ranges from zero at Navrongo to 27% at Sunyani (Table 3.5 column [13]). The average value of that absolute difference between the modified GG model and the GR method is 12%. This value is still close enough to measurements uncertainty which is typically considered to be around 10%. This finding also indicates that the modified GG model can reliably estimate ET using minimal data and represent areal ET as well. The actual ET estimates of the modified GG model vary between 51 and 74% of the average annual rainfall and the average value is 65%. This value is in excellent agreement with the globally observed average percentage of ET/P ratio of 60 to 65% (Brutsaert, 1982). The crop ET estimates of the GR method range from 52 to 78% of the average annual rainfall with an average of 62%. More statistical metrics are computed to compare the monthly estimates of the modified GG and GR methods. The RMSE ranges from 11 at Wenchi to 32 mm/month at the neighboring station, Sunyani. The average value of RMSE is 22 mm/month which is acceptable given the uncertainty of the methods and the variability of the environments. Knowing that the average Bias is 3.7 mm/month, Sunyani has the minimum Bias of -26 mm/month while Koforidua has the maximum Bias of 21 mm/month. R^2 values vary between 0.34 at Koforidua and 0.83 at Wa with an average of 0.65. As a result, it can be said that the modified GG model is providing regional-scale estimates of ET in the area of study.

The HV method tends to overestimate crop ET compared to the GR method, specifically under humid climates. The TC and JH methods are simulating slightly higher estimates compared to the GR and AL methods among the different climates, respectively. This information indicates that ET in that region is driven by radiation more than temperature. Hence, radiation methods developed under humid conditions outperform the temperature method which was implicitly developed for the study region. Therefore the use of simple methods that requires minimal data can sometimes be a good alternative to the more complex methods such as the P-M equation which is data intensive. In addition, HV method developed for west Africa cannot be readily used elsewhere. Each method constructed to a specific region is subject to verification and perhaps calibration in some cases to be applied elsewhere.

3.4.7 Comparison with Prior Studies

Acheampong (1986) computed ETP from three methods at six synoptic stations across Ghana, whereas Asare et al. (2011) recently estimated ETP at Atomic-Kwabenya site, 20 km north of Accra, using six models. Such comparative studies do not exist for actual ET estimates in the area of study. Furthermore, it is well known that actual ET significantly varies in space and time particularly in Ghana where climate changes with latitude. Therefore, regional studies are important to better manage transboundary water resources of the Volta Basin. Although Oguntunde et al. (2005) verified the complementary relationship between ETP and ET at regional level for the Volta Basin, but they also found that actual ET estimates were high (even higher than rainfall) and the values had to be validated by another method.

Remote sensing provides a good alternative for regional studies that can demonstrate the spatial distribution of ET. A remote sensing technology was applied to estimate actual ET based on Makkink's equation and compared to scintillometer observations from August to December 2002 at three stations; namely Ejura (in humid tropical region), Navrongo, and Tamale (Schuttemeyer et al., 2007). The Scintillometer observations were compared to Eddy Covariance measurements at Ejura and Tamale in another work of Schuttemeyer et al. (2006). In the Upper East Ghana, Compaore et al. (2008) used remote sensing during the dry season 2002/2003 at two spatial scales; MODIS (1000 m) and Landsat (30 m). Another study was conducted using Landsat images at Tarkwa area in southwestern Ghana from January to May 2002 to model actual ET by the triangle method (Aduah et al., 2011). In effect, prior remote sensing studies conducted in Ghana are spatially and temporally confined and more importantly required large amount of data and information for both application of the methods and validation of results.

To further assess the applicability of the modified GG model, the average annual actual and crop ET estimates are compared to the estimates from other prior studies in the region and the results are shown in Table 3.6. It should be mentioned here that average annual crop ET represents the average value of the five crop ET estimates from the different classical methods. First, comparing the estimates of the modified GG method with those of the classical methods, both sets of results have similar average values (793 and 778 mm/year) and percentage of rainfall (i.e., 65%). In addition, the areal averages were calculated for both estimates using the Thiessen polygons and these areal average values are similar to simple average values shown in Table 3.6. However, areal average values cannot be used for comparison purposes with estimates of the prior studies that only used simple average values.

The results show that the estimates from this study are closer to those of both Obuobie (2008) and Wagner (2008) who worked in the White Volta River Basin. However, Carrier (2008) and Martin (2006) overestimated actual ET and both studies used the same method. Alfa et al. (2011) applied a distributed hydrologic model, MIKE SHE, which uses the Kristensen -Jensen (K-J) method to predict ET over the Densu River Basin and their ET/P percentage is close to that of the modified GG model at Koforidua which lies within the same basin. The average annual rainfall of the entire basin for the period from 2007 to 2008 was 1126 mm (Bob Alfa, personal communication) which is much lower than that of 1384 mm at Koforidua station (2000-2005). This justifies the difference in actual ET values of Alfa et al. (2011) and the modified GG model. The remaining two studies by Andreini et al. (2000) and Friesen et al. (2005) are generic studies for the upper basin where climate is semi-arid to hyper arid. The high value of ET/P may be due to areas of high aridity where most rainfall is lost as ET. Each of these studies produce the overall average ET that is close to that of Carrier (2008) whose area of study is much wetter compared to the upper basin. This observation is also shown by the difference in ET/P ratios since the upper basin has much less water available for ET. On one hand, a recent study in the upper part of the basin, specifically southeastern Burkina Faso, had shown that ET/P ratio range from 28 to 32% only (Bagayoko, 2006). On the other hand, those ratios are much higher than those found for land surfaces particularly in parallel regional studies conducted in Africa as clearly shown by Brutsaert (1982). Therefore the ratios cannot be compared to typical values of Ghana. The estimates of the modified GG model are comparable and similar to the average from most prior studies conducted in the same region. More noteworthy is that the results of this work using the modified GG model agrees well with globally known ET/P ratio.

3.4.8 Spatial Distribution of ET

Fig. 3.6 shows the spatial distribution of ET across Ghana using simple Kernel smooth method in ArcMap 10. ET decreases from southeast to northwest, but the trend changes to northeast in northern Ghana. This trend is similar to the distribution of rainfall which is the main driver of ET. There is also strong evidence that Volta Lake is contributing significantly to the water loss in the area which was evident at Koforidua and Kete-Krachi stations. Carrier (2008) conducted a study in northern Ghana and found that the trend is from south-southwest to north-northeast in consistent with the findings of this study.

The polygons shown in Fig. 3.6 are the representative areas of synoptic stations used in this study and the numbers inside each polygon represent the total water loss as ET. The values were calculated by multiplying the area of each polygon by the average annual estimate of actual ET from the modified GG model. The total volume of rainfall is approximately 297 km^3 while the actual ET represents 66% of the rainfall volume which is about 195 km^3. The difference between these two values is the water excess that is available as soil moisture, groundwater recharge, and/or baseflow.

Andreini et al. (2000) performed a water budget analysis for the Volta Basin and found that the average total rainfall over the Volta Basin to be 400 km^3 of which 195 km^3 (or 48.8%) is the share from Ghana. The difference in rainfall of Ghana (which is 297 km^3) and this amount of 195 km^3 is around 100 km^3. This volume of rainfall comes from southern Ghana that is not covered by the Volta River Basin (see Fig. 3.2). Given the high humidity and prevailing tropical climate, rainfall in this southern part is high. Friesen et al. (2005) performed a similar water balance for the Volta Basin and found that the average annual rainfall is 401 km^3 and the average ET accounts to 357 km^3 or 89% of rainfall which is much higher than predicted by this study. The model used by that study was a modified Thornthwaite-Mather and not much details were available from the study. Hence, no obvious reason for this high value can be discussed but compared to all other studies, the ET/P ratio of 89% is too high to be realistic.

3.5 Conclusions

The distinction between actual and crop ET is important for the understanding of total water loss from the land surface as opposed to the water loss from crop related ET. Since most of the synoptic weather stations considered in this study are located in rural watersheds, agriculture is the predominant land use and the calculated ET represents mostly crop ET. In general, the estimates of the modified GG model that represents the complementary methods are in good agreement with crop ET calculated using the classical methods. In selected stations such as Kete-Krachi and Sunyani where other types of land uses such as water bodies and urban areas are present, the modified GG model captured total water loss from all sources confirming the argument that the complementary methods are capable of predicting ET independent of land use/cover information. Most importantly, the modified GG model that uses the complementary relationships requires meteorological data only making the analysis simple and straight forward. Other advantages include the ability to predict regional ET as opposed to localized values making the results more attractive to long-term water resources planning and management.

The results indicate that the actual ET estimates range from 51 to 74% of the total annual rainfall with an average of 65%. The diverse zones of climates across Ghana may justify having this wide range of ET and an average value that complies with the global estimates of 60-65% of rainfall. The spatial distribution shows that actual ET decreases from southeast to northwest direction and that trend switch to northeast in northern Ghana following the rainfall trends. The P-T equation used to compute ETW of the modified GG model is close to the P-M equation used in the GR method and the relative absolute difference of annual values is on average 9%. Comparing the ET estimates of the GG model and the GR method, the average values of RMSE and R^2 over the 10 stations are 22 mm/month and 0.65, respectively. Most importantly, this comparison shows that the modified GG model provides regional-scale estimates of ET from point observations of meteorological data only.

Estimation of actual ET is more challenging and subject to significant changes in space and time given the contrasting climates prevailing in Ghana. The need for a reliable ET model is becoming increasingly important since ET is a key component of the water budget. Although there are many ET studies conducted in this region, yet none of these studies have been rigorously tested and evaluated by ET measurements. There are a few exceptions as cited in this study that are limited in space and time and cannot be used at a national level. Therefore, prior studies cannot be blindly followed and there is a call to building a model that is data simple and can be used at regional scale with the ability to accommodate contrasting physical and climatic conditions. In this need, the modified GG model using complementary relationships is found to be providing reliable and consistent estimates of ET very close to the classical methods used in the past few decades.

References

Acheampong, P.K., 1986. Evaluation of potential evapotranspiration methods for Ghana. JeoJournal 12(4), 409-415.

Aduah, M.S., Mantey, S., Kwesi, E.A.A., 2011. Remote sensing and GIS in modeling actual evapotranspiration: A case study using the triangle method in Tarkwa, South West Ghana. Eur. J. Sci. Res. 62(2), 257-266.

Alfa, B., Hasholt, B., Jørgensen, N.O., Banoeng-Yakubo, B., 2011. Rainfall and water resources of a coastal basin of Ghana. J. Hydrol. Eng. 16(4), 316-323.

Allen, R.G., Pereira, L.S., Raes, D., Smith, M., 1998. Crop evapotranspiration: Guidelines for computing crop water requirements. FAO Irrig. and Drain. Paper No. 56, Food and Agric. Orgn. of the United Nations, Rome, Italy.

Allen, R.G., Walter, I.A., Elliot, R., Howell, T., Itenfisu, D., Jensen M. (Eds), 2005. The ASCE Standardized Reference Evapotranspiration Equation. American Society of Civil Engineers Environmental and Water Resource Institute (ASCE-EWRI).

Andreini, M., van de Giesen, N., van Edig, A., Fosu, M., Andah, W., 2000. Volta Basin Water Balance. ZEF – Discussion Papers on Development Policy No. 21, Bonn, Germany.

Armstrong, R.N., Pomeroy, J.W., Martz, L.W., 2008. Evaluation of three evaporation estimation methods in a Canadian prairie landscape. Hydrol. Process. 22, 2801-2815.

Asare, D.K., Banini, G.K., Ayeh, E.O., Amenorpe, G., 2011. Estimation of potential evapotranspiration for a coastal savannah environment by comparison of different methods. Intl. J. Sustain. Agric. 3(2), 65-70.

Bagayoko, F., 2006. Impact of land-use intensity on evaporation and surface runoff: processes and parameters for Eastern Burkina Faso, West Africa. Doctoral Thesis. University of Bonn, Germany. Ecology and Development Series No. 40.

Bouchet, R.J., 1963. Evapotranspiration reelle et potentielle, signification climatique. Int. Assoc. Sci. Hydrol. Pub. 62, 134-142.

Brutsaert, W., 1982. Evaporation into the Atmosphere: Theory, History, and Applications. D. Reidel Publishing Company, Dordrecht, Holland.

Brutsaert, W., Stricker, H., 1979. An advection aridity approach to estimate actual regional evaporation. Water Resour. Res. 15(2), 443-450.

Budyko, M.I., 1958. The Heat Balance of the Earth's Surface. trs. Nina A. Stepanova, US Department of Commerce, Washington, D.D., USA.

Carrier, M., 2008. Hydrogeological synthesis of Northern Ghana. MS thesis, Avant-Garde University, Canada.

Chiew, F.H., Leahy, C.P., 2003. Comparison of evapotranspiration variables in evapotranspiration maps for Australia with commonly used evapotranspiration variables. Water Resources Bulletin 27, 611-620.

Compaore, H., Hendrickx, J., Hong, S., Friesenc, F., Van de Giesen, N.C., Rodgersd, C., Szarzynski, J., Vlek, P., 2008. Evaporation mapping at two scales using optical imagery in the White Volta Basin, Upper East Ghana. Physics and Chemistry of the Earth 33, 127-140.

De Martonne, E., 1925. Traité de Géographie Physique, tome 1, Fourth ed. A. Colin, Paris.

Davenport, D.C., Hudson, J.P., 1967. Changes in evaporation rates along a 17-km transect in the Sudan Gezira. Agric. Meteorol. 4, 339-352.

Doorenbos, J., Pruitt, W.O., 1977. Guidelines for predicting crop water requirements, FAO Irrig. and Drain. Paper No. 24, 2nd ed., Food and Agric. Orgn. of the United Nations, Rome, Italy.

Doyle, P., 1990. Modelling catchment evaporation: An objective comparison of the Penman and Morton approaches. J. Hydrol. 121, 257-276.

Food and Agriculture Organization (FAO), 1989. Arid zone forestry: A guide for field technicians. Food and Agriculture Organization of the United Nations, Rome, Italy.

Fortin, J.P., Seguin, B., 1975. Estimation de I'ETR regionale a partir de IETP locale: Utilization de la relation de Bouchet a differentes echelles de temps. Ann. Agron. 26(5), 537-554.

Friesen, J., Andreini, M., Andah, W., Amisigo, B., van de Giesen, N., 2005. Storage capacity and long-term water balance of the Volta Basin, West Africa. Regional Hydrological Impacts of Climatic Change - Hydroclimatic Variability (Proceedings of symposium S6 held during the Seventh IAHS Scientific Assembly at Foz do Iguaçu, Brazil. IAHS Publ. 296, 138-145.

Granger, R.J., 1989. A complementary relationship approach for evaporation from nonsaturated surfaces. J. Hydrol. 111, 31-38.

Granger, R.J., Gray, D.M., 1989. Evaporation from natural nonsaturated surfaces. J. Hydrol. 111, 21-29.

Granger, R.J., Gray, D.M., 1990. Examination of Morton's CRAE model for estimating daily evaporation from field-sized areas. J. Hydrol. 120, 309-325.

Hargreaves, G.L., Hargreaves, G.H., Riley, J.P., 1985. Agricultural benefits for Senegal River Basin. ASCE J. Irrig. and Drain. Engr. 111(2), 113-124.

Hobbins, M.T., Ramirez, J.A., Brown, T.C., 2004. Trends in pan evaporation and actual evapotranspiration across the conterminous U.S.: Paradoxical or complementary? Geophys. Res. Lett. 31(L13503), 1-5.

Hobbins, M.T., Ramirez, J.A., Brown, T.C., Claessens, L.H., 2001. The complementary relationship in estimation of regional evapotranspiration: The Complementary Relationship Areal Evapotranspiration and Advection-Aridity models. Water Resour. Res. 37(5), 1367-1387.

Irmak, S., Haman, D.Z., 2003. Evapotranspiration: Potential or reference? Agricultural and Biological Engineering Department ABE 343. Florida Cooperative Extension Service. Institute of Food and Agricultural Sciences, University of Florida.

Jensen, M.E., Burman, R.D., Allen, R.G., 1990. Evapotranspiration and Irrigation Water Requirements. ASCE Manuals and Reports on Engineering Practice No. 70, Am. Soc. Civil Engr., New York.

Jensen, M.E., Haise, H.R., 1963. Estimating evapotranspiration from solar radiation. ASCE J. Irrig. Drain. Div. 89, 15-41.

Lemeur, R., Zhang, L., 1990. Evaluation of three evapotranspiration models in terms of their applicability for an arid region. J. Hydrol. 114, 395-411.

Martin, N., 2006. Development of a water balance for the Atankwidi catchment, West Africa – A case study of groundwater recharge in a semi-arid climate. Doctoral thesis, University of Gottingen. Ecology and Development Series No. 41.

Mawdsley, J.A., Ali, M.F., 1985. Modelling Nonpotential and Potential Evapotranspiration by Means of the Equilibrium Evaporation Concept. Water Resour. Res. 21 (3), 383-391.

Monteith, J.L., 1965. Evaporation and environment, in: 19th Symp. Soc. Exp. Biol., University Press, Cambridge, U.K., pp. 205-234.

Morton, F.I., 1983. Operational estimates of areal evapotranspiration and their significance to the science and practice of hydrology. J. Hydrol. 66, 1-76.

Morton, F.I., 1994. Evaporation research - a critical review and its lessons for the environmental sciences, in: Critical Reviews in Environmental Science and Technology 24(3), Taylor and Francis Group, London, U.K., pp. 237-280.

Nash, J.E., 1989. Potential evaporation and the complimentary relationship. J. Hydrol. 111, 1-7.

Obuobie, E., 2008. Estimation of groundwater recharge in the context of future climate change in the White Volta River Basin, West Africa. Doctoral thesis. University of Bonn, Germany. Ecology and Development Series No. 62.

Oguntunde, P.G., Van de Giesen, N., Andreini, M., 2005. Modeling regional evapotranspiration in the Volta Basin, West Africa: Testing the complementary relationship hypothesis. International Agricultural Research for Development Conference, Stuttgart-Hohenheim, Germany.

Penman, H.L., 1948. Natural evaporation from open water, bare soil, and grass. Proc. Roy. Soc. London A193, 120-146.

Penman, H.L., 1956. Evaporation: An introductory survey. Neth. J. Agric. Sci. 4, 9-29.

Priestley, C.H.B., Taylor, R.J., 1972. On the assessment of surface heat flux and evaporation using large-scale parameters. Month. Weather Rev. 100, 81-92.

Rietveld, M.R., 1978. A new method for estimating the regression coefficients in the formula relating solar radiation to sunshine. Agric. Meteorol. 19, 243-252.

Schüttemeyer, D., Moene, A.F., Holtslag, A.A.M., de Bruin, H.A.R., van de Giesen, N., 2006. Surface fluxes and characteristics of drying semi-arid terrain in West Africa. Boundary-Layer Meteorology 118, 583-612.

Schüttemeyer, D., Schillings, Ch., Moene, A.F., de Bruin, H.A.R., 2007. Satellite-based actual evapotranspiration over drying semiarid terrain in West Africa. J. Appl. Meteor. Climatol. 46(1), 97-111.

Shuttleworth, W.J., 2006. Towards one-step estimation of crop water requirements. Trans. ASABE. 49(4), 925-935.

Shuttleworth, W.J., Wallace, J.S., 2009. Calculating the water requirements of irrigated crops in Australia using the Matt-Shuttleworth approach. Trans. ASABE. 52(6), 1895-1906.

Sophocleous, M.A., 1991. Combining the soil water balance and water-level fluctuation methods to estimate natural groundwater recharge: Practical aspects. J. Hydrol. 124, 229-241.

Statistics, Research and Information Directorate (SRID), 2010. Agriculture in Ghana: Facts and Figures (2009). Ministry of Food and Agriculture, Ghana.

Thornthwaite, C.W., 1948. An approach toward a rational classification of climate. Geographical Review 38(1), 55-94.

Thornthwaite, C.W., Mather, J.R., 1955. The water balance. Publ. Climatol. 8(1), 14-21.

Turc, L., 1961. Estimation of irrigation water requirements, potential evapotranspiration: a simple climatic formula evolved up to date. Ann. Agron. 12, 13-49.

United Nations Environment Programme (UNEP), 1992. World Atlas of Desertification. Edward Arnold, London, UK.

Wagner, S., 2008. Water balance in a poorly gauged basin in West Africa using atmospheric modelling and remote sensing information. PhD Dissertation, University of Stuttgart, Germany.

Walter, I.A., Allen, R.G., Elliott, R., Mecham, B., Jensen, M.E., Itenfisu, D., Howell, T.A., Snyder, R., Brown, P., Echings, S., Spofford, T., Hattendorf, M., Cuenca, R.H.,Wright, J.L., Martin, D., 2000. ASCE standardized reference evapotranspiration equation, in: Evans, R.G., Benham, B.L., Trooien, T.P. (Eds.), Proc. National Irrigation Symposium ASAE. Phoenix, AZ, pp. 209-215.

Xu, C.Y., Singh, V.P., 2005. Evaluation of three complementary relationship evapotranspiration models by water balance approach to estimate actual regional evapotranspiration in different climatic regions. J. Hydrol. 308, 105-121.

Table 3.1. Characteristics of the 10 synoptic stations in Ghana.

Station	Lat. (°)	Long. (°)	Elev. (m)	Rainfall (mm/yr)	T (°C)	RH (%)	S (hr)	U (m/s)	Land cover
Navrongo	10.90	-1.10	201	963	29.3	53.8	8.0	1.5	savanna woodland
Wa	10.05	-2.50	323	1040	28.5	58.3	7.8	1.1	savanna woodland
Tamale	9.50	-0.85	168	1040	28.8	60.3	7.5	1.8	savanna woodland
Yendi	9.45	-0.02	195	1291	28.4	62.7	7.7	0.8	savanna woodland
Bole	9.03	-2.48	299	1157	27.1	66.9	6.9	1.3	savanna woodland
Kete-Krachi	7.82	-0.03	122	1353	28.3	73.2	7.2	0.8	savanna woodland
Wenchi	7.75	-2.10	339	1258	26.5	73.2	6.4	1.0	herb/bush
Sunyani	7.33	2.33	309	1197	26.4	75.3	5.4	2.2	Settlement
Koforidua	6.08	-0.25	166	1384	27.3	77.6	6.1	0.7	herb/bush
Akim Oda	5.93	-0.98	139	1432	27.3	79.2	5.3	0.6	herb/bush

Table 3.2. Climatic class of each station using different aridity indices.

Station		AI_M	Class	AI_T	Class	AI_B	Class	AI_U	Class
Navrongo		24.5	sub-humid	-48.3	semi-arid	1.68	semi-humid	0.52	dry sub-humid
Wa		27.0	sub-humid	-37.0	semi-arid	1.56	semi-humid	0.63	dry sub-humid
Tamale		26.8	sub-humid	-43.0	semi-arid	1.55	semi-humid	0.57	dry sub-humid
Yendi		33.6	humid	-15.5	dry sub-humid	1.28	semi-humid	0.85	humid
Bole		31.2	humid	-24.9	dry sub-humid	1.36	semi-humid	0.75	humid
Kete-Krachi		35.4	very humid	-6.4	dry sub-humid	1.24	semi-humid	0.94	humid
Wenchi		34.5	humid	-6.1	dry sub-humid	1.22	semi-humid	0.94	humid
Sunyani		32.9	humid	-14.4	dry sub-humid	1.19	semi-humid	0.86	humid
Koforidua		37.1	very humid	6.8	wet sub-humid	1.12	semi-humid	1.07	humid
Akim Oda		38.4	very humid	19.1	wet sub-humid	1.02	humid	1.19	humid
Class Definition									
very humid		$AI \geq 35$		$AI > 100$					
humid		$28 \leq AI < 35$		$20 < AI \leq 100$		$0 < AI \leq 1.1$		$AI \geq 0.75$	
sub-humid	wet	$24 \leq AI < 28$		$0 < AI \leq 20$		$1.1 < AI \leq 2.3$		$0.65 \leq AI < 0.75$	
	dry			$-33 < AI \leq 0$				$0.50 \leq AI < 0.65$	
mediterranean		$20 \leq AI < 24$							
semi-arid		$10 \leq AI < 20$		$-67 < AI \leq -33$		$2.3 < AI \leq 3.4$		$0.20 \leq AI < 0.50$	
arid		$AI < 10$		$-100 < AI \leq -67$		$3.4 < AI \leq 10$		$0.05 \leq AI < 0.20$	
hyper-arid						$AI > 10$		$AI < 0.05$	

Table 3.3. Average annual ETP estimates (mm) computed from different methods and the relative absolute difference (RAD) as %.

	[1]	[2]	[3]	[4]	[5]	[6]	[7]	[8]	[9]	[10]
Method	Complementary		Classical						RAD_{GR}	RAD_{AVG}
	Modified GG		ASCE					Avg.	$\frac{\lvert[2]-[3]\rvert}{[2]}$	$\frac{\lvert[2]-[8]\rvert}{[2]}$
Station	ETP	ETW	GR	AL	HV	TC	JH	[3] to [7]		
Navrongo	2662	1623	1862	2386	1905	2102	2161	2083	15	28
Wa	2547	1616	1651	2008	1767	1928	2001	1871	2	16
Tamale	2614	1609	1824	2343	1793	1856	1943	1952	13	21
Yendi	2432	1635	1527	1766	1801	1826	1964	1777	7	9
Bole	2341	1540	1540	1864	1794	1648	1801	1729	0	12
Kete-Krachi	2308	1657	1446	1609	1642	1549	1713	1592	13	4
Wenchi	2105	1497	1341	1530	1576	1460	1514	1484	10	1
Sunyani	2165	1389	1398	1736	1608	1302	1385	1486	1	7
Koforidua	2044	1523	1296	1420	1654	1364	1533	1453	15	5
Akim Oda	1882	1426	1202	1305	1614	1269	1374	1353	16	5
Min	1882	1389	1202	1305	1576	1269	1374	1353	0	1
Avg.	2310	1551	1509	1797	1716	1630	1739	1678	9	11
Max	2662	1657	1862	2386	1905	2102	2161	2083	16	28

Table 3.4. Percentage of crop cultivated in area of each station and related crop coefficients and heights.

Crop percentage (%)																
Station	maize	rice	cassava	yam	cocoyam	plantain	sorghum	millet	groundnut	cowpea	soybean	sweet potato	okra	pepper	tomato	eggplant
Navrongo	10	16	0	0	0	0	13	17	21	13	8	2	0	0	0	0
Wa	16	9	1	12	0	0	17	14	19	11	0	0	0	0	0	0
Tamale	21	10	10	12	0	0	7	10	21	4	5	0	0	0	0	0
Yendi	16	3	11	12	0	0	11	12	19	8	8	0	0	0	0	0
Bole	19	3	14	16	0	0	12	10	18	6	2	0	0	0	0	0
Kete-Krachi	30	6	29	15	2	4	3	4	5	1	3	0	0	0	0	0
Wenchi	29	1	23	24	10	9	0	1	1	0	1	0	0	0	0	0
Sunyani	26	1	26	11	18	19	0	0	0	0	0	0	0	0	0	0
Koforidua	36	0	33	4	6	12	0	0	0	0	0	0	2	4	3	0
Akim Oda	26	1	27	2	15	29	0	0	0	0	0	0	0	0	0	0
Total	229	48	175	108	50	74	64	68	103	43	28	2	2	4	3	0
%	23	5	17	11	5	7	6	7	10	4	3	0	0	0	0	0
Crop coefficients and height (Allen et al., 1998)																
$K_{c\ ini}$	0.70	1.05	0.30	0.50	0.50	0.50	0.70	0.70	0.40	0.40	0.50	0.50	0.60	0.60	0.60	0.60
$K_{c\ mid}$	1.20	1.20	0.80	1.15	1.15	1.10	1.05	1.00	1.15	1.05	1.15	1.15	1.05	1.05	1.15	1.05
$K_{c\ end}$	0.35	0.60	0.30	0.65	0.65	1.00	0.55	0.30	0.60	0.35	0.50	0.65	0.90	0.90	0.80	0.90
h (m)	2.00	1.00	1.00	0.40	0.40	3.00	1.50	1.50	0.40	0.40	0.75	0.40	0.70	0.70	0.60	0.80

Table 3.5. Computed average annual actual or crop ET (mm) and corresponding ET/P ratios as %. Diff. is absolute difference between the percentages in columns [2] and [4].

		[1]	[2]	[3]	[4]	[5]	[6]	[7]	[8]	[9]	[10]	[11]	[12]	[13]
Method		Complementary		Classical										Diff.
		Modified GG		ASCE				Other classical						| [2] - [4] |
Station	Rainfall	ET	%	GR	%	AL	%	HV	%	TC	%	JH	%	
Navrongo	963	584	61	585	61	586	61	647	67	618	64	592	61	0
Wa	1040	686	66	723	69	713	69	808	78	787	76	735	71	3
Tamale	1040	603	58	765	74	784	75	809	78	770	74	702	67	16
Yendi	1291	838	65	670	52	647	50	797	62	746	58	708	55	13
Bole	1157	739	64	683	59	684	59	831	72	714	62	668	58	5
Kete-Krachi	1353	1006	74	776	57	747	55	875	65	830	61	783	58	17
Wenchi	1258	889	71	848	67	836	66	998	79	906	72	810	64	3
Sunyani	1197	612	51	930	78	974	81	1085	91	874	73	773	65	27
Koforidua	1384	1001	72	749	54	724	52	950	69	791	57	763	55	18
Akim Oda	1432	970	68	765	53	737	51	1021	71	814	57	766	53	14
Min	963	584	51	585	52	586	50	647	62	618	57	592	53	0
Avg.	1212	793	65	749	62	743	62	882	73	785	65	730	61	12
Max	1432	1006	74	930	78	974	81	1085	91	906	76	810	71	27

Table 3.6. Comparison of annual ET estimates (mm) and percentage of annual ET to rainfall (%) of this study with results from prior studies conducted in the region.

	Present Study				[1][a]		[2][a]		[3][a]		[4][a]		[5][a]		[6][a]		[7][a]	
Method	Modified GG		Classical methods		Rushton		K-J/ Mike SHE		Rushton and WASIM		WASIM		Ritchie/ SWAT		Water Balance		Thornthwaite - Mather	
Study Area	Ghana		Ghana		Ghana		Densu River Basin		Upper East		White Volta		White Volta		Volta basin		Volta basin	
Period	2000 - 05		2000 - 05		2000 - 05		2007 - 08		2003 - 04		1961 - 00		1986 - 99		1936 - 98		1931 - 95	
ET and ET/P	mm	%	mm	%	mm	%	mm	%	mm	%	mm	%	mm	%	mm	%	mm	%
Station: Navrongo	584	61	606	63	758	79			762	76	739	75	603	74				
Tamale	603	58	766	74	862	83												
Wa	686	66	753	72	891	86												
Bole	739	64	716	62	970	84												
Yendi	838	65	714	55	919	71									910	91	892	89
Kete-Krachi	1006	74	802	59	915	68												
Wenchi	889	71	880	70	1071	85												
Sunyani	612	51	927	77	1006	84												
Koforidua	1001	72	795	57			813	71										
Akim Oda	970	68	821	57														
Average	793	65	778	65	886	80		71	762	76	739	75	603	74	910	91	892	89

[a][1] Carrier (2008), [2] Alfa et al. (2011), [3] Martin (2006), [4] Wagner (2008), [5] Obuobie (2008), [6] Andreini et al. (2000), and [7] Friesen et al. (2005).

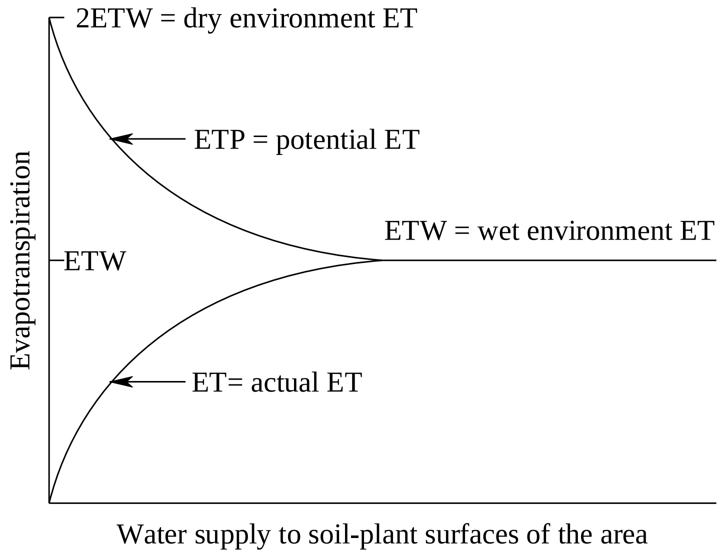

Fig. 3.1. A schematic representation of the complementary relationship between ET and ETP (after Morton, 1983).

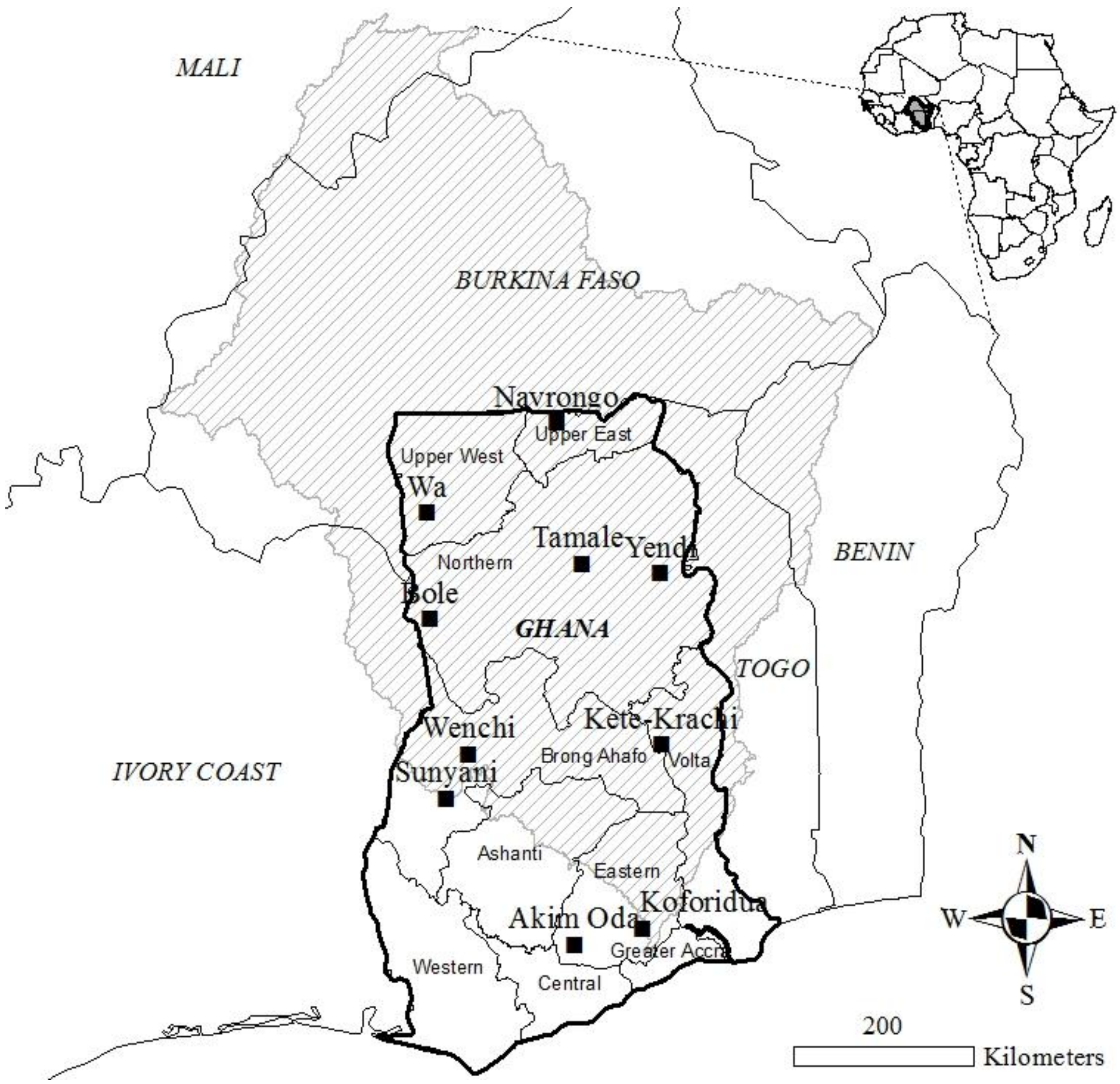

Fig. 3.2. Map of Ghana (within dark solid line) and the Volta River Basin in the hatched area. The dark squares show the synoptic stations used in the study and the interior divisions are administrative regions of Ghana.

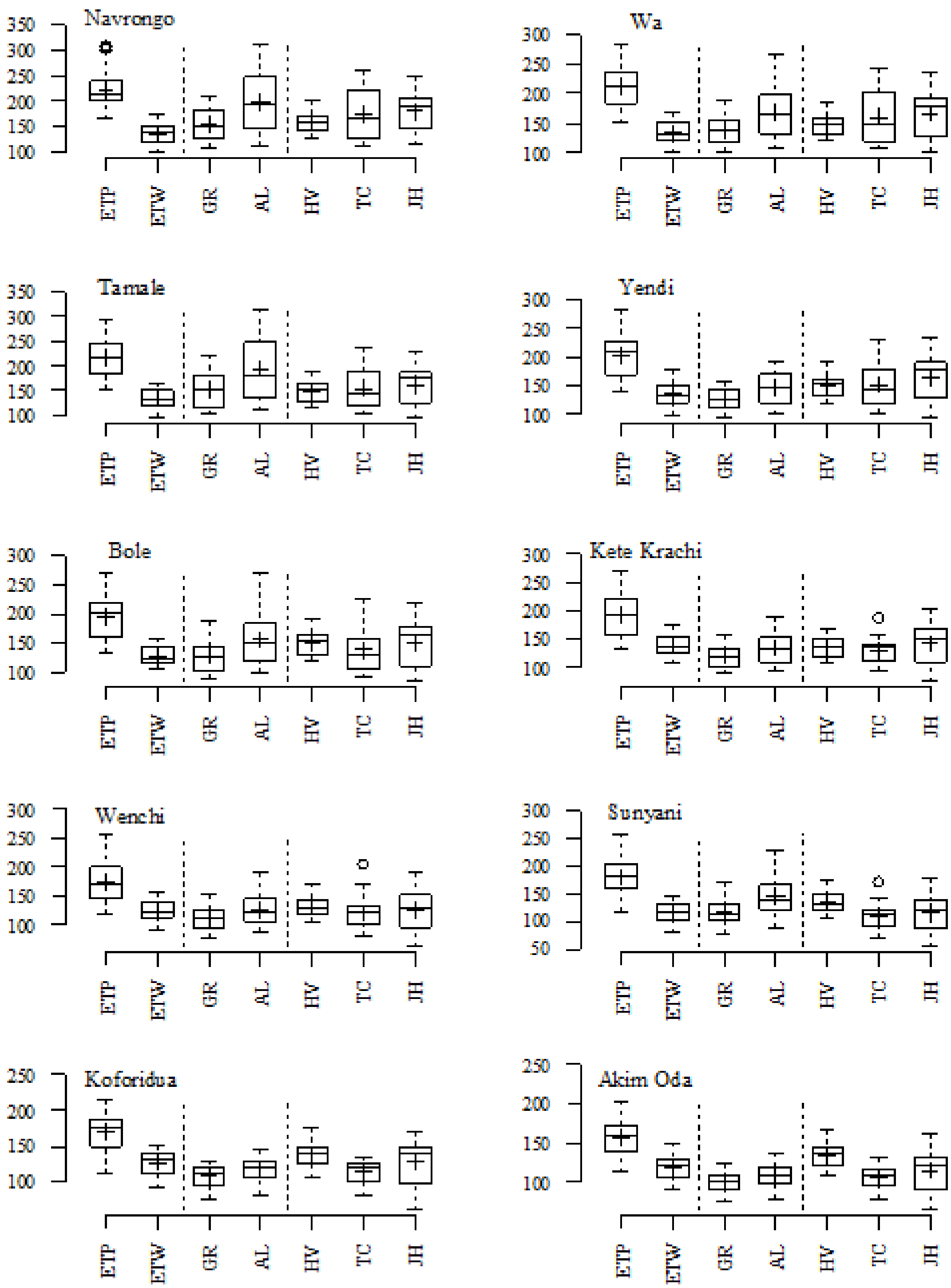

Fig. 3.3. Monthly potential evapotranspiration boxplots in mm (+: average value, ETP: GG model, ETW: GG model, GR: grass ET_o, AL: alfalfa ET_o, HV: Hargreaves ET_o, TC: Turc ET_o, and JH: Jensen Haise ET_o).

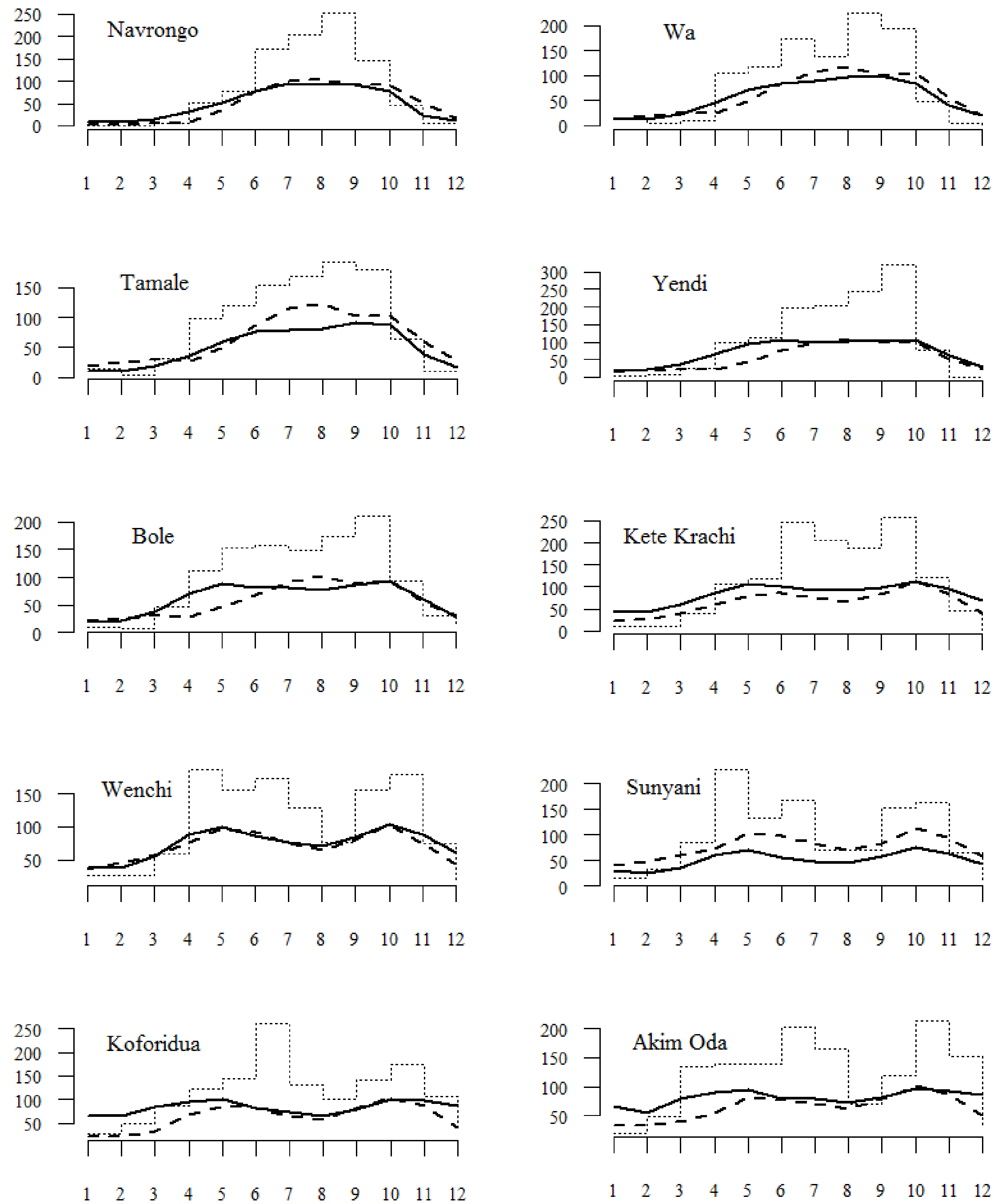

Fig. 3.4. Average monthly actual ET, crop ET, and rainfall in mm (solid line: actual ET of GG model, dashed line: crop ET of GR method, and dotted line: rainfall).

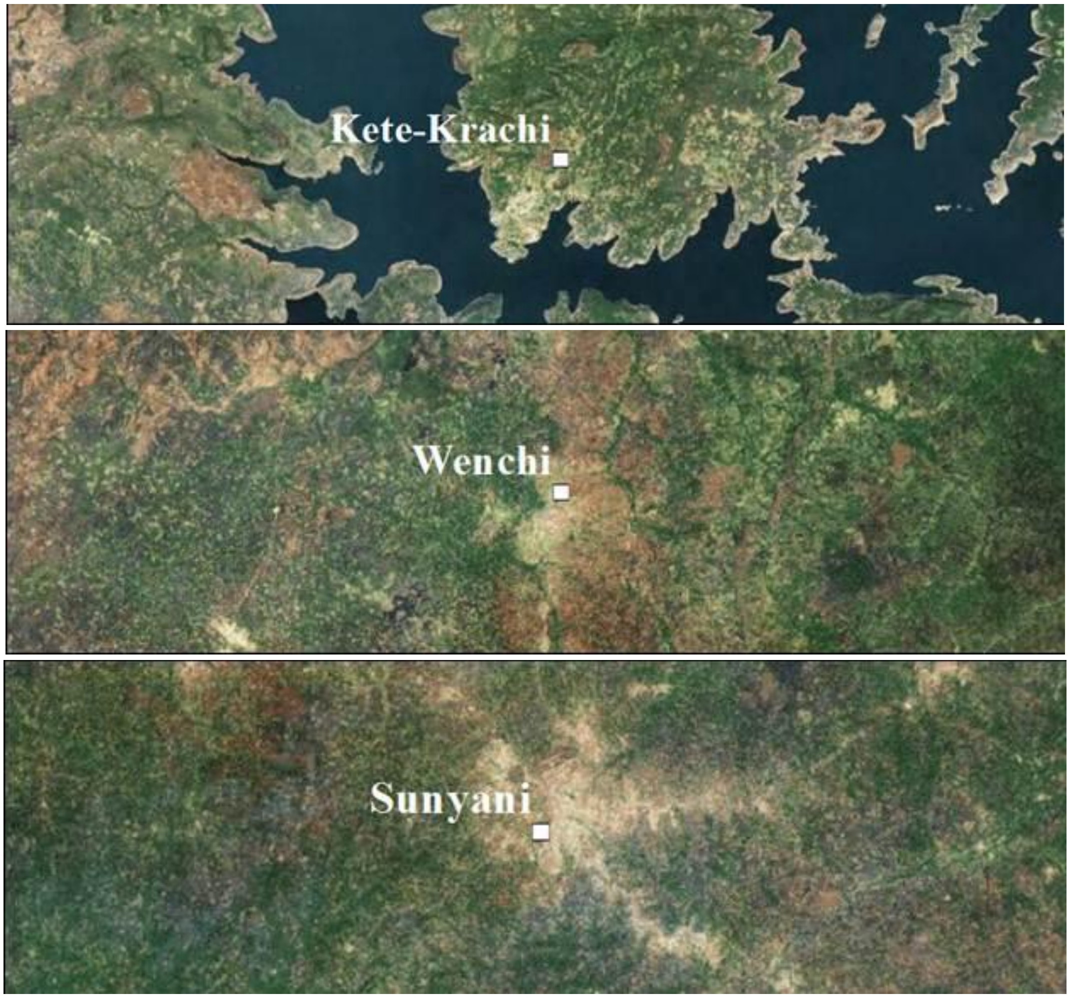

Fig. 3.5. Land use in areas surrounding Kete-Krachi, Wenchi, and Sunyani stations using the areal basemap feature enabled of ArcMap 10 at 1:250000 scale.

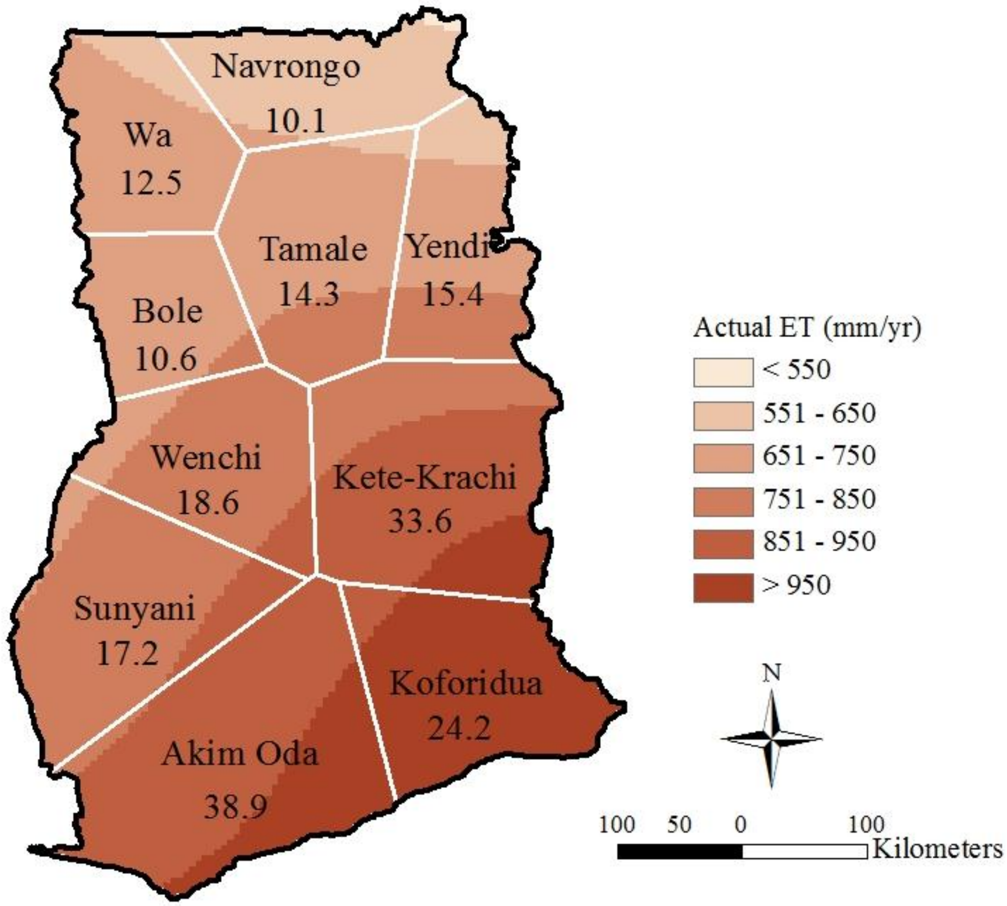

Fig. 3.6. Spatial distribution of actual ET where the polygons show the representative areas falling within each synoptic station. The number inside each polygon is the volume of annual water loss from each area in km^3.

CHAPTER 4

GLOBAL APPLICATION OF A MODIFIED MODEL OF COMPLEMENTARY EVAPOTRANSPIRATION UNDER CLIMATE CHANGE

Abstract

Recent work by Anayah and Kaluarachchi (Chapter 2) proposed a modified form of the Granger and Gray (GG) method (Granger and Gray, 1989) that can estimate regional evapotranspiration (ET) under different land use/class, and physical conditions. The proposed model was validated using measured data from 34 global sites. The purpose of this study is to investigate the applicability of this modified GG model to estimate global ET and corresponding water balance. Gridded climatological data from the Climate Research Unit, University of East Anglia (CRU CL 1.0) of 30 minutes spatial resolution are used. The output of the modified GG model comprises of potential ET, wet environment ET, and actual ET at global scale and at monthly time steps. Using the Thornthwaite water budget, monthly maps of worldwide water surplus (precipitation - ET) are produced. Given the minimal data requirement of the modified GG model to predict ET, the results show good agreement with previous studies conducted globally. Globally, the average annual precipitation, ET, and water surplus are 690, 434, and 256 mm, respectively. In the context of climate change, climatological normal for two general circulation models, CGCM3.1 and HADGEM1, are selected with the moderate A1B emission scenario for two time periods; 2050s (2040-2069) and 2080s (2070-2099). It is found that an annual increase in precipitation of 10% in 2050s will result in 2% increase in ET, however, 15% increase in precipitation in 2080s has insignificant impact on ET (-0.3%). Globally, the ET patterns are not necessarily influenced by the climate change

scenarios instead the regional climate has a strong influence. The overall results prove that the modified GG model is capable of reliably predicting regional ET using meteorological data only and can be used for the assessment of global water resources under climate change.

4.1 Introduction

4.1.1 Prior Studies

The study of the global water budget has been of interest to many over the past few decades (Baumgartner and Reichel, 1975; Berner and Berner, 1987; Budyko et al., 1962; FAO, 1973; L'vovich, 1979; Street-Perrott et al., 1983; Willmott et al., 1985). The need for worldwide estimates of water balance increases for the purpose of planning and management of water resources in large river basins especially when demand for water increases. In operational climatologic and hydrologic practices, such estimates will assist planners and policy makers better understand how the meteorological forcing fields drive land surface climate, and how uncertainties in these fields impact land surface hydrology (e.g., Guo et al., 2006). More recently, global meteorological estimates have become increasingly important as these serve as the reference to predict future projections of climate change in the 21st century using general circulation models (GCM) (New et al., 1999; Willmott et al., 1985).

The increasing attention by people, scientists, and decision makers alike reflects the importance to better assess the future water resources, to sustainably manage these resources, and make appropriate changes in management and practices to minimize climate change impacts. A significant part of that ongoing process is to understand the existing conditions. Decisions made now are undoubtedly influenced by available resources from the past generation and will affect the resources available for the future generations. It should be kept in mind that the importance of global water budget is not restricted to applications in climatology and hydrology only, but has environmental, socioeconomic, anthropogenic, and political implications too (Berner and Berner, 1987; Budyko et al., 1966; FAO, 1973).

The major water fluxes of terrestrial water budget comprises of precipitation, ET, and runoff (Baumgartner and Reichel, 1975; Thornthwaite, 1948; Zektser and Loaiciga, 1993). Groundwater recharge is sometimes embedded into the runoff component at global scale (e.g., Fan and van den Dool, 2004; Fekete et al., 2000), but, few studies focused on groundwater of the water budget. For example, Zektser and Loaiciga (1993) considered the contributions of groundwater to runoff and to the ocean. While precipitation and runoff are usually measured with uncertainties (Yang et al., 2005; Zhang et al., 2010), ET is the residual of these measurements that provide water balance closure (Baumgartner and Reichel, 1975; Zektser and Loaiciga, 1993). Independent estimation of ET, therefore, is the challenging task in the water balance estimations (Zhang et al., 2010) given that 60-65% of global precipitation is lost as ET (Brutsaert, 1982). The importance of correctly estimating ET for regional and global water resources assessment emerged over past few decades when neither computational power nor satellite images were widely available.

Thornthwaite, Mather, and others started developing a global network of precipitation and temperature back in 1947 in an effort to develop a water balance atlas of the world (Willmott et al., 1985). Since the ET estimation method of Thornthwaite (1948) is temperature-based, ET map of the world can be produced using readily available data.

Similar efforts have been made by other scientists to build ET networks that cover all continents (see Willmott et al., 1985). Ultimately, Baumgartner and Reichel (1975) produced the first maps of annual mean ET of the world. Others who did similar work included Budyko et al. (1962) and L'vovich (1979). L'vovich (1979) solved the water balance equation including ET at several levels; the entire earth, the terrestrial and maritime portions, the continents, and the countries.

4.1.2 Future of Global Water Assessment

Currently, remote sensing techniques are used in predicting and mapping ET at large spatial scales, yet, predictions need ground truthing. Eddy covariance (EC) technology measures surface energy fluxes for weather forecasting, irrigation scheduling, and hydrologic modeling (Chavez et al., 2009). The well-known FLUXNET regional networks (Baldocchi et al., 2001) use EC technology to monitor vapor and energy fluxes and data are accessible at no charge (http://fluxnet.ornl.gov/). Therefore, FLUXNET EC systems are commonly used to calibrate, validate, and evaluate hydrologic models, including remote sensing models (e.g., Chavez et al., 2009; Mu et al., 2011; Zhang et al., 2010).

These recent studies can be utilized for cross-comparison with results of the present study. However, upscaling the estimates of such methods to a global level has many difficulties that cannot be neglected. These difficulties include, but not limited to, the following; remote sensing estimates always need secondary data that are not globally available, tower fluxes data should be checked for quality, coverage, and appropriateness of use, and the empirical upscaling of local tower measurements to global scale is unacceptable (Jimenez et al., 2011).

Jimenez et al. (2011) made a comparison study of land surface flux products including satellite-based products, reanalysis fluxes, and off-line land surface model and concluded that global scale studies require "simplified formulations that are adapted to the existing global data sets and are also robust in the face of the data uncertainties." This work was part of the new initiative launched by the Global Energy and Water Cycle Experiment (GEWEX) Radiation Panel (GRP) LandFlux and named "LandFlux-EVAL" (http://www.iac.ethz.ch/groups/seneviratne/research/LandFlux-EVAL). A more specific study on ET fluxes was conducted recently to evaluate different global observations-based ET datasets and IPCC AR4 simulations (Mueller et al., 2011). Given these difficulties, the selection of an appropriate ET estimation method to independently compute global ET is challenging. There are many ET estimation methods discussed in the literature and the methods vary in complexity and accuracy.

Another major limitation in selecting an appropriate method to estimate ET is constrained by the availability of data and this is the reason for the use of simple Thornthwaite method in many studies (Fan and van den Dool, 2004; Fekete et al., 2000; Willmott et al., 1985). Presently, observed meteorological data including temperature, humidity, sunshine duration, wind speed, wet day frequency, and many other variables are readily available and digitally accessible at no charge. Such global datasets are currently available in different accuracies and resolutions (e.g., Jones, 1994; New et al., 1999; Ramirez and Jarvis, 2008). Statistics can be computed and interpolated for inter-station areas using GIS tools enabling researchers to reliably estimate ET and other hydrologic parameters.

There are several classical methods presently available to estimate potential ET whereas estimating actual ET requires detailed local data such as land cover/land use, crop pattern, growing cycle, etc. More detailed description of the methods can be found in the work of (Anayah and Kaluarachchi, Chapter 2). Typically, these classical methods are applicable to predict crop ET from crop covered areas during the growing seasons to manage agricultural water demands. Crop ET is potential ET multiplied by an applicable crop coefficient, which is called the two-step approach (Allen et al., 1998). However, the actual water loss from the land surface is not restricted to crop areas only; instead evaporation happens from open water bodies as well as from open land surfaces with minimal vegetation cover. In water resources planning, the important estimate is the total water loss from the land surface that may or may not include transpiration from crop areas. Since such methods require detailed land cover/use data and information, the use of these methods is difficult given the uncertainties inherent in the input data. A good example of such limitations is the prediction of ET under climate change where expected land cover/land use changes have yet to be projected.

In contrast, the complementary methods, including the Complementary Relationship Areal ET (CRAE) method (Morton, 1983), Advection-Aridity (AA) method (Brutsaert and Stricker, 1979), and Granger and Gray (GG) method (Granger and Gray, 1989), have the potential to provide competitive alternatives to calculate ET using meteorological data. Details of the methods including advantages, limitations, and applications can be found in a prior work of the authors (Anayah and Kaluarachchi, Chapter 2). Still the complementary methods offer a distinct advantage over the classical methods given the simplicity, availability of data, and the ability to estimate total water loss as opposed to crop ET. The complementary methods currently offer the best approach to estimate ET because the methods are simple and adaptable to available datasets according to the LandFlux-EVAL initiative of Jimenez et al. (2011) and Mueller et al. (2011). Another attractive feature of the complementary methods is the applicability in the impact assessment studies under climate change because GCM models typically project meteorological forecasts (precipitation, temperature, etc.).

Studies of climate change impact on ET started two decades ago but focused mostly on potential ET (Arora, 2002; Chattopadhyay and Hulme, 1997; McKenney and Rosenberg, 1993) because it requires meteorological data only. The studies performed so far indicate that ET estimation under climate change is poorly understood (Harmsen et al., 2009; Jung et al., 2010; Nabi, 1998; Remrova and Cislerova, 2010; Thomson et al., 2005). Such a study needs large amounts of field data and has many assumptions producing results with large uncertainties (e.g., Harmsen et al., 2009).

Global warming from increased emission of greenhouse gases will change precipitation and ET patterns worldwide. The increase in ET predicted by many studies still need verification in the light of other studies that show different and sometimes opposite patterns and trends (Harmsen et al., 2009; Nabi, 1998; Remrova and Cislerova, 2010). One reason is that “atmospheric CO_2 increases stomatal resistance which reduces ET” (Thomson et al., 2005). Since then, Thomson et al. (2005) concluded that ET patterns may vary by region more than the climate change scenario. In this regard, caution should be exercised given the large variability and uncertainty of climate change models. The complementary methods are using meteorological data already existing for the current conditions and projected values for a given emission scenario without requiring land surface information such as land cover/land use and soil characteristics. Therefore, the applicability of complementary methods to estimate ET and therefore water balance under climate change is high and attractive.

The concerns related to the original complementary methods have been addressed in a recent study by Anayah and Kaluarachchi (Chapter 2). Additionally, the proposed modified GG model was validated using measured ET data from 34 FLUXNET global sites with contrasting climatic and physical conditions. The purpose of this study is to extend the earlier work and examine the applicability of the proposed modified GG model of Anayah and Kaluarachchi (Chapter 2) to reliably predict the global distribution of ET and corresponding water resources under current and climate change scenarios.

4.2 Data Collection

4.2.1 Meteorological Data

Observed meteorological data that represent the mean monthly terrestrial climatology of the 20th century are required to have gridded seasonal ET estimates. Such global data sets are currently available in different formats and contents and for variable periods and resolutions (Hijmans et al., 2005; Hulme, 1992; Jones, 1994; Mitchell et al., 2004; New et al., 1999; New et al., 2002; Ramirez and Jarvis, 2008; WMO, 1996). Although data of Hijmans et al. (2005) are of high resolution that approaches 30 arc-seconds (latitude/longitude), but these data only provide precipitation, mean, maximum, and minimum temperatures. However, eight climate elements including relative humidity and wind speed are offered with a resolution of 10 arc-minutes by New et al. (2002). Therefore, the selection of appropriate dataset depends on accuracy of the interpolation method, space-time resolution, accessibility of data, and most importantly the purpose of this study.

In this study, the meteorological data of New et al. (1999) were selected for many reasons. Although data of New et al. (1999) are upgraded to 10 arc-minutes (minutes hereafter) resolution (New et al., 2002), but the use of 30 minutes resolution data are still adequate at global scale. Furthermore, the runoff and soil moisture datasets used in this study have 30 minutes resolution. Unlike the data from New et al. (2002), it is noteworthy that the 30 minutes resolution data are accessible as global grids that can be easily imported into the GIS applications.

The data comprise of climatological normals for the "standard" (or baseline) period 1961-1990. The climatological normal which is commonly derived from 30-year averaging period is used as the reference periods for many datasets. In the 20th century, the averaging periods 1901-1930, 1931-1960, and 1961-1990 are selected for climatological normal. However, many datasets in IPCC (2001) and IPCC (2007) are exclusively calculated for the 1961-1990 normals as the reference for the current climatic conditions. Hence, using the "standard" 1961-1990 reference period is preferred over using the more recent 1971-2000 normals which requires recalculating (updating) of many IPCC datasets that would have contained climate change projections (Trewin, 2007). For predictive purposes, scientists are still considering the 1961-1990 normals as a reference period of many GCM models (see Ramirez and Jarvis, 2008).

The nine climate variables included in the data are; precipitation, wet-day frequency, mean temperature, diurnal temperature range, vapor pressure, sunshine, cloud cover, ground frost frequency, and wind speed. The original dataset is provided by the

Climatic Research Unit (CRU), School of Environmental Sciences, University of East Anglia, Norwich, United Kingdom at (http://www.cru.uea.ac.uk/). Yet, these data cannot be easily imported into the GIS environment. Fortunately, the CRU datasets are processed, re-formatted, and provided by several institutions to disseminate good quality data free of charge for non-commercial purposes. For example, gridded data (in GeoTiff and NetCDF format) are supported by the IPCC (http://www.ipcc-data.org/) and 10-year and 30-year meteorological normals are provided for the 20th century. Unfortunately, these data do not include wind speed which is required to calculate ET estimates. To avoid this limitation, an alternative source of data (The Oak Ridge National Laboratory Distributed Active Archive Center - ORNL DAAC) is available as gridded data of precipitation, maximum and minimum temperature, vapor pressure, wind speed, cloud cover, and solar radiation (http://webmap.ornl.gov/). Solar radiation is not available in the original data sources and therefore cloud cover data were used instead. It is worth to mention that data can be downloaded using different spatial projections, resolution, extent, interpolation method, and data format.

Net radiation is calculated using the procedure of the American Society of Civil Engineers (ASCE) method (Allen et al., 2005) because Anayah and Kaluarachchi (Chapter 2) showed the ASCE method is superior to the original method of Morton (1983). It is known that net radiation cannot be computed without temperature, humidity, and sunshine duration (or cloud cover). The qualitative cloud cover data were converted into quantitative sunshine duration data using equations proposed by the CRU scientists who originally processed the raw data maps (Ian Harris, CRU, personal communication).

4.2.2 Runoff Data

Under the umbrella of World Meteorological Organization (WMO), the Global Runoff Data Center (GRDC) in Germany (http://www.gewex.org/grdc.html) provide daily and monthly discharge data for over 8000 stations distributed worldwide. In cooperation with the Water Systems Analysis Group at the University of New Hampshire (UNH), composite runoff gridded data (UNH/GRDC) were developed by combining discharge observations from GRDC with water balance runoff estimated by the UNH team (see http://www.grdc.sr.unh.edu/). These gridded runoff data are deemed to be the "best estimate of terrestrial runoff over large domains" since the data "preserve the accuracy of discharge measurements and simultaneously the spatial and temporal distribution of simulated runoff" (Fekete et al., 2000). It is good that the composite runoff data are in grid format that can be viewed and processed by GIS tools and have spatial resolution of 30 minutes which coincides with the resolution of meteorological data. The water balance calculations are based on Hamon's temperature-based potential ET and Thornthwaite soil moisture budget, and therefore, air temperature, precipitation, land cover, and soil characteristics are required (Fekete et al., 2000). Use of simple complementary methods to estimate ET is justified when there is a lack of other meteorological data across the world. It should be noted that the runoff data belong to the maximum available time series of each worldwide station (Thomas de Couet, GRDC, personal communication).

It should be mentioned that another data source for runoff is the Global Terrestrial Network – Hydrology (GTN-H) website (http://gtn-h.unh.edu/). The GTN-H is a joint project of the Global Climate Observing System, the World Meteorological Organization, and the Global Terrestrial Observing System to host and provide global hydrologic data. This project is sponsored by the UNH team, however, data maps can only be viewed not downloaded. There are many other maps that the Water Systems Analysis Group at UNH offers at regional and global scales (http://www.wsag.unh.edu/).

4.2.3 Soil Moisture Data

Typically precise measurements of soil moisture are expensive and tedious to collect (Hollinger and Isard, 1994). However, large-scale networks of soil moisture measured by remote sensing and other techniques are of coarse resolution in space and time and their accuracies are questionable at global scale (Scipal, 2002). Efforts by Scipal (2002), Wagner et al. (2003), and others have made improvements in soil moisture estimates and developed reliable maps of global soil moisture data (e.g., Naeimi, 2009). The Global Soil Moisture Data Bank (Robock et al., 2000) provides broad archive of in-situ soil moisture measurements that serve as the basis for many research studies. Different models were used to produce global soil moisture data for the 1986-1995 period by the second global soil wetness project (International GEWEX Project Office, 2002). Yet, Guo et al. (2006) showed discussed the sensitivity of soil moisture products to meteorological forcing fields. Therefore, high quality data of long-term soil moisture are not yet available globally.

Fan and van den Dool (2004) produced global soil moisture data for the period from 1948 to 2003. This time period exceeds the “standard” reference period of 1961-1990, yet this represents the highest quality data available presently. The climatological soil moisture gridded data (in GeoTIFF format) were made accessible by Matthew Rosencrans of National Oceanic and Atmospheric Administration (NOAA) (personal communication) for the period 1948-2003. The data are now available at the Global Land Surface Monitoring and Prediction/NOAA site (http://www.cpc.ncep.noaa.gov/soilmst/leaky_glb.htm).

The data from Fan and van den Dool (2004) are given at monthly time steps and 30 minutes spatial resolution. Soil moisture is a function of precipitation, ET, and runoff, but, it is mostly influenced by precipitation forcing. As stated by Fan and van den Dool (2004), ET and runoff parameterizations act as “restoring negative feedbacks on soil moisture anomalies” and “will not cause an accumulating bias or runaway effect in soil moisture.” Given this reasoning, soil moisture data can be used in this work with minimal impact on water balance estimation. Still, ET is estimated using an adjusted Thornthwaite method which depends only on temperature. Groundwater recharge is not explicitly defined and instead embedded in runoff. More importantly, five parameters to estimate runoff were derived using data from few watersheds in Oklahoma from 1961 to 1990, validated using watersheds in Illinois between 1984 and 2001, and spatially assumed constant worldwide (Fan and van den Dool, 2004).

4.2.4 Climate Change Data

In IPCC (2007), current and future projections of many GCM models exist in coarse resolutions. The mismatch between the coarse resolution of these projections and much finer resolution of watershed models can be resolved using statistical and dynamical downscaling approaches with some levels of uncertainty. Many efforts are made to have these high resolution “downscaled” data available (e.g., Mitchell and Osborn, 2005; Ramirez and Jarvis, 2008). Since this study is using data at spatial resolution of 30 minutes, downscaled ClimGen data (http://www.cru.uea.ac.uk/~timo/climgen/#refs) are available and easily downloaded as gridded data from the International Center for Tropical Agriculture (CIAT) in Colombia (Ramirez and Jarvis, 2008) (http://www.ccafs-climate.org/). It should be mentioned that the Pattern-scaling method is used to downscaling GCM projections in ClimGen dataset and more details about the method can be found in Mitchell and Osborn (2005).

For simplicity and demonstration purposes, data from two GCM models only are used in the present study: the UKMO-HADGEM1 model (Johns et al., 2006) and the CCCMA-CGCM3.1 (T47) model (Scinocca et al., 2008). From the existing models in the CIAT dataset, these two models are recent and discussed in the IPCC (2007) report. The emission scenarios SRES-A1B was used in this study and A1B suggests CO_2 emission will approach its maximum levels by 2050s and then lower rates will be emitted (see IPCC, 2001, 2007). A1B is a moderate scenario among the A1 group. The projections represent the climatological normal for a 30-year period such that results can be compared to the baseline scenario. Two time periods are selected for climate change projections with the A1B emission scenario, 2050s (2040-2069) and 2080s (2070-2099).

All forward projections were made based on the baseline of WorldClim data (Hijmans et al., 2005) available at http://www.worldclim.org (Carlos Eduardo, CIAT-CCAFS, personal communication). Downscaled data are maximum and minimum temperatures, and precipitation and other products of temperature and precipitation data while the original ClimGen (Mitchell and Osborn, 2005) data include all meteorological forcing variables required to estimate ET. Data are downloaded at 10 minutes resolution and upscaled to 30 minutes using the Bilinear technique. This lack of data issue can be resolved using many procedures discussed by Allen et al. (2005) and further discussed in the next section.

4.3 Methodology

4.3.1 Complementary Relationship

The complementary methods can estimate potential ET (ETP), wet environment ET (ETW), and actual ET using meteorological data only. In water resources systems, the concept of ETP is widely used to indicate the climate driven water demand that is only governed by atmospheric conditions and not restricted to availability of water on the surface (Fortin and Seguin, 1975). In the complementary methods ETW is ET that would occur if the soil-plant system is saturated and then ET could approach its potential rate, ETP (Granger, 1989). Actual ET, however, is the total water loss from the land surface which may or may not include vegetation, but includes evaporation from water bodies and soil moisture.

The concept of the complementary theory was initially introduced by Bouchet (1963) and states the presence of a complementary relationship between ET from an area and point ETP estimate in that area. The three types of ET used in the complementary methods are mathematically related as

$$ET + ETP = 2ETW \qquad (1)$$

where ET, ETW, and ETP are in water equivalent units (mm/day). In spite of the fact that ET is negatively correlated to ETP as shown in Eq. (1), there is no exact shape of that relationship (see Davenport and Hudson, 1967). Eq. (1) indicates that an increase in ET will be accompanied by an equivalent decrease in ETP, i.e., $\delta ET = - \delta ETP$. In other words, as the surface dries, areal ET decreases causing a decrease in humidity and an increase in temperature of the surrounding air at the same time, and as a result ETP will increase. Therefore ETP is a function of ET in contrast to the model suggested by Penman (1948) where ETP is independent of ET. This latter claim is true for large moist areas when the effect of ET on temperature and humidity is fully developed and ET and ETP are equal, and for small moist areas in which the effect of ET is insignificant (Morton, 1983).

The CRAE and AA methods use the same complementary relationship originally developed as shown in Eq. (1). However, Granger and Gray (1989) modified that relationship as follows:

$$ET + \frac{\gamma}{\Delta} ETP = (1 + \frac{\gamma}{\Delta}) ETW \tag{2}$$

where γ is the psychrometric constant (kPa/°C) and Δ is the rate of change of saturation vapor pressure with temperature (kPa/°C). Hence, Eq. (2) can be reduced to Eq. (1) only when $\gamma = \Delta$.

4.3.2 Modified GG Model

The modified GG model proposed by Anayah and Kaluarachchi (Chapter 2) is an enhanced version of the complementary methods in which two significant changes are made to the original GG method. It is found that the complementary relationship shown in Eq. (1) can precisely describe the behavior of ET fluxes better than the more generic expression derived in the original work of Granger and Gray (1989), i.e., Eq. (2). More importantly, the predictive power of the GG method is improved when the Priestley and

Taylor (1972) equation (P-T) shown in Eq. (3) is used to calculate ETW instead of the Penman (1948) equation used in the original GG method.

$$ETW = \alpha \frac{\Delta}{\gamma + \Delta}(R_n \quad G_{soil}) \tag{3}$$

where α is the coefficient of the P-T equation and equals to 1.28, R_n is the net radiation in mm/day, and G_{soil} is the soil heat flux density in mm/day. Again, the procedure described by Allen et al. (2005) is used to calculate R_n for actual ET estimates. Monthly data required to calculate R_n are simply: minimum air temperature (T_{min}), maximum air temperature (T_{max}), vapor pressure (e_a), and cloud cover (cld). Soil heat flux (G_{soil}) density is computed at monthly time periods using the procedure described in Allen et al. (2005) which requires T_{min} and T_{max} of both the previous and future months.

In the GG method, two new parameters were identified and empirically correlated together; relative drying power (D) and relative evaporation (G) shown in Eq. (4) and Eq. (6), respectively. Parameter D indicates the dryness of the surface, i.e., D increases with dryness of the surface. Parameter G is ET that occurs under similar wind and humidity conditions from a saturated surface at its actual temperature (Granger and Gray, 1989). The term E_a in Eq. (5) represents the aerodynamic ET that is generated by large scale advection effects. It should be mentioned that Eq. (7) was empirically derived using data from two stations in a semi-arid region of Western Canada. Granger and Gray (1989) claimed that it is independent of land use.

$$D = \frac{E_a}{E_a + R_n} \tag{4}$$

$$E_a = 0.35(1.0 + 0.54U)[(e_s - e_a)] \tag{5}$$

$$G = \frac{ET}{ETP} \tag{6}$$

$$G = \frac{1}{1 + 0.028e^{8.045D}} \tag{7}$$

where E_a is the drying power of air in mm/day, U is the wind speed at 2 m above ground level (m/s), e_s is saturation vapor pressure at T (mm Hg), e_a is the vapor pressure of air (mm Hg). Substituting ETP of Eq. (6) in Eq. (1) will provide an estimate of ET in the modified GG model as shown in Eq. (8).

$$ET = \frac{2G}{G + 1} ETW \tag{8}$$

4.3.3 Soil Moisture Budget

The soil moisture budget of Thornthwaite (1948) states that

$$\frac{\delta w}{\delta t} = P - ET - S \tag{9}$$

where $\delta w/\delta t$ is the change in soil moisture of the root zone (mm/day), P is precipitation (mm/day), ET is evapotranspiration (mm/day), and S is water surplus or excess (mm/day). For annual time steps, $\delta w/\delta t$ will approach zero such that S = P – ET. Water surplus needs further explanation. When there is water surplus (S > 0), the water supply (P) is basically larger than both the water need (ET) and reserve ($\delta w/\delta t$) and all water demands will be fulfilled accordingly. Initial abstractions from precipitation include interception, surface storage, infiltration (USDA-SCS, 1972), and immediate evaporation.

At this stage, infiltration is filling soil moisture storage that is consumed earlier (Thornthwaite, 1948). Then, the water surplus will generate surface and subsurface runoffs from the root zone (Willmott et al., 1985) and recharge groundwater as well (Thornthwaite, 1948). In other words, both runoff and recharge will increase accordingly.

The opposite of water surplus is simply water deficiency where elevated water demands exist. Higher water demands, mainly higher ET, indicate consuming available water on the surface and water reserved in the root zone. Water deficiency may also cause groundwater levels to lower because Chen and Hu (2004) showed that shallow groundwater contributes to ET at the surface. When ET is higher than precipitation, there are other sources of water available on the surface. A good example is irrigation where water is available from extracted groundwater, treated wastewater, reservoirs and adjacent water bodies (e.g., lakes), or any other source such as desalinated sea water. As a result, water deficiency can be interpreted as the higher water requirements (demands) of crops cultivated in that region beyond water availability from soil moisture and instead provided from other sources. The land surface model shown by Eq. (9) reflects climate affinity to water surplus or deficiency according to the physical characteristics of land cover/land use, soil properties, and “the existence of rivers, floods, lakes, or deserts” as mentioned by Thornthwaite (1948). In conclusion, the definition of water deficiency can be understood and interpreted in different ways.

Fekete et al. (2000) used earlier water budget equation to predict runoff and indicated that water surplus includes both “runoff and/or recharge.” However, there is no mention of recharge in this definition. A similar approach was taken originally by Thornthwaite (1948) when discussing water surplus in the soil moisture budget with runoff measurements from small watersheds in diverse climates in North America. In effect, the runoff component comprises surface runoff, subsurface runoff, and baseflow (or seepage). A similar distinction of runoff in the water balance equation was made by Fan and van den Dool (2004). They defined runoff to be the sum of surface runoff, base runoff, and loss to groundwater. The authors explained positive $\delta w/\delta t$ to signify the possibility of recharge occurrence. The reserve or stored soil moisture may end as recharge to the aquifer system, subsurface runoff, or ET to the surrounding atmosphere.

In the development of global scale models using grid-by-grid calculations, flow routing, for instance, is not considered. The time offset between the different hydrologic processes is also not considered. Having a rainfall storm will neither generate an immediate runoff nor change in soil moisture content. In addition, the snow-cover budget (accumulation and melt) is excluded in this study as its effect on ET estimation is minor (Willmott et al., 1985). As a result, the impact of this approach is minimal on regional ET estimates using the complementary methods in which the interactions of atmosphere with the soil-plant system will be completely developed.

4.3.4 Global Circulation Models

As mentioned earlier, the data projected from GCM models are only temperature and precipitation. The three missing climatic data for ET estimation using the complementary methods are: dew-point temperature to calculate the actual vapor pressure, the sunshine duration to compute the incoming short-wave solar radiation, and the wind speed to estimate aerodynamic ET. There are many procedures to predict these missing climatic data as explained by Allen and others (Allen, 1996, 1997; Allen et al., 1998, 2005).

4.3.4.1 Dew-point temperature

There is a relationship between the minimum and dew-point temperatures as shown in Eq. (9).

$$T_{dew} = T_{min} - K_o \tag{9}$$

where T_{dew} is the dew-point temperature, T_{min} is the minimum air temperature, and K_o is a constant that equals 2 to 4°C in semiarid and arid climates and 0°C in sub-humid and humid climates (Allen et al., 2005). The constant K_o is the difference between the two temperatures and this difference may approach 20°C and more as aridity increases (Allen, 1996). Since relative humidity data from New et al. (1999) dataset are available, the actual vapor pressure (e_a) can be calculated from which T_{dew} can be computed at every grid (30 minutes cell) at each month. As K_o becomes a characteristic of the climatic conditions at a given location, it is reasonable to assume that the difference between T_{dew} and T_{min} is similar between the current and future times. Harmsen et al. (2009) used a simple procedure assuming that K_o equals to 0°C in two humid sites and 2.9°C in humid sites.

4.3.4.2 Sunshine duration

Sunshine duration is used to compute the incoming short-wave solar radiation which can be calculated using different equations each requiring different input data (Allen et al., 2005) as shown in Eq. (10) and Eq. (11).

$$R_s = \left[a_s + b_s \frac{n}{N}\right] R_a \tag{10}$$

$$R_s = k_{Rs} \sqrt{(T_{max} - T_{min})}\, R_a \tag{11}$$

where R_s is the solar radiation (mm/day), n is actual sunshine duration (hour), N is maximum possible duration of sunshine hours (hour), R_a is extraterrestrial radiation (mm/day), a_s is a constant equals to 0.25, b_s is a constant equals to 0.5, T_{max} is maximum temperature (°C), T_{min} is minimum temperature (°C), and k_{Rs} is adjustment coefficient that equals 0.16 for interior locations and 0.19 for coastal locations (Allen et al., 2005). Allen (1997) discussed the Hargreaves-Samoni equation (Eq. 11) in more details to predict k_{Rs} properly. Since sunshine duration is calculated from cloud cover data from the dataset of New et al. (1999), it is possible to solve for k_{Rs} at each grid. Therefore, k_{Rs} becomes a characteristic of the location and assumed constant for future scenarios. Harmsen et al. (2009) used Eq. (11) with recommended values of Allen et al. (2005).

4.3.4.3 Wind speed

Wind speed is required to estimate the aerodynamic ET which plays an important role in advective environments. However, this variable is more complex than others as there is no direct correlation to meteorological variables. In the work of Allen et al. (2005), wind speed was qualitatively classified into light, light to moderate, moderate to strong, and strong wind speed, and each class was assigned an average value of wind speed. However, variations in wind speed diminish when averaged over times larger than a day (Allen et al., 2005). The impact of wind speed on global land ET was found to be of less important than other parameters (Jung et al., 2010). Therefore, instead of using a single value (average) for each month, it is possible to use available wind data at monthly time steps for current conditions and preserve spatial correlations among gridded data. It was decided to use current wind speed data given that variations on monthly basis will be insignificant.

Furthermore, Harmsen et al. (2009) indicated that “uncertainties in the assumptions made relative to the parameters are less than the uncertainties associated with the future climate predictions, and therefore, a more precise parameterization may be unwarranted.” Nevertheless, once those data are downscaled, results can be updated accordingly.

4.4 Current Conditions

4.4.1 Global Estimates

Typically, “Global” means the whole globe including land and oceans. In the present study, however, only the land (terrestrial) surfaces are considered except Oceania and Antarctic areas.

4.4.1.1 Wet environment ET

As shown in Fig. 4.1, the inter-annual variation of ETW is represented by the seasonal pattern of cumulative ETW across 3-month intervals. ETW is driven by the same meteorological forcing fields controlling the net radiation, namely temperature, humidity, and sunshine duration. Temperature is the most important that drives ETW. At the same time, climate can be lumped into “temperature” in particular when classifying the different climates. Therefore, there is indirect evidence that ETW is a function of latitude which governs the ETW cycle through the year. This is simply because latitude exerts a large control on the prevailing climate by dictating sunlight amount and intensity. ETW is a measure of climate driven water demand that is only governed by atmospheric conditions. Therefore, ETW can capture these climatic patterns dictated by latitude from the meteorological fields. There is an obvious inter-annual variation of ETW in the temperate zones (23.5 - 66.5° N and S) and in the tropics (23.5° S to 23.5° N). The tropics are exposed to high sunlight intensity for extended periods in a persistent manner making ETW high all year round. The variation is minor in the subarctic zone and almost nonexistent in the arctic zone where highest-inclined, least-intense radiation exists.

On a monthly basis, the average ETW ranges from 45.1 mm/month in December to 112.3 mm/month in July with an average of 71.9 mm/month. It is noticed that the highest monthly ETW which is 213.6 mm/month in July happens at Ras Al-Khaimah area in the United Arab Emirates. This location is in the temperate zone and not in the tropics. It is clear from Fig. 4.1 that the season of the highest water demand is June through August in which the average ETW is 316.6 mm while the December through February season has the least demand with an average ETW of 135.8 mm. The highest annual ETW is 2013.7 mm which occurs at Bosaaso area in Somalia. It is noticed that the area surrounding the Gulf of Aden particularly the Horn of Africa is experiencing the highest levels of ETW annually and the elevated levels of ETW are obvious across every season.

4.4.1.2 Actual ET

Fig. 4.2(a) shows the spatial distribution of annual ET worldwide computed using the proposed modified GG model. Here, the notion that ETW reflects the water demand should be kept in mind. Apparently, the actual ET is a function of both the energy required for ET in the surrounding atmosphere and the water available at the underlying surface. Therefore, ET is governed by the net effect of water demand and supply that describes the actual amount of water available to evaporate and transpire.

Accordingly, availability of water (in any form) will not necessarily result in elevated values of actual ET, and on the other hand, high energy is not enough in some cases to increase ET in that area. Again, it is the net balance between water supply and demand. The comparison will be made between areas of low ET, namely Greenland and North Africa. Both areas share low values of ET and have contrast climates. Greenland is in the extremely cold arctic zone while North Africa is in the critically hot temperate zone. In Greenland, precipitation (mostly snow) is much larger than that of North Africa, yet, sunlight duration and intensity is much lower such that it is not enough to evaporate (or sublimate) the large masses of snow. Solar energy in North Africa is plenty, yet, it has low precipitation rates. The Arabia desert shares the same conditions of North Africa. Australia is also known as one of the driest continents. It is expected to have high ET estimates in the tropics across Asia, Africa, and South America given the high water supply and demand. Similar trends were found by Zhang et al. (2010).

Zhang et al. (2010) estimated global monthly ET from 1983 to 2006 using remote sensing. They used a modified Penman-Monteith equation with GIMMIS normalized difference vegetation index for ET and the P-T equation to calculate open water evaporation. Data are accessible on the web (http://ntsg.umt.edu/project/et) at two spatial resolutions; 1 degree and interpolated to ~4 minutes. In ET calculations, "Barren" lands of North Africa, Middle East, Greenland, and large areas of Asia between Mongolia and Caspian Sea were excluded while water bodies were included. It is noticed that these ET estimates are the only ones published by the ORNL DAAC database.

In Fig. 4.2(b), a spatial comparison between estimates of ET from this study and estimates (ET_{Zhang}) of Zhang et al. (2010) is made as a relative difference percentage. It is noticed that ET is underestimated in all areas surrounding "Barren" lands. However, it is noticed that areas where overestimating takes place are those experiencing both moderate and high values of gradients in precipitation. Availability of precipitation suggests that plant cover in the underlying land will produce high rates of ET. It should be noted that regional ET cannot be easily predicted since it depends on many drivers such as precipitation, radiation, temperature, humidity, etc. and each acting differently. Teuling et al. (2009) found that trends in ET depend mostly on radiation in Central Europe while not in North America where precipitation is the major driver of ET trends.

The relative difference has an average value of -4.2% and areas with values of ±25% (in white) are dominating globally except in Australia. Since the two methods used here are different, it is not expected to observe a perfect match. Similar and much higher differences were found when Hijmans et al. (2005) compared precipitation data they had with those of New et al. (2002). Therefore, the values and trends of annual ET between the results of this study and Zhang et al. (2010) are in good agreement. The Environmental Change research Group at University of Oregon (http://geography.uoregon.edu/envchange/) has a website with global climate animations of ET (ET_{Oregon}) and other components of water and energy balance cycles. However, authors could not access these data in digital format for comparison. A visual comparison with ET_{Oregon} shows similar ET trends and magnitude.

This study estimated the global average annual ET is 434 mm which is 63% (ET/precipitation (P) ratio) of average annual precipitation of 690 mm. These estimates compare well to the ET/P ratio values of 60-65% found worldwide by Brutsaert (1982). In addition, Baumgartner and Reichel (1975) found average annual ET and P to be 480 and 746 mm, respectively, with an ET/P ratio of 64%. Almost identical values were found by FAO (1973). L'vovich (1979) found higher values of average annual ET and P of 540 and 834 mm, respectively because the author excluded the areas of Greenland, and the Canadian Arctic Archipelago, but still predicted an ET/P ratio of 65%. The average annual ET is expected to be lower than that of 539.3 mm/year predicted by Zhang et al. (2010) since that work ignored large land areas of low ET values as mentioned earlier. In that work, Zhang et al. (2010) predicted an ET/P ratio of only 60%. The Cayenne area in French Guiana has the highest ET value of 1493.8 mm/year. Zhang et al. (2010), however, found that the largest average ET occurs in the Evergreen Broadleaf Forest biome that consists of six stations of which two stations are located in French Guiana and Brazil.

4.4.1.3 Water Surplus (S)

Globally, the average annual S is 256 mm which matches perfectly with the D value of 266 mm predicted by Baumgartner and Reichel (1975). In that work, D is the discharge (or runoff) which is simply P – ET or S in the present study. Therefore the estimates of S can be compared to the composite runoff estimates of Fekete et al. (2000) mentioned earlier. Fig. 4.3(a) shows the distribution of S worldwide on annual basis while the S anomalies between estimates of Fekete et al. (2000) and this study are shown in Fig. 4.3(b).

Fig. 4.3(a) shows ET exceeding P as expected in arid areas in the Gulf of Aden which experiences elevated values of ET during the year. The zone of tropics is receiving excessive precipitation and therefore have high S. Underestimation in Fig. 4.3(b) mostly occurs when negative values of S are compared to S_{Fekete} runoff estimates that are kept above zero. Although North Africa and Middle East have negative values in the mid of winter season (i.e., January) on contrary to the expectation, these values are low and close to zero reflecting dry soil moisture conditions. Furthermore, water deficiency or negative

S values dominate in the Northern Hemisphere and vice versa in the Southern Hemisphere. Water surplus is mostly driven by precipitation. It should be kept in mind that since S is the residual of the water budget components, uncertainties in both precipitation measurements as well as estimates of ET and $\delta w/\delta t$ can influence the accuracy of S estimates. Again, uncertainty in precipitation can only be responsible for any abnormal anomalies such as those in the Middle East and South America.

Since the runoff estimates of Fekete et al. (2000) were originally derived from runoff observations, these estimates could be used in the water balance equation to calculate groundwater recharge if needed. Therefore, Fekete et al. (2000) estimates were compared to the S estimates of the present study. The consistency in S estimates is prominent and trends are acceptable when compared to the work of Fekete et al. (2000) in particular where anomalies around ± 250 mm/year can be considered reasonable.

4.4.2 Hemispheric Scale Estimates

Given the results discussed so far, the next set of questions is; How does the water cycle look in the two Hemispheres? Are there obvious inter-annual variations in the components of water budget? To answer these questions, the monthly average values of water budget components will be calculated for each month for both the Northern and Southern Hemispheres (Fig. 4.4) and the global water cycle results are also added to Fig. 4.4.

In the Northern Hemisphere, the annual values of P, ET, and S are 587, 387, and 200 mm, respectively. In the Southern Hemisphere, the annual values of P, ET, and S are 1110, 627, and 483 mm, respectively. These results show that the ET/P ratios are 66% and 56% in the Northern and Southern Hemispheres, respectively. Baumgartner and

Reichel (1975) found that the ET/P ratio is 64% for both Hemispheres. They also found S annual values of 243 and 316 mm in the Northern and Southern Hemispheres, respectively. The annual values match better in the Northern Hemisphere.

Undoubtedly, the global water cycle is highly influenced by the Northern Hemispheric cycle. Globally, precipitation is slightly fluctuating around its average (57.5 mm/month) except from May to August (almost JJA season) when it approaches the maximum similar to ET with a pronounced inter-annual cycle. Temperature in particular which indicates available energy in the land atmosphere is the driver for such a trend. The trend is exactly the opposite from November through February (almost DJF season). Therefore, one can infer that S will be the minimum during the JJA season. Positive S values in Fig. 4.4 indicate the existence of runoff and/or recharge throughout the year. It is noticed, however, that the ET/P ratio ranges from 41% in December (average temperature is -0.3°C) to 87% in May (average temperature 12.4°C). In May, the soil water reserves are used as $\delta w/\delta t$ values are negative for the last few months indicating dry conditions. Hence, the increase of precipitation will result in increased ET.

Comparing the results of Northern and Southern hemispheres, the annual cycle is more prominent in the latter as Fan and van den Dool (2004) found but not for ET. The precipitation data used in Fan and van den Dool (2004) study are considerably different than data used in this study. The trends in almost all components of the water budget in the present study and Fan and van den Dool (2004) study agree reasonably well. ET values are underestimated by Fan and van den Dool (2004) and this underestimation results in larger amounts of runoff compared to the S estimates of the present study. This is obvious in the Northern Hemisphere where runoff behavior is different in the months of the MAM and JJA seasons.

4.4.3 Continental Scale Estimates

It is important to determine the share of each continent to the total water budget. In Table 4.1, the average annual values of P, ET, and S are computed and compared to estimates of other studies.

It is clear that the other two studies are close to each other. The present study is in good agreement with the results of Baumgartner and Reichel (1975) and FAO (1973). The difference in ET/P ratios ranges from 1 to 11% with an exception in Australia. The ET estimates of the other two studies are much higher than that of the present study and the discrepancy cannot be easily justified. When boundaries of Australia are defined, none of the three studies considered the surrounding oceanic islands under which humid climate prevails. A possible explanation is the minimal knowledge of hydrology of Australia in the past and the elevated uncertainty of the modified GG model in such dry regions. North Africa is another example of arid regions where the ET estimates are relatively good. The difference in ET/P approaches 11% for South America. However this value is acceptable for the wettest continent in the globe where uncertainties in precipitation and other ET drivers may be significant. Another example of a humid continent is Europe where ET/P ratio of the present study matches with the estimates of the other two studies as shown in Table 4.1. Overall, Africa has the highest ET/P ratio while South America has the lowest at the continental scale. All studies agree that South America has the highest water surplus across all continents.

4.4.4 Latitudinal Patterns

It is interesting to explore the latitudinal patterns of the water budget and the ET/P ratios (Fig. 4.5). For this purpose, globe is divided into latitudinal slices each of 10° height starting from 60-50° S slice up to 80-90° N. The average annual value of the variables of interest over the latitudinal slice is calculated and plotted on the center of the slice. For example, average annual precipitation at 80-90° N slice is 171 mm and this value is plotted at 85° N and so forth.

The values of the Baumgartner and Reichel (1975) study also added to the plots (dashed line) for comparison. Overall, the two estimates are comparable to each other and agree over many latitudinal slices with the exceptions at the two extreme climates (polar and tropical zones). In tropical areas of high precipitation, the discrepancy in ET estimates is also high (Fig. 4.5(b)). This discrepancy can be measured by the difference between the two ET/P ratios. The value of this difference ranges from -16 to 50% with an average value of 7%. It should be mentioned that the value of 50% takes place at the arctic zone where ET of the modified GG model exceeds precipitation ($ET/P_{80\text{-}90° N}$ = 105%) as shown in Fig. 4.5(d). In Berner and Berner (1987), S is plotted over the continents and oceans. Berner and Berner (1987) found that S is negative in the subtropics (15° to 30° N and S) and the two poles.

The land area of each latitudinal slice varies and therefore presenting the water budget components in water equivalent units as depths of water (in mm) could be ambiguous. The distribution of land areas and volume of water for each component in every latitudinal slice is shown in Table 4.2. To compare the share of each component in each latitudinal slice, the volumes in percentage are also given in Table 4.2. As expected, the tropical zone between 10° S and 10° N has the highest share for all components of the water budget. Almost 29% of P, 22% of ET, and 41% of S resides at this latitudinal slice. Therefore it is important to have good estimates of water balance in the tropics given the significant contribution to the global hydrologic cycle. While the 60° - 70° N latitudinal slice covers the largest land area (>16%), the share is almost 10% for each component of the water budget at that slice. The total land area of earth as computed here is higher than the commonly-known number of ~148,900x10^3 km^2. The reason is the relatively coarse resolution (30 minutes) used in the calculations in which cells near coastal boundaries may include the adjoining water bodies.

4.5 Future Projections

The two GCM models used in the present study are: the UKMO-HADGEM1 (HADGEM) of Johns et al. (2006) and the CCCMA-CGCM3.1-T47 (CGCM) of Scinocca et al. (2008). The two time periods considered in this study are: 2050s (2040-2069) and 2080s (2070-2099). Therefore, the climate change scenarios presented here are (a) HADGEM-2050, (b) CGCM-2050, (c) HADGEM-2080, and (d) CGCM-2080.

Fig. 4.6 shows the anomalies of annual estimates of ET and S for the four climate change scenarios. The results show that there is a general increasing trend of ET in the arctic and subarctic zones in addition to large areas of Europe. Almost all the remaining parts of the earth are experiencing a decrease in ET.

The annual ET in the 2080s is less than that of the 2050s and this observation complies with the A1B emission scenario where greenhouse emissions will be reduced after 2050s. In general, there is no significant difference between the two GCM models. In the United States, the annual ET produced by HADGEM is less than that of CGCM in both time periods. The CGCM model is underestimating annual ET in West Africa when compared to the HADGEM model. Overall, it is noticed that the variations in ET globally are not significant given the moderate greenhouse gas emissions of the A1B scenario.

For the annual anomalies of S, it is obvious that S is highly influenced by the amount of precipitation. It is interesting to see the discrepancy in S estimation between the two models across the conterminous United States. The HADGEM model suggests that the Western States are experiencing drier climates in the future and suggests the opposite for the Eastern United States. While the predictions of the CGCM model are on the contrary but the results agree well with the work of Thomson et al. (2005).

To explore the distribution of anomalies shown in Fig. 4.6, the share of each continent and Hemisphere to water balance was computed and shown in Table 4.3. In 2050s, temperature, precipitation, and CO_2 emissions increase, and consequently ET follows the same trend but at a slower pace. It is a compromise between the competing feedbacks on the water cycle of which one parameter has a positive correlation (increases ET) while another may have a negative correlation (suppresses ET). In 2080s, however, temperature and precipitation increase but not CO_2 emissions, as a consequent ET shows negligible changes. There is an evidence of the various feedbacks that control the interaction between the atmosphere and the soil-plant system in opposite directions at the same time (IPCC, 2007). In the complementary theory, higher temperatures indicate higher values of potential ET not actual ET. This fact can be recognized when the different GCM models were applied in the 2050s and the 2080s alike (Table 4.3). It is evident that temperature is the most noticeable signature of ET in agreement with the findings of previous researchers starting from Thornthwaite (1948) who worked on temperature-based ET methods that assume that temperature is the main driver.

The higher moisture in atmosphere primarily from precipitation indicates cloudier conditions that make the surface cooler in warm areas and warmer in cold areas (IPCC, 2007). “The warming of the atmosphere by the surface may reduce its relative humidity and reduce precipitation as happens over deserts. However, it can also increase the total water held by the atmosphere, which may lead to increased precipitation as happens over the tropical oceans” (IPCC, 2007). In effect, the HADGEM model suggests an increment of 2% in ET (Table 4.3) given that the average annual temperature increases by 3.1°C in the 2050s, however, an increase of 4.8°C to the average annual temperature in 2080s results in almost no noticeable change in ET (-0.3%). Higher temperatures reflect dryer surface conditions that consequently result in lower values of ET. This is obvious when ET predictions in the 2050s and the 2080s are compared for both GCM models (Table 4.3).

Others have also found similar ET patterns given higher temperatures and rainfall conditions. Nabi (1998) developed a hydrologic model for closed canopy cover of vegetation. A sensitivity analysis showed that increases in temperatures of 3 to 4°C and increase in precipitation of 10% result in variation of ET from -9 to 24%. Remrova and Cislerova (2010) used a soil moisture model and found a stable pattern of ET by the end of 21st century with HADCM3 model and the A2 emission scenario. Although A2 scenario implies higher CO_2 emissions than A1B does, still impact on ET is trivial.

It is also noticed that changing the GCM model has minimal impact on global ET patterns in the present study. At the scales shown in Table 4.3, there is no strong evidence that ET is correlated to soil moisture as Jung et al. (2010) stated. According to Thomson et al. (2005), it could be the regional climate that has a larger impact on the water cycle variations than the GCM selected. Remrova and Cislerova (2010) concluded that climate change will be more effective at regional not global scale. This may explain having ET patterns with the same trend regardless of the GCM selected.

As shown in Fig. 4.6, the regional trends in water surplus (S) are more prominent between the two GCM models. A good example of that would be the United States where HADGEM model is expecting water deficiency in the east compared to the west while the opposite trend is being projected by CGCM model. In order to better present the differences in the GCM model projections on a regional scale, the western United States are chosen for that analysis. The analysis will take into account the

The variation in the water cycle is more prominent in the South Hemisphere recognized by the dramatic changes that will take place with hydrologic processes (see IPCC, 2007). In addition to the climate signature on the ET pattern, the distribution of meteorological fields across the gridded network in both cold and warm climates may also play an important role (as indicated by the IPCC (2007) report and Fig. 4.6) given the quality of data used, the GCM model selected, the downscaling approach applied, and emission scenario chosen.

In order to show the differences between the two GCM models selected in the present study, the area of the western United States is chosen. The analysis will consider the population growth in each state from the present through to 2050s. The population statistics were obtained from http://www.census.gov/population/www/documentation/twps0056/tabs15-65.pdf. The future population of each state in the 2050s was projected under four immigration scenarios (Martin and Fogel, 2006). The average number of population from the four scenarios is used for comparison with the present population. The water surplus in the baseline scenario is calculated by adding the values of each cell within each state and similar calculations performed for future scenarios too.

Fig. 4.7 shows the results of S per capita for the two GCM models compared to the baseline scenario as percentages. It is noticed that the two GCM models suggest different projections. The positive values in Fig. 4.7 indicates higher share of water for each person (water surplus) and vice versa for negative values (water deficiency). The S/capita ratios of the two GCM models are almost indifferent for the Pacific, Colorado, and Idaho states. The difference between the two GCM models is found to be the largest in New Mexico in which opposite projections are expected. While S/capita is expected by the CGCM model to be low in Utah (S/capita = -49%), the HADGEM model projected a much higher S/capita. The opposite trend between the two GCM models is observed for Montana. There is an agreement between GCM models that Wyoming has no concerns about the future water supply as water surplus is expected to significantly increase.

Arizona is expected to have the second highest population growth after Nevada by the 2050s and therefore it has high negative S/capita values predicted from both GCM models. While Nevada has the highest population growth in the United States by 2050s, the S/capita values are extremely high and positive. The large values in Nevada are referred to the fact that its S/capita ratio in the baseline scenario is found to be negative. This means that Nevada confronted a water deficiency in the 20^{th} century and therefore the state is dependent on water from other states such as from the Colorado river.

However, this argument does not mean that the projected increase in S will overcome the large population growth in this state. In contrast, Nevada has one of the lowest S/capita ratios among the western United States in the 2050s similar to Arizona.

Overall, this is an example illustrating the demographic implications into the future using the present study showing that accurate calculations and predictions of water resources is a prerequisite to successful planning and management of water resources.

4.6 Conclusions

In a previous work of the authors (Anayah and Kaluarachchi, Chapter 2), the complementary methods were tested over 34 FLUXNET global sites and the GG method were modified such that ET can be reliably estimated under variety of physical and climatic conditions. The modified GG model is simply using the basic complementary relationship of ET + ETP = 2ETW and predicting ETW using the Priestley-Taylor (1972) method. Data required for the model are routine meteorological variables, temperature, humidity, sunshine duration, and wind speed only. Given the simplicity of this proposed modified GG model and the minimal data requirements, this work extended the analysis to predict the global ET and water surplus patterns.

Data from New et al. (1999) were used at 30 minute spatial resolution at monthly time steps to predict the climatological normal of ET in the baseline period. The complementary methods, including the modified GG model, provide a good alternative to the classical methods of estimating ET given the minimal data requirements. In addition, the modified GG model is driven by metrological data only and therefore, this approach is attractive for ET estimations under climate change. The proposed modified GG model was applied and results were compared to estimates from others studies. The comparison showed reasonably good agreement in most cases and any discrepancy found is understood and can be explained. This good comparison provided confidence that the proposed modified GG model is reliable and consistent and can be used at global scale to predict water balance.

Globally, the average annual ET is 434 mm which is 63% (ET/P ratio) of average annual precipitation (P) of 690 mm. The estimated ET/P ratio is in close agreement to the values of 60-65% ET/P found worldwide by Brutsaert (1982), L'vovich (1979), and others. Worldwide, the average annual S is 256 mm which matches perfectly with the D value of 266 mm predicted by Baumgartner and Reichel (1975). Comparing the Northern and Southern hemispheres, the annual cycle is more prominent in the latter as Fan and van den Dool (2004) found but not for ET. Overall, Africa has the highest ET/P ratio while South America has the lowest at the continental scale. All studies agree that South America has the highest Water Surplus across all continents. As expected, the tropical zone between 10° S and 10° N has the highest share for all components of the water budget. Almost 29% of P, 22% of ET, and 41% of S resides at this latitudinal slice. Therefore, it is important to have good estimates of water balance in the tropical zone given its significant contribution to the global hydrologic cycle.

Two recent and robust GCM models are used to evaluate climate change impacts on water balance and these are HadGEM1 and CGCM3.1-T47. The greenhouse gas emission scenario considered is the moderate A1B scenario which shows a reduction in emissions after 2050s. The two time periods considered were 2050s (2040-2069) and 2080s (2070-2099). Downscaled ClimGen data (Mitchell and Osborn, 2005) were made available by Ramirez and Jarvis (2008) for temperature and precipitation only at 30 minutes resolution such that the data can be imported directly into the GIS environment. However, data are insufficient to predict ET of the modified GG model. Parameterization techniques were used to predict missing data.

Results show that ET has no significant trend across the 21st century at global level. Following the CO_2 pattern of the emission scenario A1B, ET increases up to 2050s and decrease slightly towards 2080s. An increase in precipitation of 10% in the 2050s results in 2% increment in ET while 15% increase in precipitation at 2080s is accompanied by decrease in ET of 0.3 %. It is evident that ET patterns are controlled by the regional climate (temperature) more than the climate change scenario selected. The difference between the two GCM models is obvious when compared at a regional scale. A good example is shown through the comparison of water surplus per capita values across the Western US between different states. This example shows the applicability of the present study to identify the impact of population growth on water resources under climate change and how necessary adaption measures should be considered.

References

Allen, R.G., 1996. Assessing integrity of weather data for reference evapotranspiration estimation. ASCE J. Irrig. and Drain. Eng. 122(2), 97-106.

Allen, R.G., 1997. Self-calibrating method for estimating solar radiation from air temperature. J. Hydrol. Eng. 2(2), 56-67.

Allen, R.G., Pereira, L.S., Raes, D., Smith, M., 1998. Crop evapotranspiration: Guidelines for computing crop water requirements. FAO Irrig. and Drain. Paper No. 56, Food and Agric. Orgn. of the United Nations, Rome, Italy.

Allen, R.G., Walter, I.A., Elliot, R., Howell, T., Itenfisu, D., Jensen M. (Eds), 2005. The ASCE Standardized Reference Evapotranspiration Equation. American Society of Civil Engineers Environmental and Water Resource Institute (ASCE-EWRI).

Arora, V.K., 2002. The use of the aridity index to assess climate change effect on annual runoff. J. Hydrol. 265, 164-177.

Baldocchi, D., Falge, E., Gu, L., Olson, R., Hollinger, D., Running, S., Anthoni, P., Bernhofer, C., Davis, K., Evans, R., Fuentes, J., Goldstein, A., Katul, G., Law, B., Lee, X., Malhi, Y., Meyers, T., Munger, W., Oechel, W., Paw, U.K.T., Pilegaard, K., Schmid, H.P., Valentini, R., Verma, S., Vesala, T., Wilson, K., Wofsy, S., 2001. FLUXNET: A new tool to study the temporal and spatial variability of ecosystem-scale carbon dioxide, water vapor, and energy flux densities. Bull. Am. Meteorol. Soc. 82, 2415-2434.

Baumgartner, A., Reichel, E., 1975. The world water balance: mean annual global, continental and maritime precipitation, evaporation and runoff, first ed. Elsevier Science Pub. Co., New York.

Berner, E.K., Berner, R.A., 1987. The global water cycle: Geochemistry and environment, first ed. Prentice-Hall, Englewood, New Jersey.

Bouchet, R.J., 1963. Evapotranspiration reelle et potentielle, signification climatique. Int. Assoc. Sci. Hydrol. Pub. 62, 134-142.

Brutsaert, W., 1982. Evaporation into the Atmosphere: Theory, History, and Applications. D. Reidel Pub. Co., Dordrecht, Holland.

Brutsaert, W., Stricker, H., 1979. An advection aridity approach to estimate actual regional evaporation. Water Resour. Res. 15(2), 443-450.

Budyko, N.I., Efimova, Zubenok, L.I., Strokina, L.A., 1962. The heat balance of the earth’s surface. Izv. Akad. Nauk. SSSR. Ser. Geogr. Geofiz. 1, 6-16 (in Russian).

Budyko, M.I., Drozdov, O.A., Yudin, M.I., 1966. The influence of man’s economic activity on the climate, in: Contemporary Problems of Climatology. Gidrometeoizdat, Leningrad, pp. 435-448.

Chattopadhyay, N., Hulme, M., 1997. Evaporation and potential evapotranspiration in India under conditions of recent and future climate change. Agric. For. Meteorol. 87(1), 55-73.

Chavez, J.L., Howell, T.A., Copeland, K.S., 2009. Evaluating eddy covariance cotton ET measurements in an advective environment with large weighing lysimeters. Irrig. Sci. 28, 35-50.

Chen, X., Hu, Q., 2004. Groundwater influences on soil moisture and surface evaporation. J. Hydrol. 297, 285-300.

Davenport, D.C., Hudson, J.P., 1967. Changes in evaporation rates along a 17-km transect in the Sudan Gezira. Agric. Meteorol. 4, 339-352.

Fan, Y., van den Dool, H., 2004. Climate Prediction Center global monthly soil moisture data set at 0.5° resolution for 1948 to present. J. Geophys. Res. 109, D10102.

Fekete, B., Vorosmarty, C., Grabs, W., 2000. Global composite runoff fields on observed river discharge and simulated water balances. Water System Analysis Group, University of New Hampshire and Global Runoff Data Centre, Koblenz, Germany.

Food and Agriculture Organization (FAO), 1973. Man's influence on the hydrological cycle. Irrigation and Drainage Paper, Special Issue No. 17. Food and Agriculture Organization, Rome, Italy.

Fortin, J.P., Seguin, B., 1975. Estimation de I'ETR regionale a partir de IETP locale: Utilization de la relation de Bouchet a differentes echelles de temps. Ann. Agron. 26(5), 537-554.

Granger, R.J., 1989. A complementary relationship approach for evaporation from nonsaturated surfaces. J. Hydrol. 111, 31-38.

Granger, R.J., Gray, D.M., 1989. Evaporation from natural nonsaturated surfaces. J. Hydrol. 111, 21-29.

Guo, Z., Dirmeyer, P.A., Hu, Z.Z., Gao, X., Zhao, M., 2006. Evaluation of the Second Global Soil Wetness Project soil moisture simulations: 2. Sensitivity to external meteorological forcing. J. Geophys. Res. 111, D22S03.

Harmsen, E.W., Miller, N.L., Schlegel, N.J., Gonzalez, J.E., 2009. Seasonal climate change impacts on evapotranspiration, precipitation deficit and crop yield in Puerto Rico. Agric. Water Manage. 96, 1085-1095.

Hijmans, R.J., Cameron, S.E., Parra, J.L., Jones, P.G., Jarvis, A., 2005. Very high resolution interpolated climate surfaces for global land areas. Int. J. Climatol. 25, 1965-1978.

Hollinger, S.E., Isard, S.A., 1994. A soil moisture climatology of Illinois. J. Climate 7, 822-833.

Hulme, M., 1992. A 1951-80 global land precipitation climatology for the evaluation of General Circulation Models. Climate Dyn.7, 57-72.

Intergovernmental Panel on Climate Change (IPCC), 2001. Climate Change 2001: The Scientific Basis. Contribution of Working Group I to the Third Assessment Report of the Intergovernmental Panel on Climate Change [Houghton, J.T., Ding, Y., Griggs, D.J., Noguer, M., van der Linden, P.J., Dai, X., Maskell, K., Johnson, C.A., (ed.)]. Cambridge University Press, Cambridge, U.K. and New York, NY, USA.

Intergovernmental Panel on Climate Change (IPCC), 2007. Climate Change 2007: The Physical Science Basis. Contribution of Working Group I to the Fourth Assessment Report of the Intergovernmental Panel on Climate Change [Solomon, S., Qin, D., Manning, M., Chen, Z., Marquis, M., Averyt, K.B., Tignor, M., Miller, H.L, (eds.)]. Cambridge University Press, Cambridge, U.K. and New York, NY, USA.

International GEWEX Project Office, 2002. The Second Global Soil Wetness Project Science and Implementation Plan (GSWP-2). IGPO Publication Series No. 37.

Jimenez, C., Prigent, C., Mueller, B., Seneviratne, S.I., Mccabe, M.F., Wood, E.F., Rossow, W.B., Balsamo, G., Betts, A.K., Dirmeyer, P., Fisher, J.B., Jung, M., Kanamitsu, M., Reichle, R.H., Reichstein, M., Rodell, M., Sheffield, J., Tu, K., Wang, K., 2011. Global intercomparison of 12 land surface heat flux estimates. J. Geophys. Res. 116, D02102.

Jones, P.D., 1994. Hemispheric surface air temperature variability - A reanalysis and update to 1993. J. Climate 7, 1794-1802.

Johns, T.C., Durman, C.F., Banks, H.T., Roberts, M.J., McLaren, A.J., Ridley, J.K., Senior, C.A., Williams, K.D., Jones, A., Rickard, G.J., Cusack, S., Ingram, W.J., Crucifix, M., Sexton, D.M.H., Joshi, M.M., Dong, B.W., Spencer, H., Hill, R.S.R., Gregory, J.M., Keen, A.B., Pardaens, A.K., Lowe, J.A., Bodas-Salcedo, A., Stark, S., Searl, Y., 2006. The new Hadley Centre climate model HadGEM1: Evaluation of coupled simulations. Journal of Climate 19(7), 1327-1353.

Jung, M., Reichstein, M., Ciais, P., Seneviratne, S.I., Sheffield, J., Goulden, M.L., Bonan, G., Cescatti, A., Chen, J., de Jeu, R., Dolman, A.J., Eugster, W., Gerten, D., Gianelle, D., Gobron, N., Heinke, J., Kimball, J., Law, B.E., Montagnani, L., Mu, Q., Mueller, B., Oleson, K., Papale, D., Richardson, A.D., Roupsard, O., Running, S., Tomelleri, E., Viovy, N., Weber, U., Williams, C., Wood, E., Zaehle, S., Zhang, K., 2010. Recent decline in the global land evapotranspiration trend due to limited moisture supply. Nature 467, 951-954.

L'vovich, M.I., 1979. World Water Resources and Their Future, first ed. AGU, Washington, D.C.

Martin, J., Fogel, S., 2006. Projecting the U.S. Population to 2050: Four Immigration Scenarios. Federation for American Immigration Reform (FAIR). FAIR Horizon Press, Washington, D.C.

McKenney, M.S., Rosenberg, N.J., 1993. Sensitivity of some potential evapotranspiration estimation methods to climate change. Agric. For. Meteorol. 64, 81-110.

Mitchell, T.D., Carter, T.R., Jones, P.D., Hulme, M., New, M., 2004. A comprehensive set of high-resolution grids of monthly climate for Europe and the globe: the observed record (1901-2000) and 16 scenarios (2001-2100). Tyndall Centre for Climate Change Research, Working Paper No. 55, University of East Anglia, Norwich, U.K.

Mitchell, T.D., Osborn, T.J., 2005. ClimGen: A flexible tool for generating monthly climate data sets and scenarios. Tyndall Centre for Climate Change Research, Norwich, U.K.

Morton, F.I., 1983. Operational estimates of areal evapotranspiration and their significance to the science and practice of hydrology. J. Hydrol. 66, 1-76.

Mu, Q., Zhao, M., Running, S.W., 2011. Improvements to a MODIS global terrestrial evapotranspiration algorithm. Remote Sens. Environ. 115, 1781-1800.

Mueller, B., Seneviratne, S.I., Jimenez, C., Corti, T., Hirschi, M., Balsamo, G., Ciais, P., Dirmeyer, P., Fisher, J.B., Guo, Z., Jung, M., Maignan, F., McCabe, M.F., Reichle, R., Reichstein, M., Rodell, M., Sheffield, J., Teuling, A.J., Wang, K., Wood, E.F., Zhang, Y., 2011. Evaluation of global observations-based evapotranspiration datasets and IPCC AR4 simulations. Geophys. Res. Lett. 38, L06402.

Nabi, A., 1998. A hydrologic model for studying the climate change impact on evapotranspiration and water yield in a humid tropical watershed. PhD dissertation, University of Putra Malaysia, Malaysia.

Naeimi, V., 2009. Model improvements and error characterization for global ERS and METOP scatterometer soil moisture data. PhD dissertation, Vienna University of Technology, Austria.

New, M., Hulme, M., Hones, P., 1999. Representing twentieth-century space-time climate variability. Part I: Development of a 1961-90 mean monthly terrestrial climatology. Am. Meteorol. Soc. 12, 829-856.

New, M., Lister, D., Hulme, M., Makin, I., 2002. A high-resolution data set of surface climate over global land areas. Clim. Res. 21, 1-25.

Penman, H.L., 1948. Natural evaporation from open water, bare soil, and grass. Proc. Roy. Soc. London A193, 120-146.

Priestley, C.H.B., Taylor, R.J., 1972. On the assessment of surface heat flux and evaporation using large-scale parameters. Month. Weather Rev. 100, 81-92.

Ramirez, J., Jarvis, A., 2008. High resolution statistically downscaled future climate surfaces. International Center for Tropical Agriculture (CIAT). CGIAR Research Program on Climate Change, Agriculture and Food Security (CCAFS). Cali, Colombia.

Remrova, M., Cislerova, M., 2010. Analysis of climate change effects on evapotranspiration in the watershed Uhlirska in the Jizera Mountains. Soil and Water Res. 5, 28-38.

Robock, A.K.Y., Vinnikov, G., Srinivasan, J.K., Entin, S.E., Hollinger, N.A., Speranskaya, S., Liu, S., Namkhai, A., 2000. The global soil moisture data bank. Bull Amer. Meteorol. Soc. 81, 1281-1299.

Scinocca, J.F., McFarlane, N.A., Lazare, M, Li, J., Plummer, D., 2008. The CCCma third generation AGCM and its extension into the middle atmosphere. Atmospheric Chem. and Physics 8, 7055-7074.

Scipal, K., 2002. Global soil moisture retrieval from ERS scatterometer data. PhD dissertation, Vienna University of Technology, Austria.

Street-Perrott, F.A., Beran, M., Ratcliff, R., 1983. Variations in the Global Water Budget, first ed. Springer, Boston.

Teuling, A.J., Hirschi, M., Ohmura, A., Wild, M., Reichstein, M., Ciais, P., Buchmann, N., Ammann, C., Montagnani, L., Richardson, A.D., Wohlfahrt, G., Seneviratne, S.I., 2009. A regional perspective on trends in continental evaporation. Geophys. Res. Lett. 36, L02404.

Thomson, A.M., Brown, R.A., Rosenberg, N.J., Srinivasan, R., Izaurralde, R.C., 2005. Climate change impacts for the conterminous USA: An integrated assessment: Part 4. Water resources. Climatic Change 69, 67-88.

Thornthwaite, C.W., 1948. An approach toward a rational classification of climate. Geographical Review 38(1), 55-94.

Trewin, B.C., 2007. The Role of Climatological Normals in a Changing Climate. World Climate Data and Monitoring Programme, World Meteorological Organization, WMO/TD No. 1377, Geneva, Switzerland.

United States Department of Agriculture- Soil Conservation Service (USDA-SCS), 1972. National Engineering Handbook, Section 4 - Hydrology. Soil Conservation Service, U. S. Department of Agriculture, Washington, D.C.

Wagner, W. Scipal, K., Pathe, C., Gerten, D., Lucht, W., Rudolf, B., 2003. Evaluation of the agreement between the first global remotely sensed soil moisture data with model and precipitation data. J. Geophysical Res. D: Atmospheres 108(19), ACL 9-1–9-15.

Willmott, C.J., Rowe, C.M., Mintz, Y., 1985. Climatology of the terrestrial seasonal water cycle. J. Climatol. 5, 589-606.

World Meteorological Organization (WMO), 1996. Climatological normals (CLINO) for the period 1961-1990. Secretariat of the World Meteorological Organization, Geneva, Switzerland.

Yang, D., Kane, D., Zhang, Z., Legates, D., Goodison, B., 2005. Bias corrections of long-term (1973-2004) daily precipitation data over the northern regions. Geophys. Res. Lett. 32, L19501.

Zhang, K., Kimball, J.S., Nemani, R.R., Running, S.W., 2010. A continuous satellite-derived global record of land surface evapotranspiration from 1983 to 2006. Water Resour. Res. 46, W09522.

Zektser, I.S., Loaiciga, H.A., 1993. Groundwater fluxes in the global hydrologic cycle: Past, present, and future. J. Hydrol. 144, 405-427.

Table 4.1. The average annual values of the water budget components and ET/P ratios by continent.

Reference	The present study				FAO (1973)				Baumgartner and Reichel (1975)			
Component	P	ET	S	ET/P	P	ET	S	ET/P	P	ET	S	ET/P
Units	mm	mm	mm	%	mm	mm	mm	%	mm	mm	mm	%
Africa	654	542	112	83	686	547	139	80	696	582	114	84
Asia	586	405	181	69	726	433	293	60	696	420	276	60
Australia	470	303	167	64	440	393	47	89	447	420	27	94
Europe	653	365	288	56	734	415	319	57	657	375	282	57
N. America	567	328	240	58	670	383	287	57	645	403	242	62
S. America	1499	728	771	49	1648	1065	583	65	1564	946	618	60

Table 4.2. The latitudinal distribution of the land areas in km^2, the volumes of the water budget components in km^3, and the share of each to its total value in % for every latitudinal slice.

Lat. Slice	Area	P	ET	S	Area	P	ET	S
°	$10^3 km^2$	$10^3 km^3$	$10^3 km^3$	$10^3 km^3$	%	%	%	%
89 - 90 N	3396	0.6	0.6	0	1.6	0.4	0.7	0
70 - 80 N	16015	5.3	3.1	2.2	7.7	3.7	3.4	4.1
60 - 70 N	33985	14.3	9.0	5.2	16.3	9.9	10.0	9.7
50 - 60 N	27104	15.5	9.7	5.9	13.0	10.8	10.7	10.9
40 - 50 N	24374	12.9	9.6	3.3	11.7	8.9	10.6	6.1
30 - 40 N	20371	10.5	8.6	1.9	9.8	7.3	9.5	3.6
20 - 30 N	17970	9.8	7.3	2.5	8.6	6.8	8.0	4.7
10 - 20 N	12985	9.8	6.8	3.0	6.2	6.8	7.5	5.6
0 - 10 N	11185	19.1	9.8	9.3	5.4	13.2	10.8	17.3
10 - 0 S	11929	22.8	10.0	12.8	5.7	15.8	11.0	23.8
20 - 10 S	10813	12.3	7.4	4.9	5.2	8.5	8.2	9.2
30 - 20 S	10838	6.4	5.2	1.2	5.2	4.5	5.8	2.2
40 - 30 S	5592	3.4	2.7	0.7	2.7	2.3	3.0	1.2
50 - 40 S	1766	1.3	0.5	0.8	0.8	0.9	0.6	1.4
60 - 50 S	564	0.2	0.1	0.1	0.3	0.2	0.2	0.2
Total	208888	144	90	54	100.0	100.0	100.0	100.0

Table 4.3. The differences (%) in the water budget components in the globe, by Hemispheres, and by continents for the four climate change scenarios.

Model	Variable	Continent						Hemisphere		Globe
		Africa	Asia	Australia	Europe	N. America	S. America	Northern	Southern	
2050										
HADGEM	P	31	14	-10	3	5	-4	14	-3	11
	ET	-3	2	-4	5	8	-2	4	-2	2
	S	22	5	-71	-1	5	-39	8	-32	-0.1
CGCM	P	8	16	10	9	5	2	11	7	10
	ET	-4	2	-5	6	9	-3	4	-3	2
	S	18	-7	-173	17	19	-7	9	-45	-2
2080										
HADGEM	P	37	20	-14	4	11	-7	20	-5	15
	ET	-6	-1	-8	2	7	-6	1	-6	-0.3
	S	30	15	-75	6	2.5	-45	13	-34	4
CGCM	P	6	23	16	13	11	2	15	9	14
	ET	-8	-1	-10	5	8	-6	1	-7	-0.4
	S	25	-2	-233	32	22	2	15	-55	1

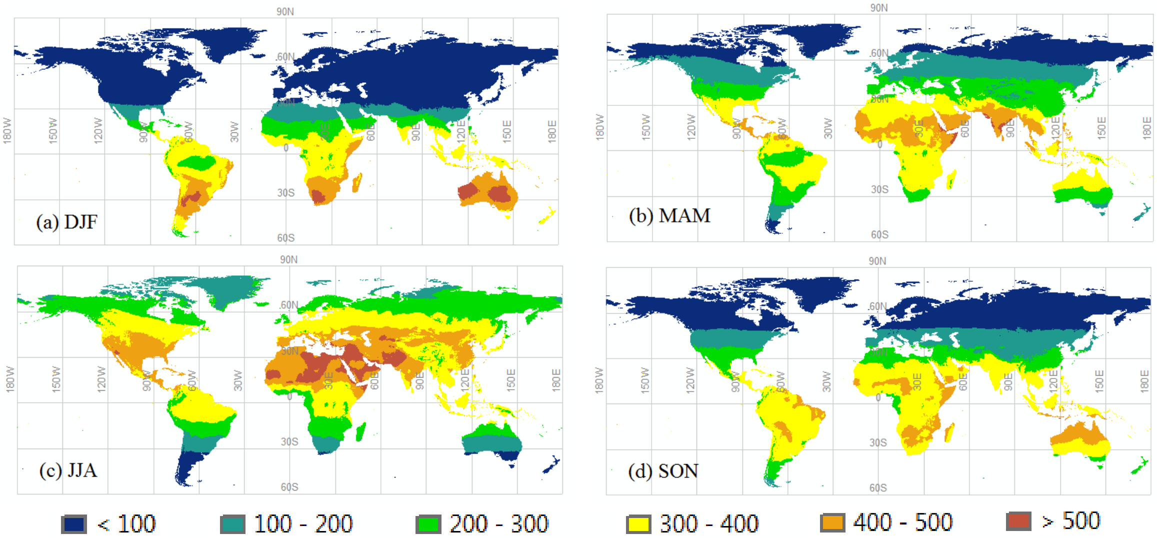

Fig. 4.1. Seasonal wet enviornment ET in mm (Priestley and Taylor equation) of: (a) DJF (Dec, Jan, Feb), (b) MAM (Mar, Apr, May), (c) JJA (Jun, Jul, Aug), and (d) SON (Sep, Oct, Nov).

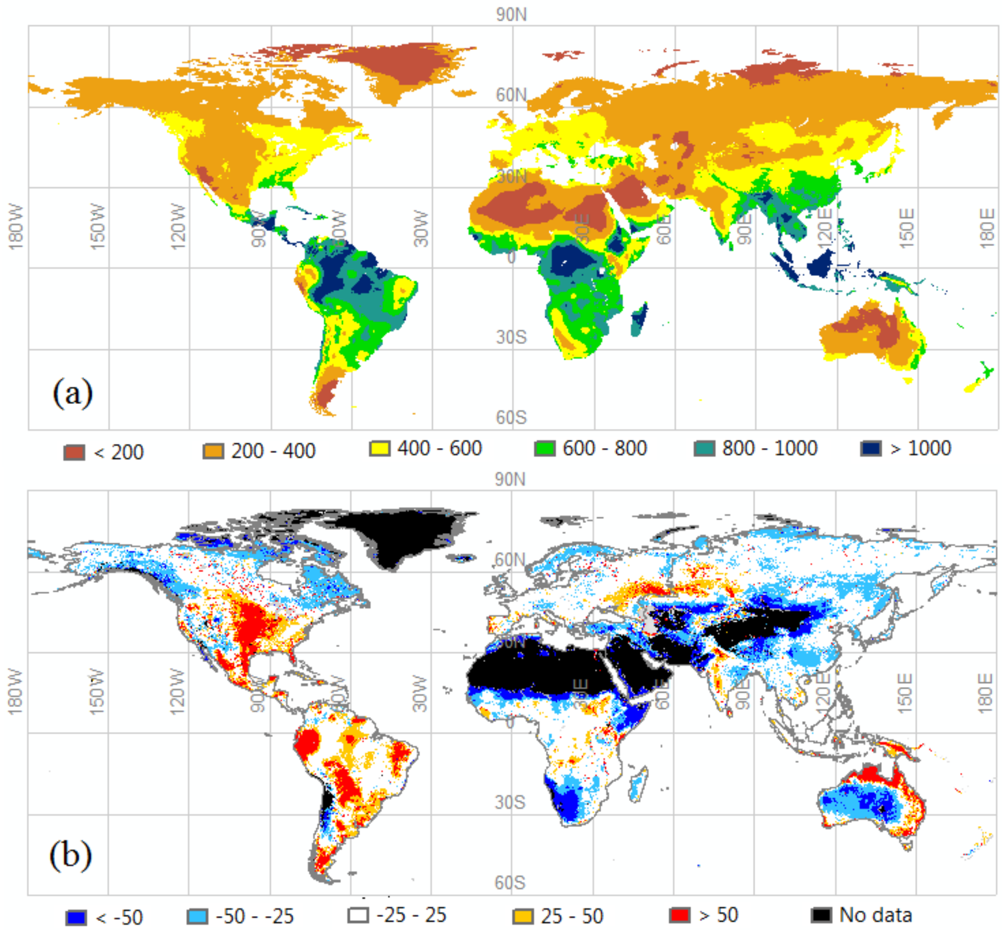

Fig. 4.2. Annual Evapotranspiration of the modified GG model: (a) actual values in mm and (b) relative difference between ET and ET_{Zhang} (Zhang et al., 2010) in %.

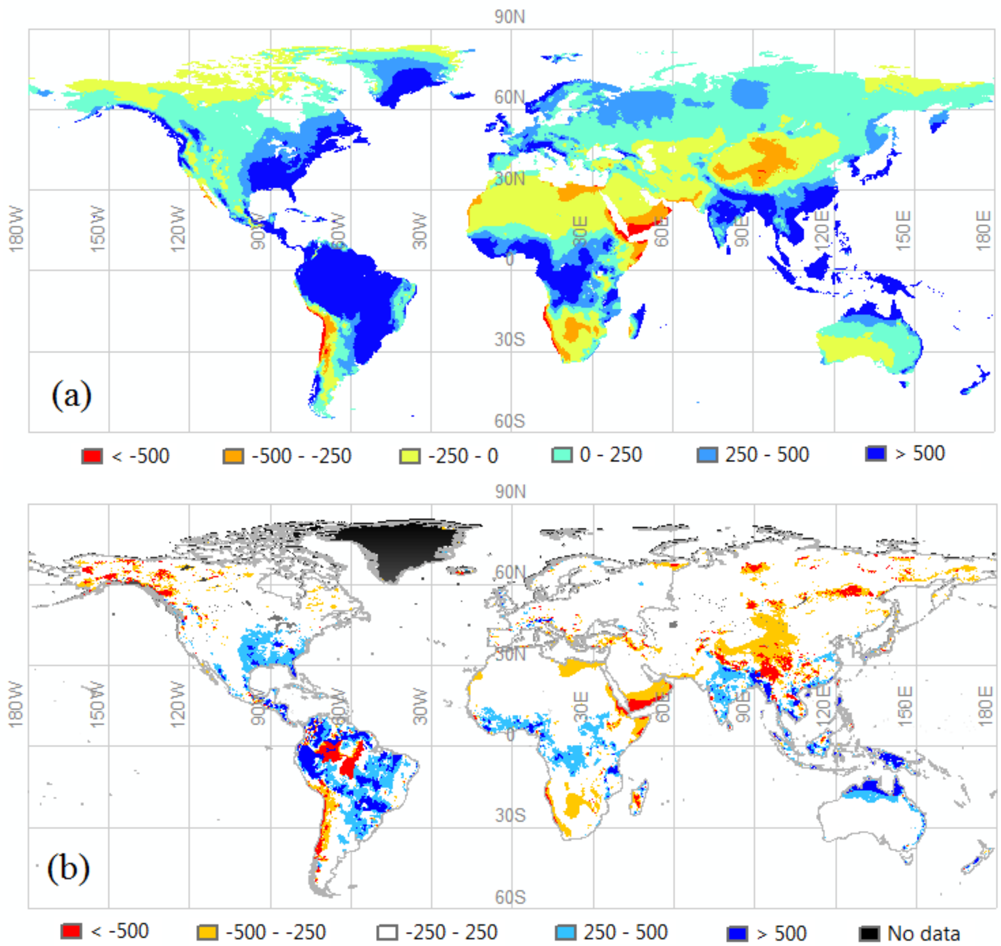

Fig. 4.3. Spatial distribution of the Water Surplus (S): (a) annual values in mm and (b) anomalies between estimates of Fekete et al. (2000) and those of present study in mm.

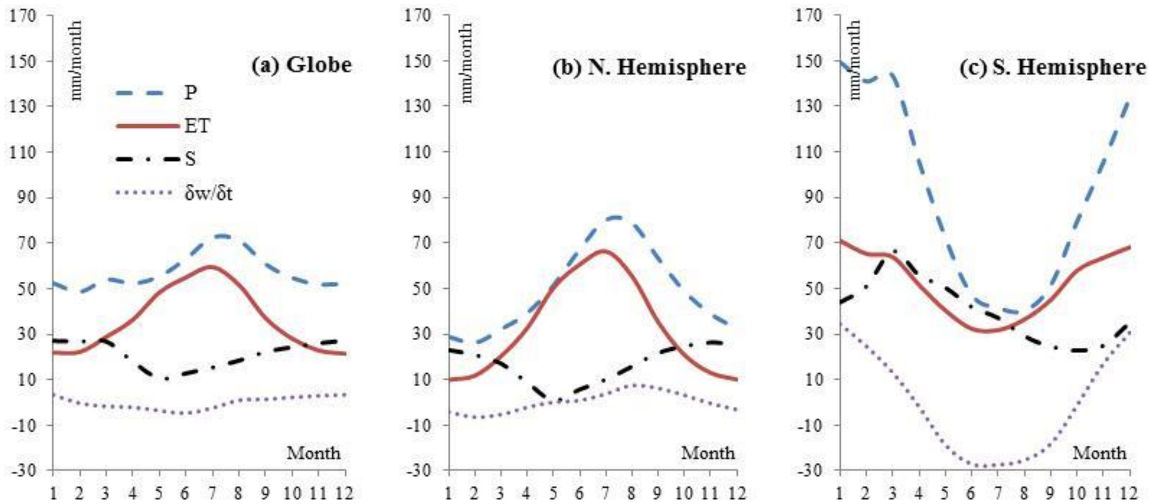

Fig. 4.4. The annual cycle of water budget components in the: (a) Globe, (b) Northern Hemisphere, and (c) Southern Hemisphere.

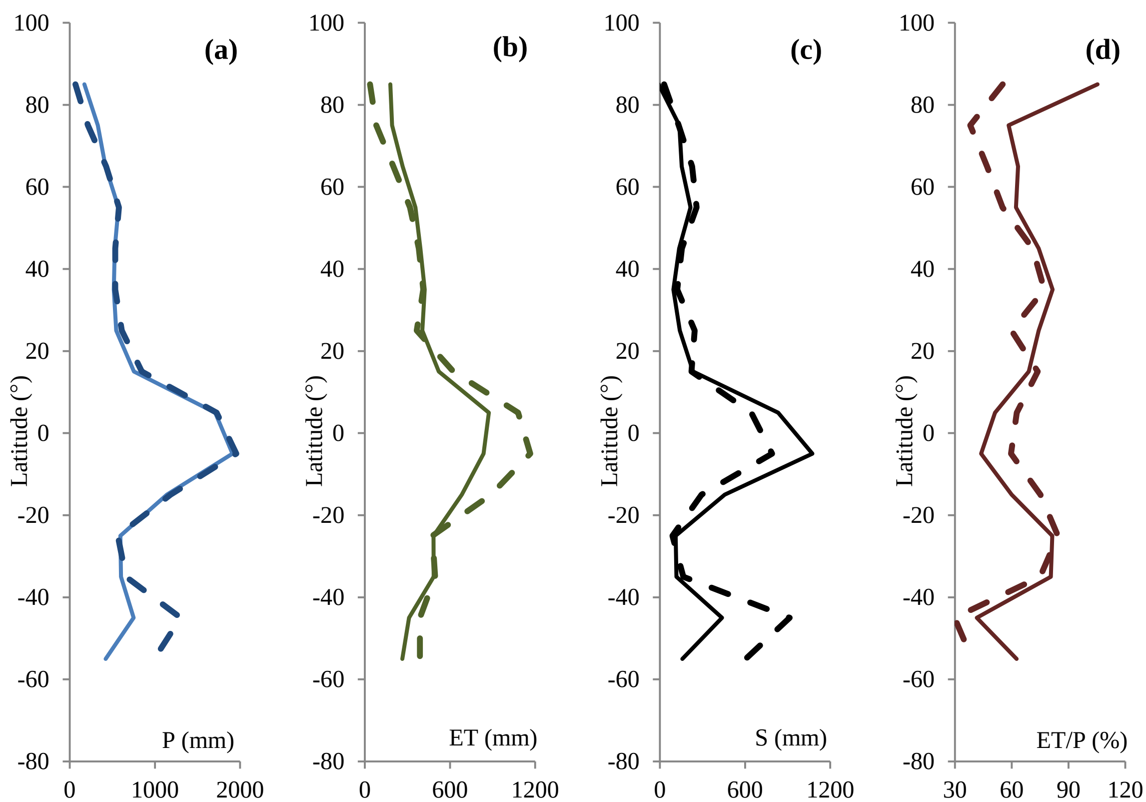

Fig. 4.5. The latitudinal patterns of the water budget components and ET/P ratios (solid line) compared to those of Baumgartner and Reichel (1975) study (dashed line).

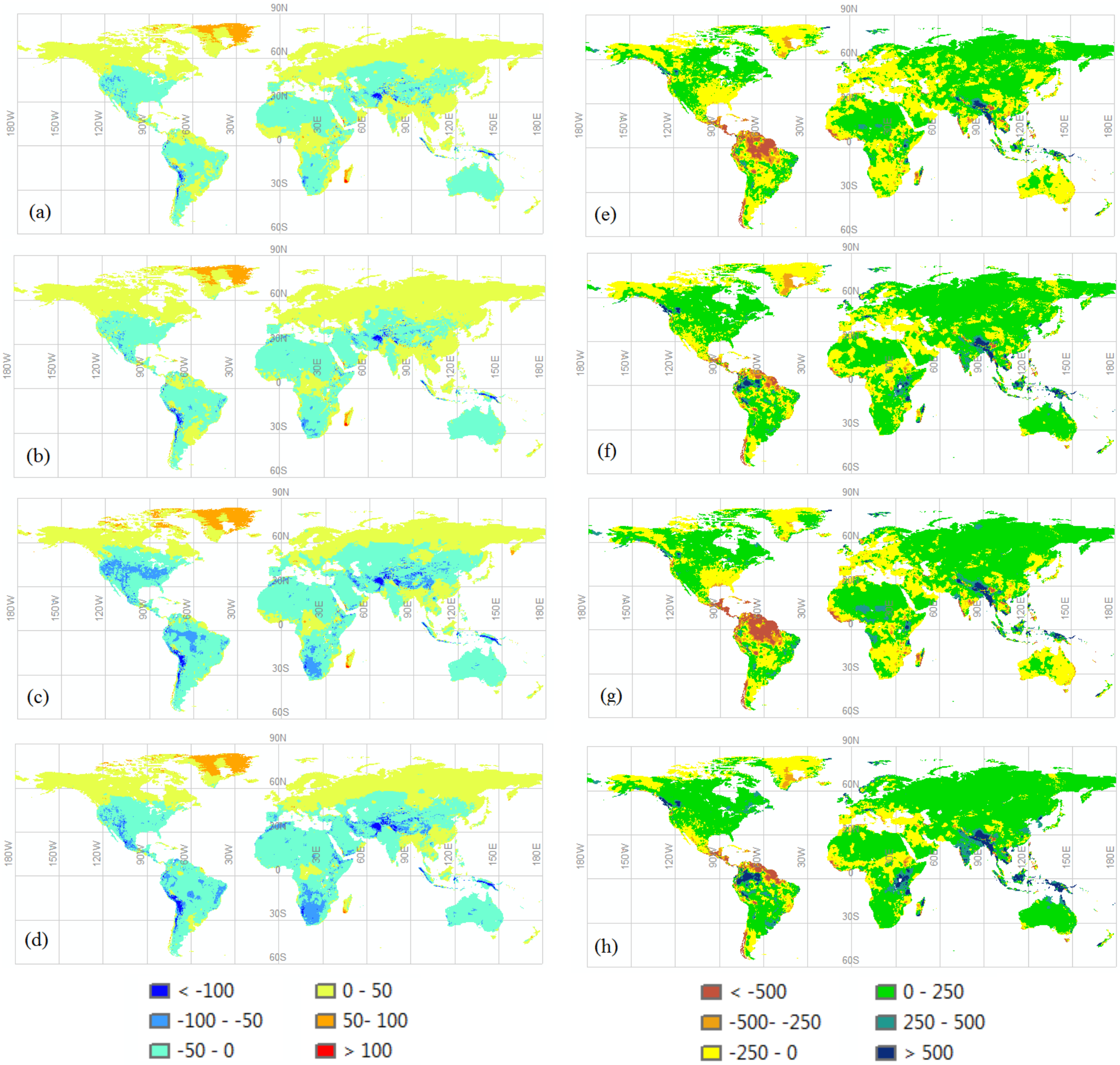

Fig. 4.6. Annual anomalies of ET for: (a) HADGEM-2050, (b) CGCM-2050, (c) HADGEM-2080, and (d) CGCM-2080 models, and annual anomalies of Water Surplus (S) for: (e) HADGEM-2050, (f) CGCM-2050, (g) HADGEM-2080, and (h) CGCM-2080 models.

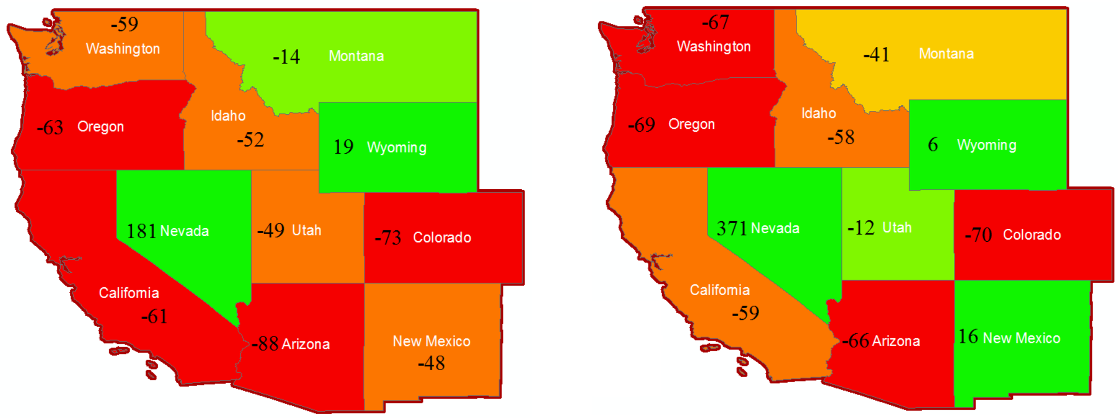

(a) (b)

Fig. 4.7. The difference in water surplus per capita ratios (S/capita) in percentage between the 2050s period and the baseline scenarios of: (a) the CGCM and (b) the HADGEM models.

CHAPTER 5

SUMMARY, CONCLUSIONS, AND RECOMMENDATIONS

5.1 Summary and Conclusions

Worldwide, ET represents a significant portion of the rainfall in the water balance especially in semi-arid regions where most rainfall is typically lost as ET (FAO, 1989). Therefore, the uncertainty in estimating ET can lead to the inaccurate prediction of water balance. There are several classical methods to estimate potential ET whereas estimating crop ET from crop covered areas during the growing seasons requires detailed local data such as land cover/land use, crop pattern, growing cycle, etc. In water resources planning, the important estimate needed is the total water loss from the land surface that may or may not include transpiration from crop areas.

Complementary methods, including the Complementary Relationship Areal ET (CRAE) method (Morton, 1983), Advection-Aridity (AA) method (Brutsaert and Stricker, 1979), and Granger and Gray (GG) method (Granger and Gray, 1989), have the potential to predict regional actual ET using minimal meteorological data. However, prior studies had used small data sets representing limited climatic variability and physical conditions and were not successful in improving the methods. This study is aimed at developing such a single step model that can compute regional scale ET independent of the land use/land class using the complementary relations which require simple meteorological data only.

In Chapter 2, 34 FLUXNET global sites with measured ET data via the eddy covariance method were used to develop the proposed model. The sites have been selected from different physical and climatic conditions to ensure the universal application of the proposed model. Using the existing three complementary methods, the analysis showed the need for improvements to the methods.

In this work, therefore, 39 different variations of model equations and parameters are considered to improve ET predictions. The selection of variations is based on the model structure and parameters used in the sub-models used to estimate ET in each of the three complementary methods. Initial results identified a set of six promising model variations. When the six climatic classes defined through the aridity index of De Martonne (1925) were reduced to three classes; wet, moderate, and dry, three promising models were identified. Statistical analyses conducted via ANOVA testing and the Dunnet method (Berthouex and Brown, 2002) showed that one model, GG18, provided the best results compared to both observed ET data and comparison with recent work of others that used remote sensing and other techniques. GG18 model is universal and does not require model calibration to suit local conditions and applicable across variety of climatic, physical and land use/cover classes.

A further comparison with existing classical methods is required to justify the applicability of the proposed modified GG model. For this purpose, Ghana was selected a study region which has contrasting climatic conditions and land use/cover. The five classical methods selected were American Society of Civil Engineers (ASCE) (Allen et al., 2005), Hargreaves et al. (1985), Jensen and Haise (1963), and Turc (1961)methods. Daily meteorological data from 10 synoptic stations in rural areas dominated by agriculture are used for monitored data. The results from Ghana when compared to five different classical methods showed good agreement between the predicted ET from the proposed GG model and crop ET from the classical methods. Water bodies and urban areas were uniquely detected by the modified GG model using the measured meteorological variables only. Most importantly, this comparison shows that the modified GG model provides regional-scale estimates of ET from point observations of meteorological data only. In essence, GG model is reliable and consistent in predicting regional ET for water resources analysis.

Given the attractiveness of the proposed GG model to predict regional ET using meteorological data only, it is obvious to assess the applicability of the model to predict global ET patterns and therefore corresponding water resources. This study therefore extended the analysis to predict regional ET worldwide and corresponding water surplus (precipitation – ET) under current conditions and climate change scenarios. For this purpose, climatological normal of the reference period 1961-1990 from New et al. (1999) are used at 30 minute spatial resolution on monthly basis. ET was estimated using the meteorological data on grid-by-grid basis and the global distribution of ET is delineated. Once the worldwide ET maps are developed, water surplus distribution was also produced. Water surplus here represents the excess water available for uses other than ET and simply can be runoff and/or groundwater recharge.

For climate change related analysis, downscaled climatological normal (Ramirez and Jarvis, 2008) for two global climate models are selected with the A1B emission scenario for two time periods; 2050s (2040-2069) and 2080s (2070-2099). The two global climate models selected are: UKMO-HADGEM1 (Johns et al., 2006) and CCCMA-CGCM3.1 (T47) (Scinocca et al., 2008). Parameterization techniques are used to predict missing downscaled data following the procedure described by Allen et al.

(1998) and others. The outputs include ET and water surplus maps in the baseline scenario and the projected scenarios in 2050s and 2080s.

Results showed that ET pattern has no significant trend across the 21st century at the global level. Following the CO_2 pattern of the A1B emission scenario, ET will increase in 2050s and decrease slightly towards 2080s. It is evident that the ET patterns are mainly controlled by the regional climate (temperature) signature more than the climate change scenario selected.

In summary, this research addressed the original research questions: 1) developing a global ET model that is verified over 34 FLUXNET global sites under a variety of physical and climatic conditions using meteorological data only, 2) validating the reliability of the proposed ET model to predict ET at country scale such as Ghana where data are limited and climate variability is significant, and 3) validating the applicability of the modified model at global scale including climate change.

5.2 Recommendations

In light of the above results and conclusions derived from this work, the following recommendations are made:

- Given the excellent results derived from the proposed methodology related to the complementary method, additional studies need to be conducted using global sites with heterogeneous land use/cover as well as climatic conditions.
- While the GG method is found to be attractive compared to the AA and CRAE methods, it is still worth to conduct additional studies using the

latter methods to identify potential advantages to further improve ET predictions using the meteorological data only.

- Besides the complementary methods, an inter-comparison study consisting of remote sensing and other recent methods will be of great interest so that inaccuracies of each method can be identified.
- In the context of climate change, the results of the present study should be used with caution given the uncertainty inherent in the global climate models, downscaling techniques, and emission scenario. A detailed study that includes the use of ensemble of global climate models with different downscaling techniques and emission scenarios is needed.
- As with many other hydrologic studies, measured data on ET are limited. Additional monitoring and measuring of ET under variety of climatic and land use/cover conditions will enable hydrologists to better use the proposed methodology in hydrologic modeling as well to make further improvement to the existing work.

References

Allen, R.G., Pereira, L.S., Raes, D., Smith, M., 1998. Crop evapotranspiration: Guidelines for computing crop water requirements. FAO Irrig. and Drain. Paper No. 56, Food and Agric. Orgn. of the United Nations, Rome, Italy.

Allen, R.G., Walter, I.A., Elliot, R., Howell, T., Itenfisu, D., Jensen M. (Eds), 2005. The ASCE Standardized Reference Evapotranspiration Equation. American Society of Civil Engineers Environmental and Water Resource Institute (ASCE-EWRI).

Berthouex, P., Brown, L., 2002. Statistics for Environmental Engineers, second ed. Lewis Publishers, CRC Press LLC, Boca Raton, FL, USA.

Brutsaert, W., Stricker, H., 1979. An advection aridity approach to estimate actual regional evaporation. Water Resour. Res. 15(2), 443-450.

De Martonne, E., 1925. Traité de Géographie Physique, tome 1, Fourth ed. A. Colin, Paris.

Food and Agriculture Organization (FAO), 1989. Arid zone forestry: A guide for field technicians. Food and Agriculture Organization of the United Nations, Rome, Italy.

Granger, R.J., Gray, D.M., 1989. Evaporation from natural nonsaturated surfaces. J. Hydrol. 111, 21-29.

Hargreaves, G.L., Hargreaves, G.H., Riley, J.P., 1985. Agricultural benefits for Senegal River Basin. ASCE J. Irrig. and Drain. Engr. 111(2), 113-124.

Jensen, M.E., Haise, H.R., 1963. Estimating evapotranspiration from solar radiation. ASCE J. Irrig. Drain. Div. 89, 15-41.

Johns, T.C., Durman, C.F., Banks, H.T., Roberts, M.J., McLaren, A.J., Ridley, J.K., Senior, C.A., Williams, K.D., Jones, A., Rickard, G.J., Cusack, S., Ingram, W.J., Crucifix, M., Sexton, D.M.H., Joshi, M.M., Dong, B.W., Spencer, H., Hill, R.S.R., Gregory, J.M., Keen, A.B., Pardaens, A.K., Lowe, J.A., Bodas-Salcedo, A., Stark, S., Searl, Y., 2006. The new Hadley Centre climate model HadGEM1: Evaluation of coupled simulations. Journal of Climate 19(7), 1327-1353.

Morton, F.I., 1983. Operational estimates of areal evapotranspiration and their significance to the science and practice of hydrology. J. Hydrol. 66, 1-76.

New, M., Hulme, M., Hones, P., 1999. Representing twentieth-century space-time climate variability. Part I: Development of a 1961-90 mean monthly terrestrial climatology. Am. Meteorol. Soc. 12, 829-856.

Ramirez, J., Jarvis, A., 2008. High resolution statistically downscaled future climate surfaces. International Center for Tropical Agriculture (CIAT). CGIAR Research Program on Climate Change, Agriculture and Food Security (CCAFS). Cali, Colombia.

Scinocca, J.F., McFarlane, N.A., Lazare, M, Li, J., Plummer, D., 2008. The CCCma third generation AGCM and its extension into the middle atmosphere. Atmospheric Chem. and Physics 8, 7055-7074.

Turc, L., 1961. Estimation of irrigation water requirements, potential evapotranspiration: A simple climatic formula evolved up to date. Ann. Agron. 12, 13-49.

CURRICULUM VITAE

FATHI "MOHAMMAD AMIN" ANAYAH

Graduate Research Assistant, Civil and Environmental Engineering

Utah State University, 4100 Old Main Hill, Logan, UT 84322-4100

Email: fathi.anayah@aggiemail.usu.edu, fanayah@hotmail.com

EDUCATION

2012	Ph.D.	Civil and Environmental Engineering, Utah State University, Logan, Utah, U.S. *Dissertation*: Improving complementary methods to predict evapotranspiration for data deficit conditions and global applications under climate change
2007	M.Sc.	Water and Environmental Engineering, An-Najah National University, Palestine *Thesis*: An Assessment of the nitrate and chloride in the West Bank groundwater resources using GIS
2007	Professional Diploma	Educational Rehabilitation, Hisham Hijjawi College Of Technology, An-Najah National University, Palestine
1997	B.Eng.	Mechanical Engineering/Thermal Power, Mu'tah University, Jordan *Project*: Modeling of fouling in heat exchangers at Mu'tah heating facility

EXPERIENCE

05/2009–04/2012	Researcher	Groundwater in sub-Saharan Africa: Implications for food security and livelihoods project, International Water Management Institute, Ghana
08/2008-present	Teaching Assistant	Groundwater Engineering Course, Department of Civil and Environmental Engineering, Utah State University, U.S.
08/2007-present	Research Assistant	Utah Water Research Laboratory (UWRL), Utah State University, U.S.
10/1999–08/2007	Vocational Teacher	Teaching classes of auto mechanics and industrial drawing, Nablus Secondary Vocational School, Palestine

06/2006- 08 /2006	GIS Trainer	Teaching courses of GIS with Engineering Applications, Al-Quds Open University, Palestine
02/1998– 10/1999	Maintenance Engineer	Working in the maintenance department, National Aluminum and Profile Company (NAPCO), Palestine

PUBLICATIONS IN REFEREED JOURNALS

Anayah, F.M., Kaluarachchi, J.J., Under review. Improving complementary methods to estimate evapotranspiration under variety of climatic and physical conditions. Water Resources Research.

Anayah, F.M., Almasri, M.N., 2009. Trends and occurrences of nitrate in the groundwater of the West Bank, Palestine. Appl. Geogr. 29, 588-601.

PUBLICATIONS IN CONFERENCE PRCEEDINGS

Anayah, F.M., Kaluarachchi, J.J., 2011. Is there a global model to reliably predicting Evapotranspiration? Spring Runoff Conference 2012. Logan, Utah, U.S. (Apr. 3-4, 2012).

Anayah, F.M., Kaluarachchi, J.J., 2012. Are actual and crop Evapotranspiration equivalent? An oral presentation at Water, Intermountain Graduate Research Symposium 2012. Logan, Utah, U.S. (Apr. 5-6, 2012).

Anayah, F.M., Kaluarachchi, J.J., 2011. Evapotranspiration estimation: complementary versus classical methods. An oral presentation at Water, Climate, and Sustainability of our Changing World, Spring Runoff Conference 2011. Logan, Utah, U.S. (Mar. 29-30, 2011).

Anayah, F.M., Kaluarachchi, J.J., 2010. Can complementary methods reliably estimate evapotranspiration in semi-arid regions? A poster presentation at American Geophysical Union (AGU), San Francisco, California, U.S. (Dec. 13-17, 2010).

Anayah, Fathi, 2009. Multi criterion decision making in agricultural planning in Qalqilya District, Palestine. An oral presentation at Climate Change and the Intermountain West: Downscaling the Future, Spring Runoff Conference and 14th Intermountain Meteorology Workshop 2009. Logan, Utah, U.S. (Apr. 2-3, 2009).

AFFLIATIONS

2009	Member	American Geophysical Union (AGU), U.S.
2008	Member	Golden Key International Honour Society, U.S.
2007	Member	American Society of Civil Engineers (ASCE), U.S.
1997	Member	Jordan Engineers Association, Jordan and Palestine